UNIVERSIDADE D
COIMBRA

Rita Leonor Martins Morgado

Robust Automatic Planning For Stereotactic Body Radiation Therapy

Dissertation in the context of the Integrated Master's in Engineering Physics, in the path of Scientific Instrumentation, supervised by Professor Joana Maria Pina Cabral Matos Dias, Professor Humberto José da Silva Rocha, and Professor Brígida da Costa Ferreira and presented to the Department of Physics of the Faculty of Sciences and Technology of the University of Coimbra

July 2024

1 2 9 0

FACULDADE DE
CIÊNCIAS E TECNOLOGIA
UNIVERSIDADE D
COIMBRA

Rita Leonor Martins Morgado

Planeamento Automático Robusto para Radioterapia Estereotáxica Corporal

Dissertação no âmbito do Mestrado Integrado em Engenharia Física, na área de Instrumentação, orientada pelos Professora Doutora Joana Maria Pina Cabral Matos Dias, Professor Doutor Humberto José da Silva Rocha e Professora Doutora Brígida da Costa Ferreira e apresentada ao Departamento de Física da Faculdade de Ciências e Tecnologia da Universidade de Coimbra.

Julho de 2024

“All our dreams can come true if we have the courage to pursue them.”

Walt Disney

Acknowledgements

This dissertation marks the end of a life cycle, whose path was fulfilled with learning journeys, with higher and lower moments, that would not have been the same without the people who have accompanied me over these years. Since all great endings deserve a much greater introduction, I will start this work by giving a special acknowledgement to all those who, directly or indirectly, have contributed to the realisation of this dissertation.

Firstly, I would like to thank to all my supervisors, Professor Joana Matos Dias, Professor Humberto Rocha, and Professor Brígida Ferreira, for giving me the amazing opportunity to work alongside them on this dissertation and for all the availability and support they provided throughout this work.

Secondly, I extend my gratitude to the Department of Physics's direction, namely, Professor Constança Providência, for giving me a place in office D9, which was an essential space to work in and complete this dissertation.

Thirdly, I am grateful for all the support, motivation, and advice that all my colleagues and friends from the course, the department, and the department's offices have given me over this academic journey. Specially, I would like to thank to Rafael, Carlos, and Tiago for all the lunches and for closely following the development of my work, as well as for all the advice and suggestions received. I also want to thank Rute and Maria Inês, who were always available to help.

Furthermore, I would like to give a huge thank you to my housemates for being my study buddies during work marathons and for all the enjoyable company and shared happy moments. In particular, I highlight the girls' group, namely Margarida, Hanna, and Fernanda, who are undoubtedly the best company I could wish for. They filled this past academic year with joyful and delightful leisure moments and created unforgettable memories I will carry with me.

Additionally, I would like to thank Francisco for always being present and ready to help, motivate, and congratulate me despite the distance.

Last but certainly not least, I express heartfelt gratitude to my family. Specially, I would like to give a huge praise to my mother for her unwavering and unconditional support during my master's dissertation elaboration process. Her belief and incentives were priceless, and it is with all the honour and honesty that I am deeply grateful for her encouragement, which motivated me to give my best throughout my master's dissertation.

Abstract

Purpose: In radiotherapy, treatment plans must be optimised to ensure the best coverage of target volumes while sparing organs at risk from unnecessary radiation that could damage them. Since photon radiotherapy treatments are typically fractionated into multiple sessions, to ensure that all uncertainties are adequately considered throughout the treatment period is essential. Specifically, in the case of stereotactic body radiotherapy (SBRT), the treatment consists of a small number of fractions, with each fraction delivering a higher radiation dose than other techniques such as intensity-modulated radiotherapy (IMRT). This work aims to study the influence of uncertainties in the delivery of radiotherapy treatments, taking into consideration the impact of the number of fractions and irradiation directions used. It also aims at testing a new treatment planning approach, in which different treatment plans are applied in each daily fraction of the treatment, to see if this diversification strategy is able to mitigate, to a certain extent, the impacts of uncertainty.

Methods: In a first phase, the impact of the number of fractions and the choice of angular configuration on dosimetric results was studied being uncertainty explicitly taken into account when evaluating these plans. In a second phase, six different treatment plans were compared in five cases of prostate cancer, evaluated in such a way that uncertainty is also explicitly considered. All the approaches tested consider treatment plans calculated automatically and without manual intervention by the planner. Monte Carlo simulation was used to compare these approaches.

Results: From the computational experiments carried out, it was possible to observe that the smaller the number of fractions used, the greater the expected impact of uncertainties. It can therefore be considered that the use of a greater number of fractions naturally contributes to an increase in the robustness of the treatment plans. It was also possible to verify that the number of irradiation directions influences the impact that uncertainties can have, with a greater number of directions corresponding to an increase in the robustness of the plans and coverage of the target volumes.

Conclusions: When the five prostate cases were studied, and six different treatment plans were compared, the main conclusion to be drawn is that even treatment plans that fulfil all the medical prescription constraints can correspond to treatment plans that end up not fulfilling these restrictions when they are evaluated with the impact of uncertainty being taken into account explicitly. Thus, the use of margins (Planning Target Volume) does not appear to be sufficient as a mitigation measure against uncertainties. The angular configuration plays a fundamental role in the robustness of treatment plans and the diversification of the treatment plan by treatment fraction could help mitigating the impact of uncertainties.

Key words: Treatment planning optimisation, SBRT, Monte Carlo simulation.

Resumo

Objetivo: A otimização dos planos de tratamento de radioterapia tem, como principal objetivo, garantir o cumprimento da prescrição médica, irradiando de forma adequada os volumes a tratar e poupando, o mais possível, os órgãos em risco. Os tratamentos de radioterapia são, habitualmente, fracionados em várias sessões e estão sujeitos à influência de incertezas de diferentes origens. No caso específico da radioterapia estereotáxica corporal (SBRT), o tratamento é composto por um número bastante reduzido de frações e, em cada uma dessas frações, é administrada maior dosagem de radiação do que é habitual em outros tratamentos com maior número de frações como a radioterapia de intensidade modulada (IMRT). Neste trabalho pretendeu-se analisar o impacto que a incerteza pode ter no tratamento que é administrado, nomeadamente tendo em conta o número de frações e as direções de irradiação que estão a ser consideradas. Foi também testada uma nova abordagem de tratamento, que se baseia na utilização de diferentes planos de tratamento em cada fração de tratamento, para verificar se esta diversificação poderia ser uma medida interessante de mitigação dos impactos das incertezas.

Métodos: Numa primeira fase foi estudado o impacto do número de frações e da escolha da configuração angular nos resultados dosimétricos quando se tem em conta, de forma explícita, a incerteza na avaliação destes planos. Numa segunda fase, foram comparados seis planos de tratamento diferentes em cinco casos de cancro de próstata, avaliados por forma a que a incerteza seja, também, explicitamente considerada. Todas as abordagens testadas consideram planos de tratamento calculados de forma automática e sem intervenção manual do planeador. Para comparação destas abordagens foi utilizada simulação de Monte Carlo.

Resultados: Das experiências computacionais levadas a cabo, foi possível observar que quanto menor o número de frações utilizadas, maior o impacto esperado das incertezas. Assim, pode considerar-se que a utilização de um número maior de frações contribui, de forma natural, para um aumento de robustez dos planos de tratamento. Também foi possível verificar que o número de direções de irradiação influencia o impacto que as incertezas podem ter, sendo que um maior número de direções corresponde a um aumento da robustez dos planos e cobertura dos volumes alvo.

Conclusão: Quando se estudaram os cinco casos de próstata, e se compararam seis planos de tratamento diferentes, a principal conclusão a retirar é a de que mesmo planos de tratamento que cumprem todas as restrições da prescrição médica podem corresponder a planos de tratamento que acabam por não cumprir com estas restrições quando são avaliados considerando de forma explícita o impacto da incerteza. Assim, a utilização de margens no volume tumoral parece não ser suficiente. A configuração angular tem um papel fundamental na robustez dos planos de tratamento e a diversificação do plano de tratamento por fração de tratamento poderá contribuir para a mitigação do impacto das incertezas.

Palavras-chave: Otimização do planeamento de tratamento, SBRT, simulação de Monte Carlo.

Contents

List of Acronyms

AI Artificial Intelligence
BAO Beam Angle Optimisation
CSC Cancer Stem Cell
CT Computer Tomography
DAO Direct Aperture Optimisation
DL Deep Learning
DNA Deoxyribonucleic Acid
DSB Double Strand Break
DVH Dose-Volume Histogram
ESTRO European Society for Radiotherapy and Oncology
EUD Equivalent Uniform Dose
FMO Fluence Map Optimisation
FSRT Fractionated Stereotactic Radiotherapy
Gy Gray
ICRU International Commission on Radiation Units and Measurements
IGRT Image-Guided Radiation Therapy
IMPT Intensity Modulated Proton Therapy
IMRT Intensity Modulated Radiation Therapy
ITV Internal Target Volume
LAPC Locally Advanced Pancreatic Cancer
linac Linear Accelerator
LNS Local Neighbourhood Search
MLC Multileaf Collimator
MRI Magnetic Resonance Imaging
NSCLC Non-Small Cell Lung Cancer
NTCP Normal Tissue Complication Probability
OARs Organs at Risk
PET Positron Emission Tomography
PRV Planning Organ at Risk
RE Robust Evaluation
RO Robust Optimisation
RT Radiation Therapy
SBRT Stereotactic Body Radiotherapy
SRS Stereotactic Radiosurgery
SSB Single Strand Break
TPC Tumour Control Probability
TPS Treatment Planning System

List of Figures

List of Tables

Chapter 1 Introduction

1.1. Motivation

Cancer is a severe disease that affects millions of people around the world, being the second-leading cause of death in the United States [1]. Eurostat stands that in a total of 5.29 million deaths in European Union (2021), around 84% were among people aged 65 years and over. Of these, cancer was one of the top two leading causes of death [2]. Furthermore, the World Cancer Research Fund International states that cancer incidence is higher in more developed countries and, in 2020, the first five countries with the highest cancer rate for men and women combined were European [3].

According to the World Health Organization, in 2022 there were an estimated 20 million new cancer cases and 9.7 million deaths related with cancer. About 1 in 5 people develop cancer sometime during their lifetime, and approximately 1 in 9 men and 1 in 12 women die from this disease [4]. Meanwhile, European Cancer Information System estimates that both cancer cases and deaths have increased by 2.3% and 2.4%, respectively, between 2020 and 2022 [5]. The European Cancer Information System predicts that from 2020 to 2040 [6], a relative increase in cancer incidence of 21% will happen in the 27 countries of the European Union, as well as a mortality relative increase of 31.8% [5]. Moreover, around the world, over 35 million new cancer cases are being predicted for 2050 which is a 77% increase from the estimated 20 million cases in 2022. Nevertheless, the high Human Development Index countries are expected to experience the greatest absolute increase in cancer incidence, with an additional 4.8 million new cases predicted in 2050 compared with 2022 [4].

The numbers presented above show the importance of studying cancer disease and its possible treatments. Depending on the type and stage of cancer development, several treatments are commonly used, either alone or concomitantly: surgery, chemotherapy, immunotherapy, radiotherapy, hormone therapy, stem cell transplant (bone marrow transplant), among others. One of the key aspects of cancer treatments is the need to be patient-specific, taking into account effectiveness and all the specific patient demands.

Radiotherapy is one of the most widely used therapies for cancer treatment and strongly relies on adequate treatment planning. Treatment planning plays a substantial role in the overall success of the entire treatment since it is responsible for all treatment parameters that must be considered in the treatment delivery, such as radiation intensity and direction. Therefore, automatic and robust treatment planning plays a significant role, being a complex procedure constantly pursuing further improvements in order to achieve better treatment outcomes, more accurate and precise plans calculated in less time with lower human intervention, and consequently fewer human mistakes.

1.2. Dissertation Objectives

Cancer data presented above motivates further improvements regarding its treatment. The treatment of a disease has several steps that must be followed, but all starts with treatment planning. Several decisions must be taken during treatment planning, assuring proper target coverage and organ sparing, with inevitable compromises that may not be consensual between planners. Most of the time, treatment planning is a time-consuming process and depends on the human planners' point of view and expertise. This dissertation aims at contributing to this vast research area of cancer disease by trying to improve treatment planning robustness and automation.

This work starts by presenting the context associated with radiotherapy treatment planning, considering also the impact of uncertainties on the dosimetric results when different decisions are made, namely number of irradiation angles used and number of treatment fractions.

The second research phase consists of comparing six different treatment plans in five distinct cases of prostate cancer for SBRT. The assessment made of all the treatment plans explicitly take into account uncertainties in accordance with the conclusions taken from the first phase of this study. Moreover, from the six treatment plans tested, five follow the current clinical practice of considering the same treatment plan throughout the SBRT whole treatment duration, and the sixth is a new treatment planning approach that aims to test the role of diversification as a measure to deal with uncertainty.

The experimental part of this work is, thus, divided in two study phases, where all the tested approaches will consider automatically calculated treatment plans that do not rely on the planner's manual intervention, as well as Monte Carlo simulations to compare all the tested approaches.

1.3. Dissertation Outlines

This dissertation is organised into five chapters. First, a brief summary of the reason for the conducted study and its objectives are emphasised. Secondly, a review of the state-of-the-art regarding the basic subjects concerning the steps of treatment planning that will be used in this work development or to which the knowledge and understanding are important for a better comprehension and enforcement of the work presented. Thirdly, the materials and methods used to perform this dissertation's computational experiments are outlined. In the fourth chapter, the results obtained are presented and discussed, in order to provide a smoother reading of the analysis of these results. In the last chapter, the main conclusions of this work are highlighted, and future work suggestions are presented.

Chapter 2 External Radiotherapy

2.1. Framework and Objectives

This chapter presents a brief review of the current state-of-the-art considering external Radiation Therapy (RT) treatments, aiming to describe the treatment planning workflow in external RT for some of the most used RT techniques, presenting a general overview of these techniques' characteristics and the current automation solutions developed to solve each step of the treatment planning process. Firstly, a contextualization of the external radiation therapy is provided. Secondly, a description of the general aspects of treatment workflow are briefly described, followed by a highlight of the most important findings regarding automated image segmentation and treatment planning. Thirdly, a general review of the uncertainties in RT is presented, along with the techniques to mitigate them, namely Robust Optimisation (RO).

There are common treatment planning problems for external RT despite the type of RT technique used. Thus, the analysis of the planning problems covers different types of RT techniques, highlighting the common points, research questions, and problems that this dissertation tries to answer.

2.2. Introduction

Radiotherapy (also known as radiation therapy, RT) aims to deliver an adequate dose of radiation to cancerous cells to sterilise the tumour and ensure that the surrounding healthy organs and tissues (usually called Organs At Risk, OARs) will suffer minimal damages, preventing changes in their main functions from happening. In other words, radiotherapy takes advantage of the fact that cancerous cells are focused on fast reproduction and have lower repair capability than healthy cells [7].

RT treatments can be divided in external RT and Brachytherapy. In the first, the radiation source is outside the patient's body and directed to the tumour location using specific treatment units. The second one involves the placement of radioactive sources within or very close to the tumour, allowing the delivery of a high dose of radiation to the cancerous cells while sparing the surrounding normal tissue [8].

The most common form of radiotherapy is external beam radiotherapy, and two types of radiation can be used: photon radiation and particle radiation [7], [9].

In radiotherapy with photons, the emission of secondary electrons will cause Deoxyribonucleic Acid (DNA) damage within the cancerous cells by direct or indirect effects [10]. Dose deposition induces cell death, i.e., emitted radiation causes cell sterilization actions by breaking DNA strands [10]. As illustrated in Fig. 1, there are two different types of DNA strand breaks that can occur: double or single. Single Strand Breaks (SSB) are usually repaired by unbroken strands due to the structural support. Double Strand Break (DSB) is the most effective and results from the break of two strands close to each other [10]. Even though each patient displays different treatment responses based on tumour volume, radiosensitivity of tumour cells and the repair mechanisms of tumour cells, it is known that for a radiation dose of 1 Gray (Gy) approximately 10^5 ionizations occur per cell and the yield of DSB is about 40% [10], [11].

Regarding patients' radiation resistance and insensibility to radiation therapy, several reasons have been suggested such as intratumoral hypoxic areas protecting carcinoma cells, mutations

in genes related to DNA damage and repair, affected cell cycle regulation, or compromised cell death machinery. Recently, the theory of Cancer Stem Cell (CSC) has been proposed, and its role in tumour formation, development and response to radiotherapy is under investigation. In 2015, the review led by Skvortsova et al. [12] concluded that ionizing radiation could not eradicate carcinoma cells equally due to CSCs despite the high efficiency of radiation therapy.

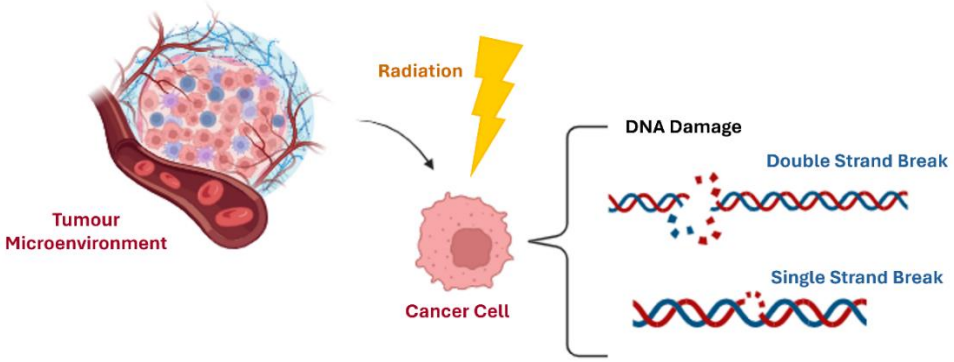

Fig. 1. Effect of radiation therapy in cancer cells.

To ensure the best result in cancerous cells sterilization and organ sparing, a RT treatment plan is made aiming to deliver a specific prescribed radiation dose to the target volume each day for a certain amount of time (i.e., weeks or months). Preceding treatment planning, the delineation of OARs and target volumes (for example, gross target volume, clinical target volume, planning target volume, etc.) must always be made using a Computer Tomography (CT) scan, Magnetic Resonance Imaging (MRI), or Positron Emission Tomography (PET) [7].

Conformal radiotherapy describes RT treatments that attempt to conform the dose to the target, i.e., treatments that use specific systems to deliver radiation from several directions and shape it to better conform with the volume to be treated [13]. In this domain, Three-Dimensional Conformal Radiation Therapy (3DCRT), Volumetric Modulated Arc Therapy (VMAT), Intensity-Modulated Radiation Therapy (IMRT), Stereotactic Body Radiation Therapy (SBRT), and Intensity-Modulated Proton Therapy (IMPT) are commonly used types of conformal RT.

Photon radiation can be from beams of X-rays or gamma rays and is mainly used in IMRT and SBRT. On the other hand, particle radiation can be from an electron, neutron, or proton beam, and is used, for example, in IMPT [9].

The 3DCRT is based on three-dimensional treatment planning, incorporating the use of imaging technologies to create 3D images of the patient. In this technique the beams are shaped according to the target volume outlined mainly from CT imaging. CT images allow the 3-dimensional localization of the tumour and critical normal organ structures. Using these images alone or combined with MRI or PET, the radiation oncologist outlines different target structures with margins to safeguard uncertainties due to organs' motion and setup variations [9], [14]. The clinical introduction of 3DCRT shifted the RT workflow [10]. It transitioned from a simulator-oriented "beam-adjusted" approach to an information-driven, computer-based process with a treatment planning system that determines machine settings for treatment delivery [10]. This system facilitated the inclusion of realistic dose calculations, allowing for manual optimisation of free variables such as beam directions, beam weights, and field shapes [10]. This technique showed an improvement in tumour targeting and reducing radiation in the surrounding normal tissues, however further improvement in dose conformity and normal tissue sparing could still

be accomplished [15]. This fact led to the development of other RT modalities as, for instance, IMRT allowing the delivery of non-uniform radiation fields, producing a highly conformal dose distribution to the volumes to treat. IMRT became one of the most conformal and effective techniques in radiotherapy [14].

Typically, radiation is generated by a Linear Accelerator (linac) mounted on a gantry that can rotate along a central axis (see Fig. 2). For the delivery of modulated radiation beams, IMRT uses a Multileaf Collimator (MLC), a device that equips the head of the gantry, consisting of movable leaves on both sides that can generate a variety of field openings. Since the patient is immobilised on a couch that can rotate, combining the couch and gantry rotation allows radiation delivery from almost any direction around the tumour. For the delivery of intensity modulated fields there are two distinct operation modes for an MLC. One is called dynamic collimation, and the other is known as multiple static collimation, depending on whether the MLC leaves move continuously during irradiation or not (the latter also known as "step and shoot mode"). The configuration of the leaves in a given moment is called an aperture. These apertures make it possible to discretize the beam into a set of smaller beams with a specific and independent fluence time or intensity. The originated small beams are called beamlets – see Fig. 2 (b). This procedure generates a discrete set of intensity maps that allow a high degree of conformity and intensity modulation of the delivered dose distribution with the shape of the tumour [7]. This ability to conform the dose distribution to the target in IMRT is proved to enhance organ sparing [16].

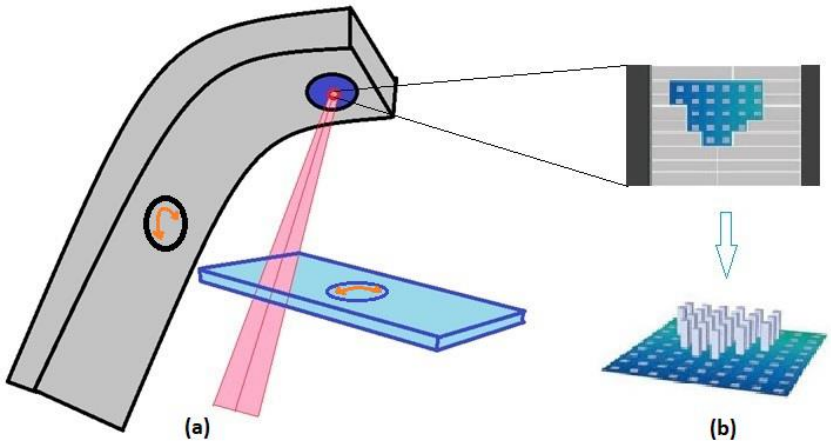

Fig. 2. (a) Illustration of a beam exiting the head of a gantry rotating around the treatment couch that can also rotate. (b) The head of the gantry is equipped with a multileaf collimator with nine pairs of leaves illustrating the discretization of the beam into small sub-beams called beamlets. (Adapted from [17])

Another well-known RT technique that employs modulated fields is VMAT [14]. The VMAT technique delivers rotational IMRT using a conventional C-arm linear accelerator design while moving from both multileaf collimator leaves and gantry (arc movements) simultaneously [14]. Therefore, in VMAT, the gantry moves continuously [14]. VMAT has proven to be more efficient than 3DCRT while providing increased OAR sparing, reduced toxicity, and improved survival rates [18]. A primary advantage of VMAT techniques is that they can deliver treatments for each patient much faster than fixed-field IMRT [14].

In 2020, the consensus from the German Society for Radiation Oncology and the German Society for Medical Physics stated that, generally, stereotactic radiotherapy is defined as a method of percutaneous external beam radiotherapy, in which a clearly defined target volume is treated with high precision and accuracy with a biologically high radiation dose in one single or a few fractions with locally curative intent [19]. Furthermore, this consensus asserts that stereotactic

RT is divided into three types, which differ from each other regarding the spectrum of indication, fractionation, and quality requirements [19]:

- Stereotactic Radiosurgery (SRS): a treatment of intracranial malignant or benign tumours and functional or vascular disorders with one single irradiation fraction.
- Fractionated Stereotactic Radiotherapy (FSRT): for intracranial malignant or benign tumours and functional or vascular disorders.
- Stereotactic Body Radiotherapy (SBRT).

SBRT is commonly used to treat extracranial malignant or benign tumours and functional or vascular disorders where treatment fractions are irradiated to extracranial targets, i.e., a high radiation dose in one single or very few fractions are administrated with high precision and accuracy to a defined target volume with locally curative intent. The SBRT principles can be applied to both photon and particle therapy. It can use either a traditional linac equipped with image guidance technology, accelerators specifically adapted for SBRT or dedicated delivery systems, which can be performed using linacs Edge (Varian Inc., Palo Alto, CA, USA) and Versa HD (Elekta AB) or specific devices for this type of treatment, such as Gamma Knife (Elekta AB, Stockholm, Sweden), or CyberKnife (Accuray Inc., Sunny-vale, CA, USA) [19], [20].

This type of treatment relies on three-dimensional imaging, such as CT, MRI, and PET/CT, to stereotactic locate the tumour or abnormality within the body to determine the exact coordinates of the target. Since the radiation beams are designed to converge to the target volume from different directions, the images taken before the treatment procedure are vital since they guide treatment planning. It is essential to ensure correct patient positioning during the treatment sessions so, usually, SBRT relies on dedicated immobilisation systems to immobilise and maintain patient position. After guaranteeing the patient's position, highly focused gamma-ray or x-ray beams will converge to the tumour or abnormality. Sometimes, Image-Guided Radiation Therapy (IGRT) is used to confirm the location of a tumour immediately before the treatment and, in some situations, during the delivery of radiation [19], [21], [22].

Proton beams were proposed for the first time in the 1950s and are increasingly being used in cancer treatment. Proton therapy gained popularity due to its unique absorption profile in tissues, which allows the deposition of maximum destructive energy at the tumour location while minimising the damage to healthy tissues along their path [9]. This unique depth-dose characteristic of proton beams comes from protons slowing down as they penetrate matter; their rate of energy transference increases with depth and stops abruptly right after the point where energy deposition is maximum, producing the so-called Bragg peak. This means that proton therapy does not have an exit dose to tissues beyond the Bragg peak point [23]. Excellent tumour irradiation can be obtained, while adjacent OARs can be significantly spared compared to photon beam RT [24]. Proton therapy has been associated with decreased incidence of secondary cancers in several paediatric cancers and has shown to be able to deliver radiation in adults with tumours located near critical structures [23].

A sophisticated mode of proton therapy is IMPT (also called "pencil beam proton therapy"). This treatment is analogous to IMRT; however, due to proton delivery characteristics, IMPT allows greater degrees of freedom to produce optimised dose distributions and can be promising for head and neck treatments that need dose escalation with OARs sparing. Particle accelerators, such as cyclotron or synchrotron, extract charged particles from hydrogen gas and accelerate them towards the speed of light [23]. In IMPT, a particle accelerator originates the proton "pencil" beams which are manipulated to treat the desired cancerous location. This

manipulation consists of changes in the number of protons (local dose deposition), energy (local penetration), and magnetic deflection (off-axis coverage) once IMPT relies on electromagnetic control of the beam to achieve target coverage while reducing the integral dose delivery. Despite the potential of this technique, still to be further explored, it also has some drawbacks, namely regarding the need to ensure the robustness of the treatments, since proton therapy is significantly vulnerable to a number of different sources of uncertainty like proton range [25]. New developments regarding on-board image guidance resources, robust optimisation algorithms, standardisation of patient-specific quality assurance programs and CT verification protocols, are expected to provide adequate approaches to deal with IMPT current limitations [26].

2.3. Radiotherapy treatment workflow

The workflow of RT treatment planning consists of three different steps, independently of the treatment modality [27], Fig. 3:

1. Immobilisation, imaging, and target volume definition.
2. Treatment planning.
3. Treatment delivery and set up verification.

First, medical images of the patient need to be obtained for proper imaging and target volume definition (usually called planning CT). This planning CT is different from the diagnosis CT scan, and it is used to define the volumes to be treated, considering the clinical examination findings and the diagnostic images from CT scan, MRI or PET [7], [27].

The medical doctor decides on the medical prescription, defining admissible tolerance doses for OARs and prescribing dose(s) to the tumour volume(s). Based on the medical imaging and medical prescription, the treatment is planned. When a treatment plan is approved, then the treatment is delivered, requiring a setup verification [27].

Most of the times, RT treatments are fractionated in several daily treatment sections until the prescribed radiation dose is totally administrated (which may take several weeks). Taking this into account, to ensure that the patient is correctly positioned in every treatment fraction is of the utmost importance. The position of the patient must be as close as possible to the position that corresponds to the planning CT, aiming to ensure accurate delivery during all the treatment sections. To reach this objective, most of the times the patient needs to be appropriately immobilised in a comfortable and reproducible way [27].

Looking with more detail into step 2, several decisions need to be made, namely:

1) Beam angle optimisation: choosing the number and directions of the radiation beams.
2) Fluence map optimisation: calculating the optimal intensity maps for each of the radiation beams.
3) Realisation: deciding on the movement of the MLC leaves.

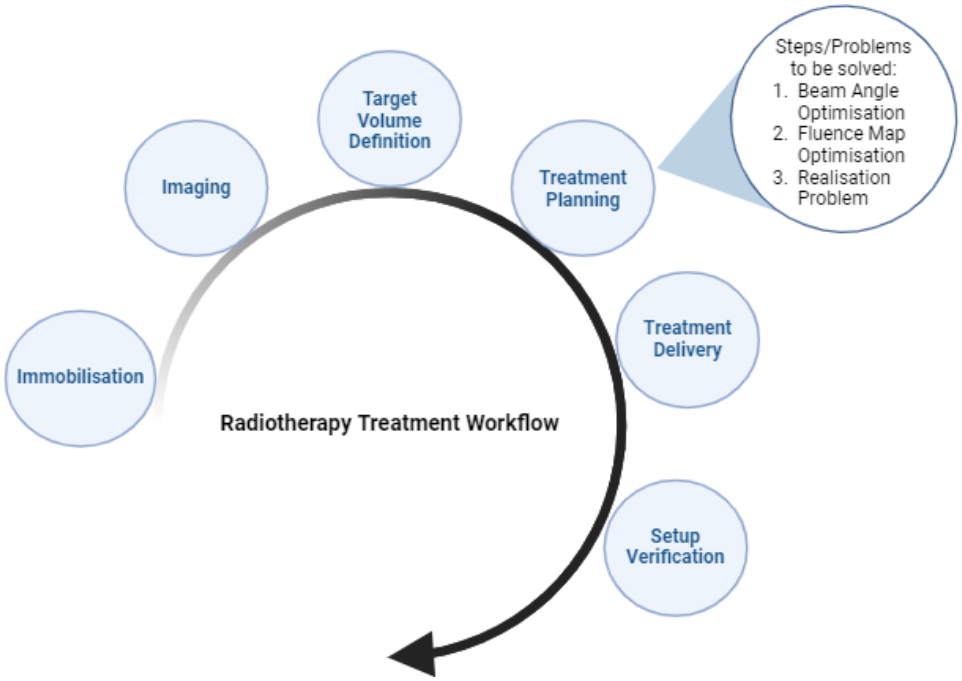

Fig. 3. Scheme of radiotherapy treatment workflow and treatment planning steps/problems that need to be solved.

As illustrated in Fig. 4, with the 3-dimensional images from the planning CT, it is possible to delineate three major mandatory target structures and their uncertainty margins. The Gross Tumour Volume (GTV) represents the volume of the known tumour. There is a possible microscopic spread in the GTV, so the Clinical Target Volume (CTV) represents the addition of the spread margin to the GTV. A marginal volume is added to the CTV as a safety measure to prevent possible inaccuracies due to organ or patient motion (known as geometrical uncertainties). This volume surrounding the CTV with a margin for geometric uncertainties is called Planning Target Volume (PTV). Around each target structure, margins are delineated to compensate for inaccuracies due to changes in size, shape and position of the organ, besides patient movement. For example, as shown in Fig. 4 Internal Target Volume (ITV) is an optional volume that can be delineated, and it describes CTV plus and internal margin, i.e., the margin for the uncertainties in size, shape and position of the CTV within the patient [7], [28].

The OARs represent the organs nearby the tumour that can be damaged by radiation when irradiated. Damages in the OARs can result in significant morbidity. Therefore, the delineation of these structures is mandatory in treatment planning. Furthermore, it is also possible to consider a margin that can be added to the OARs, accounting for uncertainties and variations in the OARs position. This margin is known as Planning Organ At Risk Volume (PRV) [7], [28].

From a treatment planning point of view, OARs can be divided into serial-like organs or parallel-like organs. Serial-like organs are such that if even only a limited percentage of the volume is over irradiated the organ can lose its functionality. This means that if the absorbed dose exceeds the tolerance value in a certain segment of the organ, it may result in loss of function to the whole organ (for example, spinal cord or oesophagus). In contrast, parallel-like organs have functional units that act independently from each other, so damages in one segment do not compromise the functionality of the others, meaning that the organ can still maintain its functionality even if a small part is affected [28].

In Fig. 4, all the structures mentioned above are outlined. In summary, the GTV, CTV, and OARs have an anatomical basis, while ITV, PTV and PRV are built considering margins introduced to mitigate uncertainties. Moreover, it is important to acknowledge that PRV and PTV margins may overlap [28].

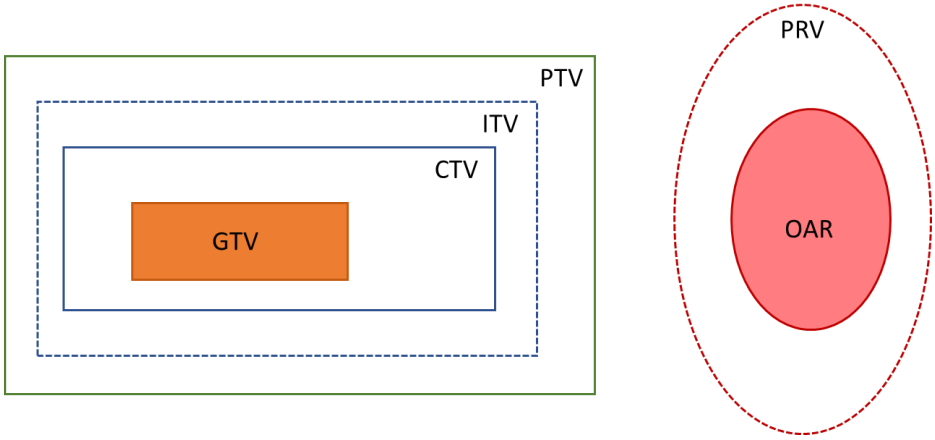

Fig. 4. Diagram to illustrate the volumes GTV, CTV, ITV, PTV, OAR, PRV delineated in radiotherapy planning.

2.3.1. Image Segmentation

Image segmentation is a crucial task routinely performed in RT workflow to identify patients' treatment targets and anatomical structures, called regions of interest, traditionally based on CT scans and, more recently, MR simulation scans. Moreover, the efficacy and safety of RT plans rely on an accurate segmentation of these regions of interest since they are used to optimise and evaluate the plan's quality [29]. Depending on the technique used to perform the segments, segmentation methods can be divided into three categories: manual, semiautomatic, and automatic [30].

Manual segmentation is typically made by a physician and reported to be significantly time-consuming, since regions of interest will need to be defined considering every CT slice. Furthermore, manual segmentation can be somewhat subjective since it is based on prior knowledge and experience of the expert performing it, which can lead to potential inconsistencies in targets and OARs segmentation that have already been reported and analysed in several studies [29]. Therefore, to rectify the intra and inter-observer divergences inherent and standardise procedures of manual segmentation, consensus guidelines were created by International Commission on Radiation Units and Measurements (ICRU), European Society for Radiotherapy and Oncology (ESTRO), etc.

The reported variabilities that are inherent to manual segmentation can have a significant detrimental impact on quantitative and dosimetric analyses [29]. Therefore, to solve these problems, the semiautomated segmentation and then automated segmentation were developed.

Semiautomatic segmentation uses algorithms to assist manual segmentation, reducing the effort and time required for this process [30]. Usually, the proposed semiautomated methods require user input for one or more of the following steps: segmentation parameters, feedback, or evaluation, including refinement and validation of segmentation [31]. For example, in 2018, Shahedi et al. [32] proposed a semiautomatic learning-based technique that uses shape and texture analysis to generate a three-dimensional segmentation for prostate CT images. This

semiautomatic segmentation method led to a faster, more accurate, and more robust performance than manual segmentation.

Automatic segmentation, or auto-segmentation, does not rely on human interactions and has two categories: learning and nonlearning based [30]. The research field regarding automatic segmentation has grown over the last two decades, and its techniques have been grouped into first, second, third, and fourth-generation algorithms [29]. Also, it is important to note that auto-segmentation is helpful if it leads to treatment plans comparable with or better than those achieved with manual segmentation but with a clinical time reduction [33].

Regarding the third generation, the multiatlas-based and hybrid techniques are considered state-of-the-art since studies from the early 2000s have shown that multiatlas segmentation minimised variability effects and was one of the most effective segmentation approaches in several grand challenges [29]. For example, in 2013, an investigation regarding the delineation of lymph node regions for RT planning of head and neck and prostate tumours was conducted by Sjöberg et al. [34], concluding that multiatlas-based segmentation achieved a reduction in time delineation compared to the use of single atlas segmentation, and the same quality of segmentation in comparison to manual segmentation. Another similar example from 2010 is a fully automatic multiatlas-based method for segmenting the whole heart and cardiac chambers implemented by Kirisli et al. [35] and evaluated using multicenter computed tomography angiography data, that demonstrated to be an accurate and robust method to 1420 multicenter data sets.

More recently, in 2020, Vrtovec et al. [36] overviewed the existing studies for automatic segmentation of OARs in the head and neck region from 2008 until 2020, concluding that, in terms of methodology, atlas-based methods for segmentation were dominating, but current approaches have shifted to deep learning, which has a superior performance. Later, in 2022, in agreement with that overview, according to Harrison et al. [33], the commercial offerings for radiotherapy segmentation have been dominated by atlas-based auto-segmentation; however, research activities regarding deep learning methods, namely fully conventional neuronal networks, have been conducted and are starting to supersede. As reported by this review, the shift from atlas-based methods to deep learning started around 2016. For example, a study from 2023 regarding validation of clinical acceptability of deep learning in RT treatment planning by Lucido et al. [37] showed that it was possible to reach highly accurate auto-segmentation of OARs of head and neck, demonstrating to be significantly time saving and achieving contours that needed only minor revisions, with potential to be used in for clinical cases. So, this work led to the development of an interventional clinical trial to assess the author's model capability in patient care.

Thus, the fourth generation has arrived with deep learning-based automatic segmentation development, which is the current state-of-the-art in radiotherapy segmentation [29]. However, due to the lack of standardisation of contouring protocols, robustness in small image acquisition changes, and trust among planners, where auto-segmentation has been used clinically, it relies on the combination of manual editing [33]. Despite inherent drawbacks, manual segmentation is still used clinically along with semiautomatic and automatic segmentation, and the choice between them depends on specific clinical scenarios, such as the complexity of the segmentation task and the available resources, as different comparison studies between all the segmentation categories led to independent and distinct results. For example, in 2020, for the specific case of quantifying vestibular schwannoma, Mcgrath et al. [31] comparison concluded

that semi-automated segmentation is significantly faster, less temporally and physically demanding, and has approximately equal performance than manual segmentation, presenting some improvements in accuracy but some limitations yet to overcome. Similarly, also in 2020, a study proposed by Kuisma et al. [38] that assessed the performance of fully automated segmentation in prostate cancer concluded there was a good agreement, repeatability, and clinical robustness when compared to manual segmentation; however, some structures remain needing important manual adjustments.

Therefore, much research and development are still needed in this field of RT workflow automation.

2.3.2. Radiotherapy treatment planning

In external RT, treatment planning is the process of determining the number, orientation, intensity, and delivery of radiation beams. Usually, treatment planning is performed with the assistance of a computerised Treatment Planning System (TPS) [39].

In order to design a treatment plan, the structures of interest are discretized into voxels, each representing a dose-point. This discretization is possible due to the CT digital medical images. Dose-points are points where the absorbed doses are calculated, and the total absorbed dose in each body region is computed as a weighted sum of the absorbed doses (expressed in Gy units). Typically, the dose distribution is represented graphically by an isodose distribution, where each set of voxels receiving a certain amount of radiation dose constitutes an isodose volume. The treatment plan defines the percentage of radiation dose for each isodose volume, aiming to ensure the quality of the treatment [7].

The quality of the treatment plan can be evaluated using various metrics, namely coverage, conformity, and homogeneity. Coverage is the ratio of the PTV enclosed by the isodose surface prescribed to the total PTV volume. Conformity is the ratio between the volume inside the isodose surface prescribed and the volume of the PTV inside that isodose surface. Homogeneity is the ratio between the maximum and minimum dose PTV receives [7]. Furthermore, the dose distribution quality is often analysed with Dose-Volume Histograms (DVHs), which represent the absorbed dose received in specific volume structures, allowing to compare and analyse different plans. The DVHs can be used to determine values such as minimum dose, median dose or maximum dose [28], [40]. Lastly, when verifying quality, it is usual to analyse the existence of cold spots (the low-dose regions where the tumour can spread during treatment sessions) and hot spots (the high-dose regions where the structure's function is compromised) [7], [28]. In Fig. 5, an example of a DVH graph is presented.

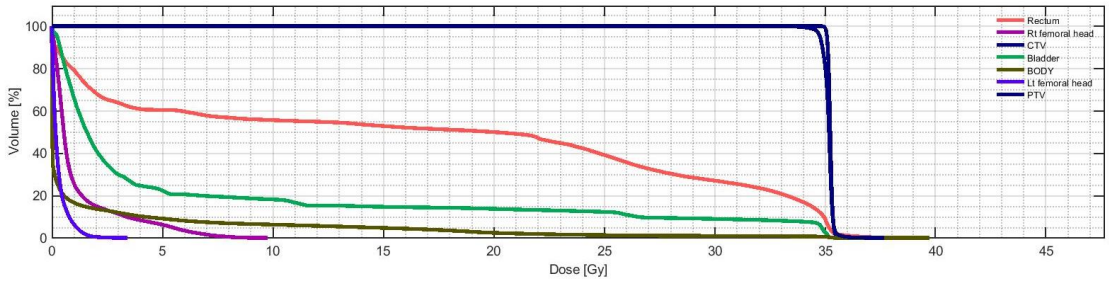

Fig. 5. Illustration of a DVH graph for a prostate cancer case displaying dosages in different structures.

The RT medical prescription is determined by what is known as the therapeutic window. The therapeutic window refers to the optimal dosage range where the probability of cure (Tumour Control Probability-TCP) is high while minimising damage to normal tissues (Normal Tissue Complication Probability-NTCP). The Tumour Control Probability (TPC) models are well stablished and provide a framework that reflects the treatment efficacy by accounting for the overall absorbed dose and the radiosensitivity of tumour tissue. These models distinguish between repairable, sub-lethal DNA SSB and unrepairable, lethal DNA DSB. Additionally, along with TPC, many institutions also use Normal Tissue Complication Probability (NTCP) for ranking competing almost equivalent treatment plans, and for evaluating candidate treatment protocols [10], [11]. Furthermore, there are more extensive models that incorporate other factors, such as tumour repopulation, tumour heterogeneity, differences in dose rate and linear energy transfer, and heterogeneous dose distributions [11].

Equivalent Uniform Dose (EUD) is a biological index, defined as the uniform dose causing equal cell surviving fraction, so it translates the biological responses into equivalent doses. This biological index is aimed for automated optimisation. On the other hand, despite not being well-suited for automated optimisation engines, conformity indexes are important for characterisation of treatment plans, since they typically focus on physical dose-volume criteria, aiming for a homogeneous dose coverage of the target and minimal dose outside [10].

The medical prescription, considering the therapeutic window, will establish dose-volume constraints for all the structures of interest.

For reporting the treatment plan, the recommended dose-volume specification can be found on cumulative DVH as the dose value specified at a percent volume, where cumulative DVHs are histograms of the volume elements that receive at least a given absorbed dose, D. In ICRU Report 83, a recommendation was made to report the near-maximum absorbed dose, e.g., D_2, where 2% represents a minimal absolute volume element within which the absorbed dose can be calculated with sufficient accuracy. This volume element is chosen to take into account the calculation grid size and considerations that pertain to dose-calculation accuracies in a single voxel. In contrast, the near-minimum dose can be given by D_{98} (or D_{95}), which is the minimum dose that covers 98% (or 95%) of the volume. The near-minimum dose was introduced in the same report as the near-maximum dose, and it ensures that the volume element in which the low dose is calculated is sufficiently large to maintain dose-calculation accuracy, which is not possible in a D_{100} value because that dose can be influences by a single voxel and the minimum dose is highly sensitive to the resolution of the calculation and the accuracy of the delineation [28].

Often, in IMRT and SBRT, to achieve dose homogeneity, the absorbed dose should be as close as possible to the near-minimum dose D_{98} or D_{95} in the PTV [20], [28]. Therefore, regarding PTV doses, the recommended reporting minimum is D_{98}, and the maximum is D_2 [20].

The dose metrics for OARs depend on whether they are parallel or serial structures. In the case of serial-like structures, the dose metric can be the maximum point dose ($D_{\max}$). In contrast, for parallel-like organs, it is recommended to use a mean dose (D_{mean}) [28]. Additionally, other dose-volume specifications can be reported [28].

Another parameter is the Van't Riet conformation number, which gives the volume of the isodose region receiving a certain amount of the dose [41]. For example, V_{59} is the volume that receives a dose larger or equal to 59 Gy [20]. This parameter may be helpful for plans that contain multiple targets [20].

Typically, RT treatment planning is divided into three steps/problems, which are described next and that are usually tackled in a sequential way.

2.3.2.1. Beam Angle Optimisation Problem

One of the challenges in IMRT, IMPT, and SBRT treatment planning is appropriately deciding how many radiation directions should be considered and what these directions should be, i.e., the number of radiation beams and their angles. This challenge is known as the Beam Angle Optimisation (BAO) problem or geometry problem, and its solution can lead to plan quality improvement [25], [42], [43].

In current clinical practice, for IMRT treatments, the BAO problem is usually handled by the treatment planner with manual selection of the number of beams and their orientation, typically resorting to previous experience, existing institutional protocols, or based on trial-and-error procedures [42]. A similar procedure happens in IMPT and SBRT [25], [44]. Despite this fact, to overcome these issues, several studies have been conducted regarding the automation of the BAO problem in IMRT, IMPT, and SBRT planning.

In IMRT, several studies concerning BAO optimisation have already been conducted. For example, in 2012, Breedveld et al. [45] proposed an *a priori* multicriteria approach to beam angle and intensity optimisation, named Erasmus-iCycle, achieving clinically feasible calculation times for a fully automated plan generation that proved to meet better the clinical goals than equiangular or manually selected configurations. Also, in 2022, Schipaanboord et al. [43] presented an approach that integrates BAO with segmentation, called TBS-BAO, that could automatically generate plans with reduced computational time compared with the Erasmus-iCycle BAO approach and manually generated. However, this novel approach showed similar plan quality compared to both methods. Furthermore, hybrid approaches that combine local gradient-based search algorithms with heuristics have been explored, such as applying a derivative-free multi-start framework with a pattern search algorithm, proposed in 2015 by Rocha et al. [42] that showed to be suitable for improving treatment plan quality. More recently, the application of Artificial Intelligence (AI) for BAO automation is being explored, as in 2020, Sadeghnejad Barkousaraie et al. [41] developed a fast and flexible beam orientation selection method that uses Deep Learning Neural Networks, which learns the connection between the patient's anatomy and the optimal set of beam orientations from the patient's anatomical features.

For IMPT, a few automation approaches for beam angle optimisation were tested and led to satisfactory results. For example, in a single mathematical framework developed in 2018 by Gu et al. [46], a novel optimisation algorithm to simultaneously select noncoplanar beam orientations and scanning spot intensity proved to be computationally efficient, dosimetrically superior, and having more delivery-friendly IMPT plans than manual planning methods for a brain and three unilateral head-and-neck cases. Despite needing more patient studies for further validation, Cao et al. [47] introduced in 2012 an uncertainty-incorporated BAO algorithm for IMPT that uses a deterministic scenario-based approach to account for uncertainties, employing a worst-case optimisation that starts with a set of initial beams and performs a local search to identify beams that improve dosimetric quality and robustness. This algorithm performed well for three prostate cancers and two skull base chordoma cases and was shown to be efficient.

For a small number of candidate beam angles in IMPT and IMRT, Lim et al. [48] developed in 2014 an effective and robust hybrid BAO framework that takes advantage of both global and local search, i.e., first finds a good feasible solution through stochastic and deterministic methods quickly and secondly finds a locally optimal solution using Local Neighbourhood Search (LNS).

Lastly, for SBRT, since the early 2000s, studies regarding automated BAO problem-solving have been conducted. For example, Magome et al. [49] developed in 2013 a computer-aided method for determination of beam arrangements based on similar cases for SBRT lung cancers, achieving usable automatically generated beam arrangements with no statistical differences from the original beam arrangement. More recently, based on that study, Haseai et al. [44] developed in 2020 a similar-case-based automated treatment planning approach with beam angle optimisation using water equivalent path length considering the doses of OAR for lung SBRT, that revealed to be efficient avoiding organs defined as OAR and automatically generating treatment plans along the planners' policies. In 2015, Rossi et al. [50] developed a beam angle class solution as an alternative to the time-consuming process of individualized beam angle selection for prostate SBRT, achieving an efficient and automated BAO that maintained plan quality and reduced computational time.

All these past studies in IMRT, IMPT, and SBRT show the importance of developing automated treatment planning approaches for BAO problem solving and potential advantages compared to manual solving, which is the most used method.

The BAO problem is a highly non-convex problem with many local minima on an ample search space, which makes it difficult to solve. The main objective of this problem is to find the minimum number and directions of beams that fulfil the treatment plan goals. The incidence angles can be either coplanar, i.e., angles that lay in the plane of rotation of the gantry, or non-coplanar. However, in clinical practice, coplanar angles are predominant possibly because this choice simplifies the solution of the BAO problem [7], [42].

Nevertheless, there is also evidence that non-coplanar incidence beam directions can lead to better treatment plans than the ones that use coplanar directions [42]. In 2003, Meedt et al. [51] studied beam direction optimisation in IMRT with coplanar and non-coplanar beams and showed that, for two cases, the non-coplanar approach outperforms the manual and the equispaced coplanar approaches. A similar comparative study between automated non-coplanar and equiangular coplanar beam setups done in 2008 by Pooter et al. [52] showed that optimisation of non-coplanar setups leads to a substantial improvement of treatment plans in IMRT for SBRT. In 2020, Ventura et al. [53], using two different algorithms for BAO optimisation, showed plan quality improvements on non-coplanar beam geometries when compared with the equivalent coplanar arrangement, achieving higher target coverage and better sparing of the normal tissues. Furthermore, in 2015, Rocha et al. [42] obtained similar conclusions regarding non-coplanar BAO optimisation in IMRT using a pattern search algorithm. Lastly, for IMPT, Kamal Sayed et al. [54] provided a method for multicriteria optimisation of the full noncoplanar beam orientation in 2020 using a multimode multi-GPU cluster and Monte Carlo dose calculation engine, automatically achieving optimised noncoplanar beam orientation plans in less time and same target coverage than manually planning.

2.3.2.2. Fluence Map Optimisation Problem

Fluence Map Optimisation (FMO) problem, or intensity problem, is the problem of determining the optimal intensity of beam profiles aiming to generate high quality treatment plans. Usually, this problem is handled after solving the BAO problem, since it is necessary to measure the impact in the dosimetric space accurately [41].

To handle the FMO problem it is possible to consider constrained or unconstrained models [17]. Typically, this problem is modelled as the minimisation of a weighted sum function where constraints are often implemented as objectives [42]. The constraints define dosimetric thresholds of the anatomical structures, such as PTVs and OARs and are, generally, dose-volume constraints, i.e., constraints that consider the relation between a percentage of radiation dose deposited on a certain percentage of the volume structure. These constraints must be respected for the clinical admissibility of the treatment plans [17]. One example of an objective function for the FMO problem is presented in equation 1. This quadratic function was used in several studies (for example [17], [55], [56], [57]) where N represents the number of beamlets and D the dose matrix, such that D_{ij} represents the contribution of unit intensity of beamlet j to the total dose deposited in voxel i. The total dose received by voxel i is calculated as $\sum_{j=1}^{N} D_{ij} w_j$, where w_j represents the weight/intensity of beamlet j. The set of structures to be considered is defined as S, and the upper and lower bounds associated with structure $s \in S$ are U_s and L_s respectively. Lastly, the penalty weights of underdose and overdose of structure s are represented by $\underline{\lambda}_s$ and $\overline{\lambda}_s$, respectively (with $s \in S$), and $(.)_+ = max\{0, .\}$.

$$f(\omega) = min_{\omega \geq 0} \sum_{s \in S} \sum_{i \in S} \left[\underline{\lambda}_s \left(L_s - \sum_{j=1}^{N} D_{ij} w_j \right)_+^2 + \overline{\lambda}_s \left(\sum_{j=1}^{N} D_{ij} w_j - U_s \right)_+^2 \right] \quad (1)$$

For this intensity problem, many different mathematical optimisation models and algorithms have already been proposed, as linear models, mixed integer linear models, nonlinear models, and multiobjective models [7]. The planner steers these mathematical models by interacting with the TPS software, where the upper and lower thresholds of each structure are defined, and a weight is considered to penalize the deviations that may occur from those thresholds. However, this definition of thresholds and weights is complex and not straightforward because, despite knowing the dose-volume thresholds that must be respected for the treatment plan to be admissible, it is complicated to know the inputs that must be given to the TPS to reach that admissible plan [17]. This is the major drawback of the manual selection of the parameters to apply in the optimisation models.

Many strategies to handle the FMO problem have been studied for the last two decades, mainly regarding IMRT treatments. In 2016, a study by Dias et al. [56] proposed the use of the quadratic unconstrained continuous programming model (1) and iteratively solve the corresponding FMO problem with the objective function parameters being defined by a fuzzy inference system. This method achieved high-quality plans within reasonable computational times. However, this methodology only considered equidistant beam solutions. In a more recent study from 2021, Eikelder et al. [58] used a conic optimisation approach to FMO that allowed nonlinear evaluation criteria, showing that the theoretical advantages of conic optimisation indeed translate to very stable convergence and good solution quality.

Additionally, in 2014, Zaghian et al. [59] proposed to solve the FMO problem for IMPT by testing an iterative approach to satisfy dose-volume constraints using a multi-objective linear

programming model. This algorithm was tested in five lung cancer cases and one prostate cancer case selected from the authors' institutional database. This method was able to satisfy the dose-volume constraints without increasing the complexity of the problem, and it alleviated the tedious effort of selecting initial values of model parameters (which were iteratively chosen).

Opposed to the automated planning process generally used and studied in the literature, few publications have focused on direct fluence map prediction, i.e., radiotherapy plans where standardised dose constraints and beam settings can be directly created by predicting the fluence maps without optimisation or dose mimicking. To do so, recently, approaches using deep learning models have been proposed, among which in 2020, Wang et al. [21] presented a novel deep learning framework for direct fluence map prediction using it in clinical pancreas SBRT cases with a single PTV. Later, in 2021, a more extensive study led by Wang et al. [60] presented a novel deep learning (DL) framework for pancreas SBRT treatment planning in scenarios involving simultaneous integrated boost (i.e., multiple PTV prescriptions). This framework utilizes two convolutional neural networks to predict beam dose and fluence maps sequentially, which enables a faster IMRT plan generation by avoiding the need for time-consuming inverse optimisation. This study conducted a retrospective analysis of 100 pancreatic cancer SBRT cases, completing the DL-based planning on average in under 2 minutes, and achieved a similar dose distribution to benchmark plans. So, this new approach showed a rapid and efficient generation of high-quality IMRT plans and a valuable tool for clinical application.

In this work, FMO will be solved with an automatic method that is based on the quadratic programming model (1) and is detailed in sub sub-section 2.3.3.1.

2.3.2.3. Realisation Problem

Usually, the BAO problem and FMO problem are solved sequentially, after which comes the challenges and difficulties of delivering the computed beam intensities effectively and accurately. Finding an efficient way to deliver, as close as possible, the optimised intensity profiles is a challenging optimisation problem. This third challenge is called the realization problem (or delivery problem) [7].

Similarly to the FMO problem, the realization problem is handled with mathematical optimisation models and algorithms [7]. Research regarding these mathematical methods for the IMRT realization problem has been done since the end of the nineties and early 2000s.

So, concerning the IMRT realization problem, it can be solved by selecting one of the existing techniques (for example, [61], [62], [63], [64], [65]), aiming to create apertures and intensities that allow the dose that is calculated by the FMO to be delivered. Additionally, numerous studies presented algorithms designed to implement arbitrary fluence distributions by segmenting multileaf fields by overlaying beams of varying shapes to allow flexible molding of the delivered fluence pattern [10]. Furthermore, differences between the planned intensity optimisation maps and the ones that are actually delivered arise from different issues, such as leaf collision and leaf perturbation of the adjacent beamlet intensities, among others, and all of them have already been addressed (for example, [66]). Despite already being addressed, these problems remain a prosperous field of research.

For example, in 2018, Baatar et al. [67] introduced a new mathematical approach to address the realization problem in IMRT, which consists of a lexicographic approach to find the minimum beam-on time and decomposing cardinality for linacs with limited MLC width. This new

approach showed an efficient reduction in the shape of the generated matrices compared to other mathematical methods, and the authors recognized that more studies must be led in the future regarding considerations for heuristics to tackle challenging instances.

Several studies defend that the three problems regarding IMRT treatment planning cannot be solved separately, i.e., these works support the idea that there is a straightforward linkage between BAO and FMO problems and a more difficult linkage between FMO and Realization problems that will define the treatment planning quality [57], [68]. The problems regarding the linkage between these last two problems have been studied. For example, in 2012, Rocha et al. [68] showed the numerical deterioration of plan quality that occurs due to the transition from FMO to the realization problem and discussed this loss based on two clinical examples. Moreover, to overcome this issue, this study proposed a combinatorial optimisation approach based on dose-volume criteria and a binary probabilistic search method that showed a better transition and increased plan quality for two clinical cases of head and neck cancer. After, to show that their approach was replicable for more clinical cases, the same authors used their proposed formulation for more clinical cases and state that it can always achieve a better transition regardless of the clinical case [57].

Other methods simultaneously tackle FMO and Realization problems instead of looking into them as separate and sequential problems. One of these methods was first introduced in 2002 by Shepard et al. [69] and is called Direct Aperture Optimisation (DAO), which uses an automated planning system to directly optimise the shape and weights of apertures for MLC devices, maintaining the advantages of explicitly including the discretization of leaves movement, and is designed to harness the dosimetric benefits of IMRT. This innovative approach in RT planning revolutionized the conventional methods. Recently, other works using the DAO method are still being conducted; for example, in 2023, Moyano et al. [70] proposed a hybrid local search strategy with mathematical programming to generate RT treatment plans by solving the DAO and testing it in a set of prostate cases. This approach achieved acceptable delivery times and produced highly competitive treatment plans in terms of the obtained objective function values compared to the traditional IMRT sequential approach.

Despite these advances, more studies must be conducted on this.

2.3.2.4. Treatment Planning Automation

The evolution path of RT seems to be going in the direction of faster and more complex treatments, with higher doses, shorter fractionation schemes, and smaller target margins [71]. Furthermore, TPS are required to be more accurate, increasingly automated, more sensitive to patient biology, and integrated with treatment machines [71]. As mentioned in the previous sections, several efforts to eliminate manual trial-and-error, time-consuming, and planner-dependent procedures in treatment planning have been made. Many of these studies lead to works that belong to the “automatic treatment planning” classification [17].

Ultimately, the most challenging part of automated treatment planning is assessing the quality of the plans since it is patient-specific, i.e., it is a patient-dependent definition, and the plan must achieve clinical goals for each patient that vary with every specific situation.

An example of a clinical available solution is the AutoPlanning in the Pinnacle TPS from Phillips, that relies on an automated rule implementation and reasoning system [72], [73].

In 2011, Zhang et al. [74] created a new methodology to automate the treatment planning process of IMRT, which the authors called the mdaccAutoPlan system. The mdaccAutoPlan system was implemented in the Pinnacle TPS, and the authors aimed to automatically generate beam angles sets, planning structures, and objective/cost function parameters without manual adjustments. This new approach starts with a selection of the beam angles from a treatment plan expert database, from which 19 selected beam angles (5 noncoplanar and 14 coplanar). Next, the planning structures and initial objective function parameters are set up based on planners' segmentation. After, an optimisation of the objective function parameters is made by the algorithm based on dose constraints, for instance, the mean lung dose constraint of no more than 22 Gy for lung cancer cases. The parameters regarding OARs could be changed during the process depending on the objective values of the current solution. Then, a ranking of the 19 beams shows the 11 best beams to be selected. These 11 selected beams will be used in the treatment plan. Lastly, the authors demonstrated that their new methodology could generate treatment plans that were better or, at least, no worse than the plans designed manually by planners in a consistent way, improving the quality and consistency of IMRT treatment planning for lung cancer.

The autoplanning solution mCycle uses an *a priori* multicriteria optimisation algorithm called Erasmus-iCycle, that was first developed and implemented in the Erasmus MC Cancer Center Institute, and, at the time, this algorithm needed to be converted to Monaco plans to generate clinical plans [45], [72]. More recently, this algorithm was implemented, for example, into Monaco TPS (Elekta AB, Stockholm, Sweden) [72], [73]. Actually, according to Meyer et al. [72], studies show that mCycle plans are considered better than manual plans in 75% of cases. In multicriteria opimisation approaches the objective is to generate a Pareto optimal treatment plan, meaning that no other plan should exist where all the objectives could be simultaneously improved (improvement in one objective must come at the expense of another objective). Erasmus-iCycle relies on a set of cost functions categorised as hard constraints or planning objectives with assigned priorities and goal values, which compose the wish-list that defines the protocol for automated plan generation, where the established constraints are never violated, and goal values are met as close as possible considering the constraints and ascribed priorities [75]. So, planning objectives are optimised sequentially based on their priorities while never violating the imposed constraints [75]. To ensure that the previously achieved function value is preserved while minimising lower-priority objectives, a new constraint is introduced to the optimisation problem following each objective function optimisation [75]. Wish-lists are treatment site-specific and developed through an iterative tuning process in collaboration with the treating physician [75].

Since 2012, the multicriteria treatment planning system Erasmus-iCycle has been clinically used for intensity-modulated photon RT and VMAT in its founding institution [76]. For proton beam scanning and IMPT optimisation, Erasmus-iCycle has already been used in several studies (and is still scarce), but clinical validations are still lacking [76].

In 2020, Bijman et al. [75] developed an automated treatment planning workflow for assessing patient-specific trade-offs between several treatment aims, using a set of treatment plans with a priori defined different balances. This study was led for fifty prostate cancer cases, where all treatment plans were automatically generated using Erasmus-iCycle [75].

Later, in 2021, Schipaanboord et al. [77] proposed a fully automated multicriterial optimisation (AUTO MCO) treatment planning for 2 MLC-based robotic RT and validated it for prostate SBRT

by comparison of the generated automated plans with high-quality, manually generated reference plans. This was the first fully independent system that generated deliverable plans integrating automated non-coplanar BAO, FMO, and segmentation all together [77]. In this novel treatment planning solution, plan generation was performed using Erasmus-iCycle for pencil-beam-based FMO and BAO, followed by MLC segment generation aiming at close reproduction of pencil-beam optimised 3D dose distributions (AUTO MCO 3D) while taking into account every potential beam at once, instead of replicating the fluence maps [77]. Moreover, a stand-alone version of the clinical dose distribution engine is employed to accurately calculate all pencil-beams, segment dose depositions, and final dose distributions [77]. This new automated optimisation workflow ensured high-quality treatment plans while reducing planning workload and time constraints compared to manual planning with the commercial TPS [77].

Additionally, the recent introduction of linacs coupled with MRI scanner, such as the MR-Linac treatment units, has made an increase in the demand for high-quality treatment plans, generating the need for faster and more accurate planning [73], [78]. In MR-Linac, the translational shifts can be corrected, as well as all interfraction setup errors, such as translations, rotations, and organ deformations that appear on the MRI scan and are translated into the daily recontoured PTVs and OARs, which can be corrected by reoptimisation starting from the fluence map [73], [78]. Due to these unique characteristics and the design of these treatment units, some treatment planning challenges arise in comparison to conventional treatment [73], [78]. With this in mind, Bijman et al. [78] developed a workflow for fully automated multicriterial planning using Erasmus-iCycle for IMRT at MR-Linac for rectal cancer and compared to the manual planning regarding planning workload and time, plan quality, treatment time, delivered monitor units, and dosimetric delivery accuracy. Similarly, for prostate cancer SBRT, Naccarato et al. [73] performed a preliminary plan comparison study of the feasibility of plans generated using mCycle versus expert planner (manual plans) on the MR-Linac.

RapidPlan from Varian is a system that uses patient contours, beam setup, dose prescription, and an associated estimation model to provide DVHs estimations that will be used to generate automatic objectives for planning optimisation [72], [73]. It is an example of a knowledge-based/atlas-based planning solution [72].

RayStation v9B autoplanning is based on machine learning approaches. The machine learning process assigns a dose value to each voxel in this system. Subsequently, the generated dose map is transformed by a “mimicker,” converting the dose distribution into an objective function. The optimisation module then uses this optimised function to ensure deliverability [72].

In 2014, Zarepisheh et al. [79] developed an optimisation model that considered treatment planning optimisation based on the DVH curves of a reference plan. This reference plan can be chosen from a library of clinically approved and delivered plans of previously treated patients with similar medical conditions. A voxel-based optimisation model was used to automatically update an FMO objective function and navigate the dose distribution Pareto surface to approach a plan with similar DVHs to the ones in the reference plane, i.e., voxel weights were iteratively adjusted in order to fit the plan with similar DVH to the reference plan. Ultimately, the authors developed a novel optimisation algorithm capable of automatically adjusting the voxel weights and generating highly efficient clinical optimal plans, improving the plan’s quality and efficiency in automatic treatment planning.

In 2019, Jia et al. [80] developed a treatment planning process that relies on an OAR-3D dose distribution prediction. In this approach, OAR-related constraints that support FMO are

determined by the dosimetric values predicted, which consider all the voxels within an OAR as research subjects, taking their doses as outputs and incorporating individualized geometrical features such as location and volumetric information as inputs. To ensure PTV coverage, this method employs hard constraints utilizing an artificial neuronal network to predict dose distributions for OAR. These predicted distributions are used as objective goals, guiding the current dose distribution to align as closely as possible with the predictions. This framework does not consider BAO, and the FMO objective function is not dynamically updated to account for dosimetric achievements. The results obtained in this study show that this novel automatic optimisation method ensures the output plan quality for IMRT, showing plan quality improvement with PTV dose coverage maintenance and major dose sparing of OARs.

2.3.3. Fuzzy Inference System: concept

In the materials and methods section of this work, the fluence map optimisation will be solved resorting to an automated algorithm that is based on a quadratic programming model (1), with the model parameters being iteratively changed by a fuzzy inference system [56]. This fact motivates this subsection, where the basic behaviour of fuzzy inference systems will be explained.

In 1965, Zadeh [81] founded the mathematical theory of fuzzy sets. This was the first milestone of the introduction of fuzzy sets in the scientific and technological area that, in the last 60 years, made theoretical improvements such as fuzzy logic, fuzzy probability theory, fuzzy topology, fuzzy algebra, and technical progress in application systems, e.g., fuzzy control, fuzzy expert systems, fuzzy clustering and data mining [82]. Thus, fuzzy sets and application systems have become widely known in mathematics, engineering and, more recently, in quantum mechanics and medicine [82].

In the domain of medicine, particularly for RT treatment planning, the application of fuzzy logic techniques has been studied in several aspects, such as parameters optimisation (e.g., [17], [56], [83], [84], [85]), tumour tracking (e.g., [86]), margins' estimation (e.g., [87]), etc.

The fuzzy inference system (FIS) is a reasoning process based on fuzzy logic consisting of three main components: fuzzifier, inference engine, and defuzzifier [83], [84]. It was first developed by Mamdani and implemented in various industrial applications [83].

In Fig. 6 a schematised illustration of FIS main components is presented. First, inputs are represented resorting to membership functions that allow natural language concepts to be represented mathematically [83]. Then, the fuzzifier processes the inputs based on their membership functions [83]. Subsequently, the resulting values from the fuzzifier process are handled in the inference engine, which computes the consequences accordingly to a base of fuzzy rules [83]. Lastly, the defuzzifier converts the consequences into final outputs [83].

Thereby, the behaviour of FIS mainly relies on the components of the fuzzy rules, such as fuzzy sets for both the antecedent and consequent parts of each rule [83]. These fuzzy sets partition different spaces for input and output variables [83]. Thereafter, appropriate functions are established to map input/output spaces to real numbers, which are known as membership values, based on this partitioning [83].

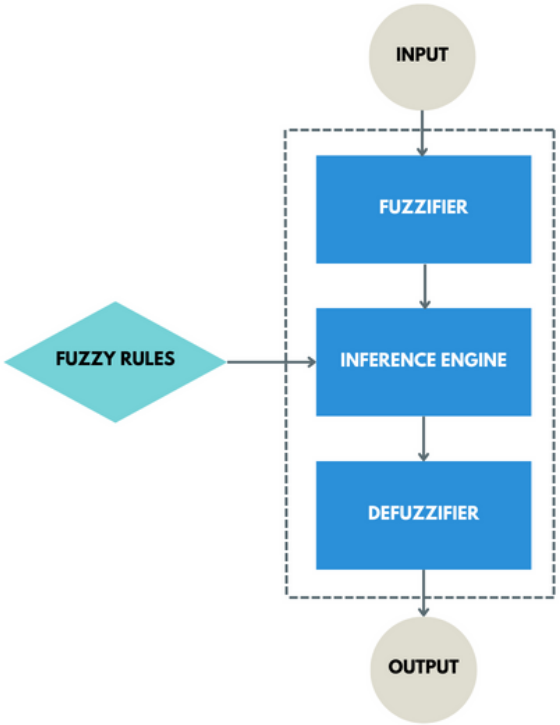

Fig. 6. Simple flowchart of the FIS.

The FIS hereby is developed to perform inference similarly to humans, making it suitable to solve problems as parameter optimisation in inverse planning [84]. With this concept in mind, several authors studied optimisation in RT treatment planning. For example, Yan et al. [84] developed a FIS to guide the optimisation of weighting factors in an inverse treatment planning for IMRT. Similarly, Stieler et al. [83] introduced an automation of the parameter optimisation process for IMRT treatment planning based on a machine learning technique that utilises FIS for function approximation. This technique allowed the automation of parameter optimisation using prior knowledge collected from human planners' trial-and-error processes [83].

Additionally, there are also studies that mix the FIS technique with AI. For example, in Yan et al.[85], the FIS is used to automatically modify and accomplish a compromise between weighting factor, dose specification, and dose prescription parameters in IMRT inverse treatment planning. Meanwhile, the dose distribution is automatically achieved by an AI-guided inverse planning system[85].

As mentioned in section 2.3.2.2, the method described in [56] iteratively changes IMRT treatment planning parameters through a FIS that mimicked the planner's trial and error procedure in an efficient, optimised, and automated way. This FIS method will be used in this dissertation's computational simulations, thus the following section 2.3.3.1 describes it in detail.

All the mentioned studies attempt to help replace or reduce the time spent in the trial-and-error approach led by the planners, testing different combinations of parameters to achieve the best dose distribution possible and, consequently, a better plan's quality. These studies emphasise that fuzzy logic can properly handle this aspect of human knowledge and experience and successfully apply it to inverse treatment planning.

2.3.3.1. Fuzzy Inference System for Automated FMO

As mentioned in the previous section, fuzzy logic is based on fuzzy sets with unclear boundaries, which allows sets of elements to have a degree of membership [56]. The method presented in [56] mimics the reasoning of the human planners when they need to change parameters associated with the fluence map optimisation, by using a set of simple fuzzy rules. Most of the times, if, for a given volume of interest, the dosimetric values obtained with the current plan are close to the desired ones, then the corresponding parameters are only slightly changed. If the dose-volume metrics are far from the desired ones, then substantial changes must be considered.

In this methodology, the natural language concepts used are represented by membership functions that are trapezoidal or triangular. These membership functions will represent concepts like “low”, “medium” or “large”. The percentage of deviation between the prescribed dose and the actual dose received is the input of the fuzzy inference mechanism. The input measures the extent of the constraint violation. The percentage of change in the corresponding bound gives the output. The methodology used is not very sensitive to the shape or the threshold values of the input and output membership functions. The input and output membership functions are connected by a set of fuzzy rules that must be evaluated simultaneously [56].

In this methodology, there are three fuzzy rules as follows: if the deviation is large/medium/low, then the change in the corresponding parameter is large/medium/low. The FIS simultaneously evaluates these rules, and through a defuzzification procedure, a final crisp value is calculated, which is the final output of the FIS [56].

In this case, the FMO model considers a voxel-based convex penalty non-linear model described in (1), where for each structure of interest, the function evaluates the sum of the weighted squared difference between the dose delivered to each one of the voxels belonging to the structure and the lower/upper bounds that have been set for that structure[17], [56].

First, as a standard procedure in treatment planning, a physician outlines constraints that define a dose prescription that must be achieved for the treatment to be considered admissible. In Dias et al. [56], this prescription will give the initialization parameters for the objective function’s upper and lower bounds that define the FMO objective function (see section 2.3.2.2).

In this methodology, the PTVs have both upper and lower bounds, since they are generally associated with both maximum and minimum dose-volume constraints, while OARs only have upper bounds. The parameters that must be defined for FMO, namely lower and upper bounds and also weights, can be considered as steering parameters for the optimisation results since they can be seen as technical tools to guide the optimisation process toward regions where the treatment plan is admissible. This method chooses to change bounds first and only adjusts weights if is strictly needed. According to the authors, changing the bounds first produces a smoother iterative process, that converges faster [56].

The weights are considered to be exactly the same for every voxel belonging to the same volume The initial weights for each structure can be set as being equal to 1. The only exception is if structures are overlapping. In these situations, a greater weight should be assigned to the inner structures because each voxel within the inner structures will belong to more than one structure (the overlapping structures) and possibly have conflicting constraints. Thus, this methodology has a simple initialisation logic for the weights with one exception in the case of overlapping

structures where the relation between the inner and outer structures must be: the smaller the volume, the greater the weight [56].

In its original version, the FIS procedure is organised in two phases. In the first phase, the FIS iteratively changes the parameters associated with all the volumes of interest in order to find a treatment plan complying with all the existing dose-volume constraints [17]. After this admissible plan is calculated, then the approach will still try to improve either PV coverage or OAR sparing, depending on the priorities defined by the user [58], [60]. This second phase of the algorithm continues until no more improved solutions can be found in a determined number of iterations or a global maximum number of iterations is reached [56].

In this work, only the first phase of the method is considered, meaning that the algorithm will stop as soon as a treatment plan complying with all the constraints defined by the medical prescription is found. The main reason that justifies this choice has to do with the fact that the objective is to study the impact of uncertainty in treatment delivery when treatment planning complies with the medical prescription, and bias could be introduced in the analysis and in the comparison of the different treatment plans if treatment planning could be even more demanding than the medical prescription. As an example, being more demanding with a given OAR could bias the result of CTV coverage when uncertainties are explicitly considered, since an extra effort would be made for OAR sparing during treatment plan optimisation.

The flowchart of the described method is presented in Fig. 7.

To the best of our knowledge, this is the first work to use the first phase of the FIS method described above to automate FMO in SBRT treatment planning.

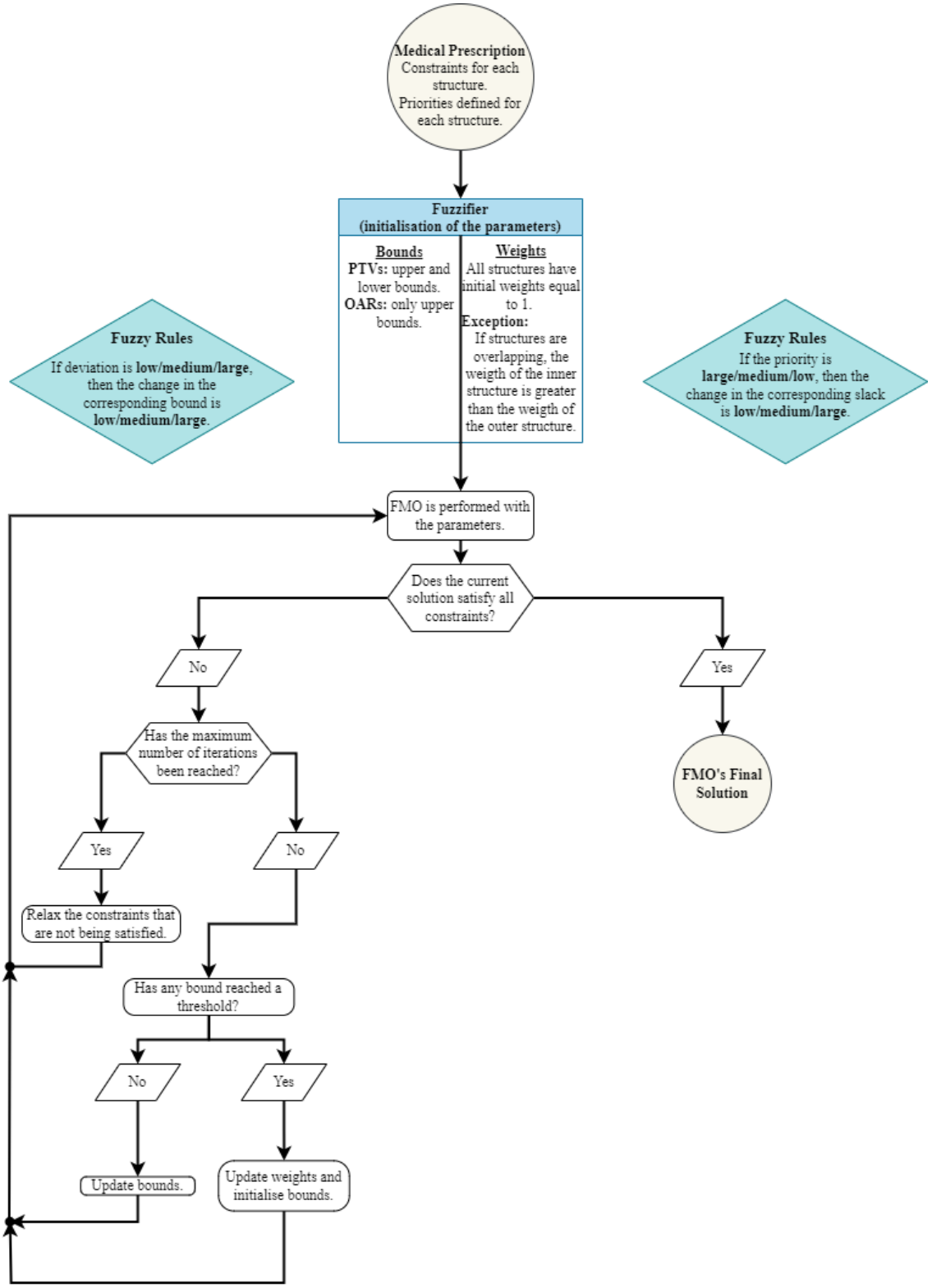

Fig. 7. Flowchart of the first phase of the FIS method for automated FMO.

2.4. SBRT treatment planning

As the focus of this work is to study SBRT treatment, this section will be emphasising the specific properties and characteristics of SBRT treatment.

SBRT is commonly used to treat extracranial malignant or benign tumours and functional or vascular disorders [19]. The joint disease sites where this treatment is used or investigated are the lungs, liver, abdomen, spine, prostate, head-and-neck. For the treatment of inoperable non-small cell lung cancer (NSCLC), SBRT has shown a survival rate of 56% at three years, a high rate of local tumour control (3-year primary control rate of 98% and three-year locoregional control of 87%), and moderate treatment-related morbidity [88]. SBRT achieves excellent results in local control for locally advanced pancreatic cancer (LAPC) [89]. Studies comparing the outcome of SBRT delivered with different technologies, such as VMAT, helical tomotherapy and non-coplanar static fields, have been a research field with conclusions that vary according to the studied organ. In the case of the lungs, VMAT SBRT showed superior conformality and better local control compared to helical tomotherapy and non-coplanar static fields. Despite belonging to the acceptable limit range, toxicity parameters had higher values for helical tomotherapy SBRT than the other two modalities [90]. For cervical and thoracic spine SBRT, the plan quality of VMAT is better than step-and-shot IMRT, with adequate target coverage, comparable delivery accuracy, better conformity and a lower dose to the spinal cord [91].

For SBRT is required MLC with leaf width inferior to 10 mm or cylindrical collimators with an equivalent size. However, in the case of nearby radiation-sensitive critical structures, the leaf width should be inferior or equal to 5 mm or cylindrical collimators of equivalent size and systems allowing non-coplanar beam directions [19]. In respect to treatment unit accuracy, for SBRT, the geometric accuracy with three-dimensional spatial dose placement requires maximum inaccuracies of 1.25 mm in non-moving and 1.5 mm in moving phantoms. In proximity to radiation-sensitive critical structures, the recommended maximum inaccuracies are 1 mm [19].

In SBRT, advanced precision technologies are required for focused planning and delivery of a reduced number of high-dose radiation treatment fractions. Due to these high doses administrated in each fraction, it is crucial for the RT team to be aware of the importance of the dose-volume constraints, particularly concerning normal tissues [92].

Nowadays, most of SBRT is performed using conventional linear accelerators and planned on the same TPS as those used for three-dimensional external beam radiotherapy. However, SBRT is very different from three-dimensional external beam radiotherapy, especially in considerations such as ensuring geometric and dosimetric accuracy [92].

The general treatment planning process for SBRT follows the same path as the one already described in this section. First, there is an imaging study from which the physician defines the GTV. If there is too much target motion, four-dimensional imaging data should also be analysed to define the target motion. These analyses generate the inclusion of the ITV margin to account for the internal motion of the target. Lastly, the PTV must also include an additional margin regarding setup uncertainties [92].

Secondly, the planning physicians or dosimetrists define the anatomical contours of the normal tissue and may add structures to enhance the conformity and gradient of the high-dose volume around the target. Therefore, the target's specific dose and fractionation, as well as the dose and dose-volume limits to OARs near the target, become defined [92].

Thirdly, one or more treatment plans are generated for a single patient, which may use several beam arrangements, including fixed fields, conformal arcs, IMRT, or VMAT delivery. The plans must be generated by optimisation on the basis of the dose constraints requested by the planning physician who is responsible to ensure that target coverage, dose gradient, and normal tissue dose sparing are within acceptable limits. Then, they may suggest revisions to the plan or approve it for patient-specific quality assurance and treatment [92]. Through treatment planning optimisation, it is possible to achieve higher dose conformity around irregular target volumes and a better ability to conform doses away from specific OARs near the target [92].

The steps described regarding the general treatment planning process for SBRT are illustrated in Fig. 8.

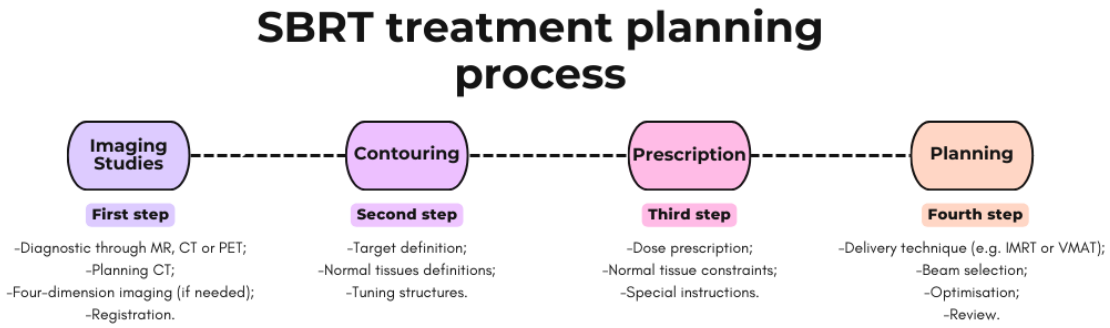

Fig. 8. Schematic illustration of SBRT treatment planning process.

Concerning prostate cancer treatment planning platforms, the use of SBRT techniques have showed to be dosimetric superior with higher dose conformity, higher PTV coverage, and lower doses to adjacent bladder and rectum in lieu of the use of IMRT techniques [92]. Furthermore, flattening-filter-free mode available on linac-based SBRT allowed achieving a reduction in overall treatment time contributing to more patient convenient treatments, although there is less awareness of the radiological implications [92].

Regarding fractionation schemes in prostate cancer SBRT treatment planning, a prospective and multi-institutional analysis of 1 100 patient showed that the most common regimens (89%) consist in the use of 35 to 36.25 Gy in five fractions delivered either daily or every other day [92].

2.5. Robust Optimisation

Treatment errors can be divided into two components: systematic and random. Systematic errors remain constant across all treatment fractions and are typically introduced during treatment planning, such as an extreme position of the prostate in the planning CT scan that differs from the mean position of the prostate. In contrast, random errors vary daily and are associated with daily variations in patient anatomy and setup during fractionated treatments [93].

The most common errors in treatment planning are, for example [94]:

- simulation errors: due to incorrect representation of the patient or the radiation distribution.
- contouring errors: errors due to incorrect segmentation of target or normal tissue.
- plan optimisation errors: for example, incorrect solving of BAO or FMO problems).

- delivery errors: when the treatment delivery differs from representation.

During a RT treatment, both random and systematic uncertainties can occur due to several factors, such as the definition of volumes of interest, image artefacts, patient immobilisation and setup, organ movements between and during treatment sessions, physiological changes, or the process of treatment delivery itself since a machine always has uncertainties. Furthermore, the positions, shapes and sizes of diseased tissue can change during treatment sessions in a way that has not precisely been considered. Moreover, treatment time may cause involuntary internal motion or patient movement, leading to uncertainties. In addition, temporary changes can occur during a treatment, for example, if during prostate cancer therapy, the rectal or bladder fills up, it can create uncertainties in dose delivery [92].

Geometry uncertainties is the name given to changes in the patient geometry, including, for example, the intrafraction and interfraction motion of organs. These geometry uncertainties and uncertainties in dose calculation throughout the treatment are the most prominent reasons for the appearance of setup errors. Dose calculation errors arise from dose calculation algorithms and techniques, i.e., uncertainties in the dose distribution delivered to the patient arise from the potential discrepancies between the dose distribution shown in the treatment planning system and the actually delivered dose [93].

For all the reasons mentioned above, although treatment planning is traditionally based on the medical images acquired at the beginning of the RT workflow, it is clear that these images are not a totally accurate representation of the patient during the whole treatment duration or even during the time period one treatment fraction takes to be delivered.

Thus, it must be recognised that uncertainties will inevitably be part of the treatment delivery and should be explicitly considered during treatment planning [92].

External radiation therapy treatments have uncertainties in treatment planning and delivery that can cause undesirable outcomes and can compromise the benefits of the treatment [95].

The robustness of the treatment plan is defined by the resilience of the intended dose distribution to uncertainties and changes depending on the treatment site, technique, and modality [95].

To mitigate effects of uncertainties regarding dosimetric accuracy delivery, techniques of geometrical margins and probabilistic optimisation have been implemented. Usually, the International Commission on Radiation Units and Measurements recommends a common benckmark of $\pm 5\%$ for dosimetric accuracy delivery in external RT [95].

Regarding the technique of geometrical margins, it consists of implementing safety margins as described in the section 2.3. of this work. The implementation of this margins depends on the treatment technique used and the image guidance schedules. In fact, studies have shown that the modality used for image guidance can change the magnitude of the margin, and advances in image guided RT techniques, such as real-time fiducial tracking and advanced anatomic imaging, have been developed to continuing to improve and adapt margins [95]. The concept of safety margins has its inherent limitations, and according to a report from 2022 about the results of ESTRO 2020 by Kaplan et al. [96], until a few years ago, it was the only universally used method to optimise and evaluate plan robustness. The major assumption of safety margins is called static cloud dose approximation, and it considers that the shape of the spatial dose distribution is unchanged under the influence of errors [96]. This assumption is possibly inadequate for highly modulated photon treatments [95], [96].

Robust Optimisation (RO) has been used to overcome the limitations of safety margins, as well as Robust Evaluation (RE) [96]. These two methods follow the same concept, i.e., RO directly calculates the dose changes induced by simulated scenarios, taking into account patient-specific anatomy and dose distribution characteristics. Meanwhile, RE recalculates and evaluates the optimised dose in a simulated error scenario [96]. It is important to note that the same error distributions to optimise (i.e., RO) and evaluate (i.e., RE) treatment plans may introduce an estimation bias. Thus, it is recommended for those error distributions to be different [96].

The RO follows a different approach from the traditional method (i.e. margins) to achieve target cover and organ sparing [97]. This approach addresses uncertainties explicitly, optimising dose distributions for several scenarios instead of just one [97]. Each scenario represents all the treatment fractions (i.e. a possible treatment course) and must include the specification of all errors that may be present to calculate the final dose distribution. Since in fractionated treatments there is always random setup errors, the use of scenarios in the RO approach includes the setup errors in all individual fractions [97]. Lastly, the final optimised plan considers all the scenarios at once (using worst-case scenario or mini max approach) or a combination of scenarios where each one as a certain probability (using a probabilistic approach) [97].

Several works from the late 1990s showed that RO is a highly successful methodology for solving many types of optimisation problems, such as linear or non-linear problems under data uncertainty [98]. Furthermore, RO was first implemented in a commercial TPS in 2014 for RT [97] and has been routinely used in clinical proton planning with pencil beam scanning ever since [99]. On the other hand, there have been fewer reports on applying RO planning in photon therapy [99].

Regardless of using the traditional method or RO, the RE evaluates the way dose distribution changes in comparison to the nominal dose, offering the possibility of quantifying the uncertainties in DVHs and other dose metrics regarding variations in patient set-up and anatomy [97].

Treatment plan robust optimisation can be translated into different mathematical terms that can be categorised as probabilistic (or stochastic) approaches, which optimises the expected dose distribution, and minimax approaches, which optimises the dose distribution for the worst error considered [93], [97]. A possible and not exhaustive schematic view of robust optimisation approaches to handle uncertainties is presented in Fig. 9.

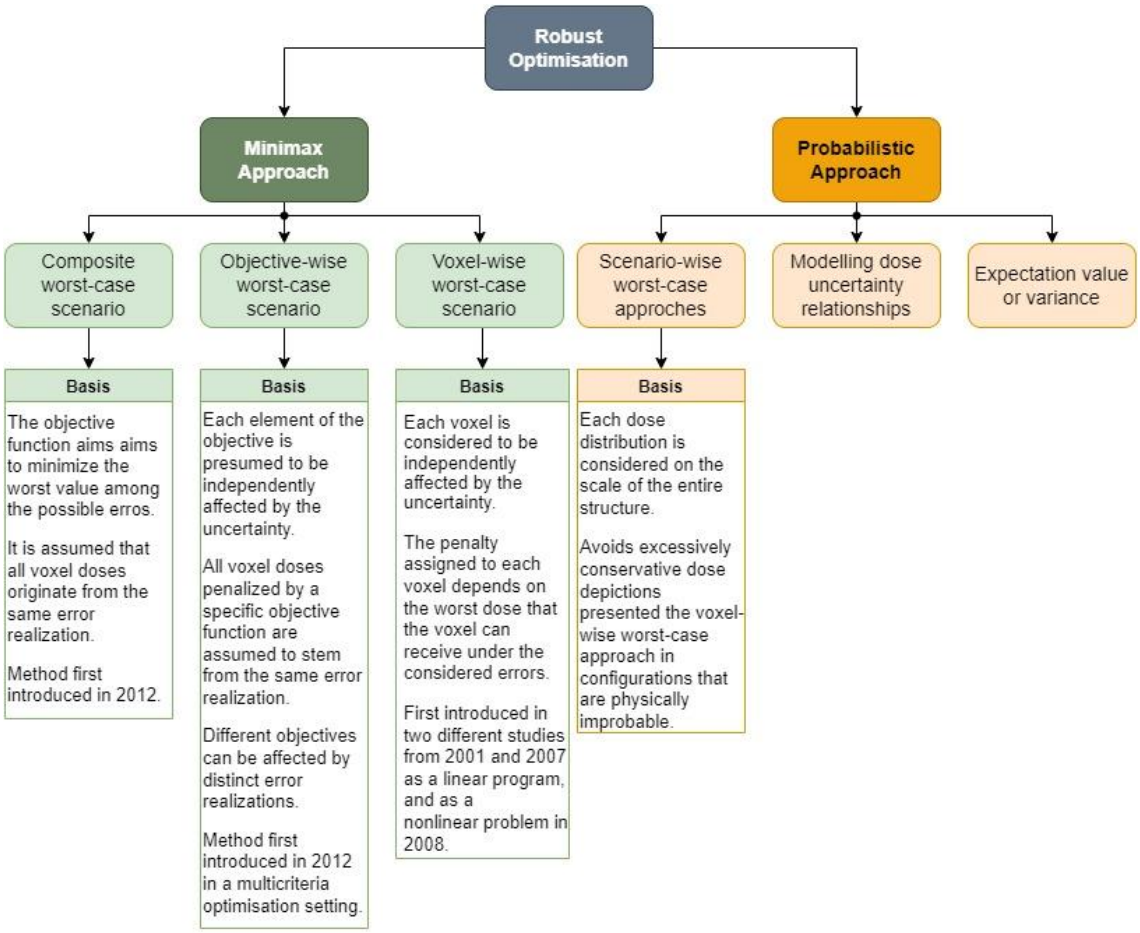

Fig. 9. Schematic view of robust optimisation approaches based on [100] and [95].

The minimax optimisation method aims to minimise the objective function to ensure that the prescription remains valid even under the worst-case scenario (worst error considered possible) [101]. In minimax approaches, the worst-case method can focus on three scenarios: composite worst-case, objective-wise worst-case, and voxel-wise worst-case [97]. The definitions of these three methods are presented in Fig. 9. These three worst-case methods were evaluated, compared, and analysed in a study from 2014 by Fredriksson and Bokrantz [100], and a new technique to examine robust treatment plan optimisation was suggested. This study was evaluated for IMPT robust optimisation concerning treatment planning for prostate subject to systematic setup errors and concluded that none of the three worst-case methods was remarkably superior to the others, all showing different and particular behaviours. Ultimately, the authors recommend making a case-by-case choice guided by each method's pitfalls [100].

Additionally, scenario-based margins are a method for robust planning to handle setup uncertainties, where plan evaluation criteria is optimised over multiple scenarios, incorporating voxel-wise penalties weighted by distribution coefficients [102]. This method works in a way to be mathematically equivalent to the conventional geometric margins when the scenario doses are calculated using the static dose cloud approximation [102].

The probabilistic approaches for plan robustness evaluation are an alternative to margins for handling uncertainties [95]. This technique is used in photon and proton radiotherapy plans, but IMPT has been the primary radiotherapy method for the development of probabilistic robustness analysis techniques, where the dose distribution is determined under several uncertainty conditions [95]. This uncertainty scenarios to ensemble dose can be represented by

approaches such as the voxel-wise worst-case approach, the scenario-wise worst-case approach, or describing the simulation of scenarios according to the expectation value or variance of the delivered dose or using a model relating the dose to uncertainty values [95].

In 2020, Teoh et al. [103] used probabilistic scenarios to make a comparative study of plans sensitivity to setup uncertainties between IMPT and photon VMAT for locally advanced non-small cell lung cancer. This study considered minimax RO and PTV optimised IMPT and VMAT nominal plans [103]. This research showed that setup errors do not influence robustness when analysing the whole treatment, regardless of the planning technique utilized [103]. Nonetheless, VMAT and minimax IMPT plans had superior fraction doses and subsequent excellent target robustness on the fraction level compared to PTV-IMPT plans [103]. Therefore, the authors concluded that VMAT and minimax IMPT plans have comparable sensitivity to setup uncertainties for non-small cell lung cancer. In addition, the probabilistic analysis allowed a fast and practical method to evaluate plan robustness in the different techniques analysed in this study [103].

In summary, it is important to note that there are several methods to quantify treatment plans' robustness [103]. Currently, there has not been a consensus neither for a definition of robustness nor for its ideal assessment metric [103]. Nevertheless, diverse studies have already been conducted regarding several metrics. The common point of all these methods is that they rely on simulating treatment plans under extreme conditions, which has the downside of overestimating errors [103].

2.5.1. Examples of RO techniques for uncertainties management in IMRT

As mentioned above, there are fewer reports about the application of robust planning in photon therapy than in proton therapy. Nevertheless, the concept of examining dose uncertainties for IMRT plans and applying robust planning had been proposed over two decades ago [99]. As a matter of fact, studies from the early 2000s have shown that the RO approach for treatment planning of IMRT provided a more accurate representation of patient's motion and setup uncertainties than traditional methods (such as safety margins) [104]. Consequently, the RO has been suggested to mitigate the effects of breathing motion uncertainty during IMRT treatment planning for breast and lung cancers [105]. For instance, in 2015, Mahmoudzadeh et al. [106] investigated the advantages of applying a RO approach for tangential breast IMRT in treating left-sided breast cancer. The authors' approach focused on optimising the tails of the dose distribution and incorporating dose-volume limits under breathing motion uncertainty [106]. Their study demonstrated that the RO approach had the potential for better heart-sparing in comparison with the clinical method at free-breathing and unravelled a path to potentially reduce the need for breath-hold techniques [106]. One year later, in terms of setup variation, Byrne et al. [107] also studied the potential of RO on breast IMRT, concluding that the achieved RO plan was comparable to other established planning methods when ensuring coverage of breast CTV with variations in patient surface position. Nonetheless, the authors considered that the benefits of RO in ensuring coverage in breast planning outweighted the additional optimisation time required compared to the other planning methods, therefore recommending the RO planning method in clinical use [107]. Miura et al. [108] studied the position dependence between full-arc and partial-arc VMAT techniques for both PTV-based and RO plans. Their investigation demonstrated that RO plans provided better homogeneous dose distribution for peripheral CTV positions than the ones achieved with conventional PTV-based plans [108].

Additionally, in 2018, to test RO in OAR sparing for IMRT treatment plans, Zhang et al. [101] conducted a dosimetric study comparing internal target volume-based RO plans and conventional PTV margin-based plans. This study selected 20 lung cancer patients with tumours at various anatomical regions and generated plans for IMRT and VMAT. The robustness of the generated plans was evaluated through perturbed doses with setup error boundaries from the isocenter. The study showed that RO plans had better target coverage, conformity index, and lower OAR doses than the PTV margin-based plans. Furthermore, the RO plans required fewer monitor units. Thus, the study concluded that RO was a promising approach for planning lung cancer RT.

Recently, in 2024, an approach regarding chest motion in RO treatment planning for chest wall postmastectomy RT was suggested by Myasaka et al. [109], where respiratory movement was considered a setup error. This study analysed 20 patients, created three treatment plans for each case, and compared them (RO plan, planning target volume plan, and virtual bolus plan). The isocenter was shifted to reproduce the chest wall movement pattern, and the doses were recalculated for comparison for each treatment plan. In conclusion, the authors showed that the RO plan demonstrates comparable tumour doses to the planning target volume plan and exhibited robustness for respiratory motion compared to the other two plans. Nevertheless, the RO plan had a slightly higher OAR dose than the other two plans, which leads to a reminder of careful consideration when applied to clinical use. On the other hand, the RO solutions for IMRT have the downside of being overconservative, only optimising for the worst-case scenario, which often is very unlikely to occur and its performance in non-worst-case scenarios is unclear [105]. So, to tackle RO downsides the Pareto RO approach was recently introduced, aiming to have better performance in non-worst-case scenarios than RO solutions, but maintaining the plan outcomes regarding worst-case scenarios [105], [110]. A subtle criticism regarding RO states that by only focusing on the worst-case outcomes, the minimax/maximin criteria may result in multiple optimal solutions, and consequently it may generate Pareto inefficiencies in the decision process [110].

In 2023, a study by Ripsman et al. [105] provided a light Pareto RO method for IMRT for five database left-sided breast cancer patients. It assessed its clinical viability for enhancing average-case plan quality while preserving robustness compared to plans optimised using RO and Pareto RO. The results of this study showed that light Pareto RO allowed increased dose drop-offs while generating high-quality and viable IMRT plans without sacrificing robustness guarantees or non-worst-case performance, which are typical downsides of RO models. This article showed that it is not necessary to lose robustness in order to improve dose conformity in IMRT treatment planning if the light Pareto RO is used.

In Fig. 10, a schematic view of the problems solved by RO planning in IMRT as well as its downsides are presented.

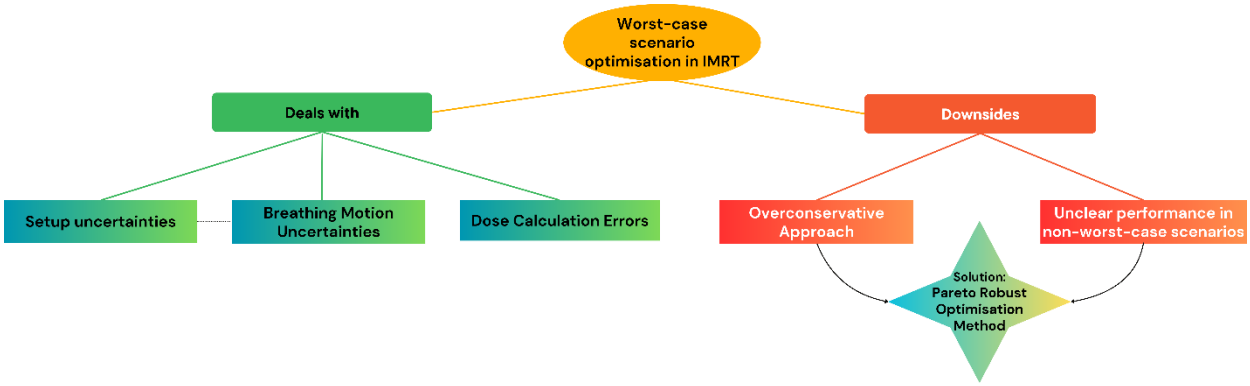

Fig. 10. Schematic illustration of upsides and downsides of Robust Optimisation planning in IMRT based on the information from [105], [106], [109], and [110].

2.5.2. Examples of RO techniques for uncertainties management in SBRT

In SBRT, the targets are irradiated with very large ablative fractionated doses, which makes setup uncertainties a significant issue. Furthermore, there is a cognizant knowledge that, even in systems with rigid immobilisation, there is a geometrical setup uncertainty. This uncertainty in positioning due to internal motion or setup error may affect OARs sparing and PTV coverage [92]. In fact, many automated optimisation routines are available to minimise these uncertainties and handle issues such as small adjustments in treatment cone size or isocenter position to improve target coverage or avoid abutting structures [92]. In terms of treatment plan evaluation, is important to carefully review and analyse both the DVH for parallel organs and the dose displayed on the CT image volume for serial organs to ensure a safe delivery of the SBRT plans [92].

For SBRT, studies regarding RO have been conducted since early 2000s, mainly for liver, lung, pancreas and head and neck cancers. For example, in 2020 a comparison study between RO and planning target volume-based optimised plans for VMAT SBRT concerning treatment plan quality, robustness, complexity and accuracy was conducted by Miura et al. [111] for ten liver cancer patients. This study concluded there was no significant difference between the two optimised plans for doses in CTV and monitor units [111]. However, RO plans showed slightly smaller variations in the CTV doses and lower complexity and position errors than planning target volume-based optimised plans. Thus, RO plans for VMAT SBRT of liver cancer is feasible and can be useful [111].

FMO can be used to account for the setup uncertainties of the delivery dosage, ensuring that the absorbed dose to the target meets the prescription dose, by considering the geometric concept of PTV in SBRT treatment planning [99]. However, in lung cancer, the PTV-based plans for SBRT have been questioned since the PTV contains low-density lung tissue, and margins such as ITV and GTV have been proposed to account for the varying dynamics of the PTV in lung SBRT [99]. Albeit the density issue for the prescribing target is solved, the setup uncertainty issues remain [99]. Thus, in 2019, Liang et al. [99] suggested the first clinical study to explore a RO for lung SBRT planning to simultaneously address the density issue in the ITV-to-PTV margin and the setup uncertainty issue. This study showed that accounting for setup uncertainties in SBRT planning is feasible by comparing PTV-based plans with ITV-based RO plans, where the second exhibited lower normal lung tissue dose, lower intermediate-to-high dose spillage to the body, and lower integral dose while preserving the dose coverage under setup error scenarios [99]. Nevertheless, to ensure the clinical effectiveness of this novel approach, the authors suggest

that further clinical studies must be conducted [99]. Furthermore, within the same year, Beldford et al. [112] studied an alternative to prescribing dose to the ITV while including the effects of positional uncertainties in 4D SBRT for lung. This study demonstrated that employing a robust probabilistic approach to planning SBRT for lung treatments leads to a dose closer to the intended prescription in the ITV than when using a static approach and prescription to the PTV. Notwithstanding this progress, the results obtained from the approaches were very close to each other [112].

Leung et al.[113] analysed the potential of RO to overcome the limitations of PTV for the median dose prescription for lung SBRT. This study intended to provide insights into the combination of SBRT planning concept and prescription method, producing the optimal dosimetric quality and robustness in target and organ dose during treatment. Thereby, the authors tried to improve consistency in dose reporting and multicenter clinical outcome assessment. The conclusions reached showed that both PTV-based plans and RO with worst-case method presented inconsistencies in GTV doses. Additionally, prescription by coverage had a major impact on the consistency of GTV dose, and GTV median dose can effectively decrease the inter-patient and inter-optimisation method variability of the GTV dose.

In 2018, Goddard et al. [114] compared proton and photon-based SBRT dose distributions accounting for uncertainties in target positioning and range uncertainties in order to investigate which was the preferable modality for high-dose hypofraction prostate cancer treatment. This study led to the conclusion that the treatment plans generated with IMPT and VMAT were similar in terms of target coverage, target conformity, and OAR sparing when range and Hounsfield unit uncertainties are disregarded. On the other hand, if these last two uncertainties are taken into account during RO, the VMAT plans outperform the IMPT plans regarding achievable target conformity and OAR sparing.

Chapter 3 Materials and Methods

Considering the review of the literature that was done, this work aims at exploring the impact that uncertainty may have on SBRT treatments namely considering the potential influence of a reduced number of fractions. It aims also to study whether the use of PTV as the main mitigation measure against uncertainty is enough, and if it is capable of guaranteeing a proper CTV irradiation and OAR sparing. Moreover, as most of the robust optimisation approaches consider the use of additional structures and/or worst-case scenario analysis, this work considers a different way of addressing uncertainty, inspired by what is done in decision-making situations under uncertainty in other areas of application. In many other application areas, diversification is a known mitigation measure against the effects of uncertainty. One possible example, among others, of using diversification as a mitigation measure can be observed in the optimisation of financial investments, where choosing a diversified set of financial assets with different characteristics is known to reduce risk. This follows a Portuguese saying: "do not put all eggs into the same basket". Actually, diversifying investments, resources, or options has the potential to mitigate overall risk, rather than concentrating everything in a single option. This helps protect against losses from any one option failing. In this work, instead of considering treatment plans that are kept constant throughout the total treatment duration, a diversified treatment approach is tested where a different treatment plan is considered for each treatment fraction.

Two computational experiments were set. In a first computational experiment, to assess the potential impact of the small number of fractions in SBRT treatment regarding the inherent uncertainty that exists, namely in terms of patient positioning, IMRT treatments with varying numbers of fractions are considered and assessed explicitly taking uncertainty into account. In these first experiments, different number of irradiation directions are also tested, to understand if the number of beam angles can have an influence on the impact of uncertainty. Our hypothesis was that a higher number of fractions would contribute to decrease the impact of uncertainty, meaning that special care must be taken when planning SBRT treatment plans due to the reduced number of fractions. We also hypothesised that an increased number of beams would result in more robust treatment plans.

In the second computational experiment, we consider prostate cancer cases to test the diversified treatment planning approach. A total of five cases were considered as a proof of concept, considering SBRT treatments with five daily fractions.

All the computational simulations conducted were performed using matRad, an open-source software for radiation treatment planning of intensity-modulated photon, proton, and carbon ion therapy [115]. This software was developed for academic purposes and is entirely written in MATLAB [115]. It mimics the behaviour of a clinical TPS. It allows us to develop our own algorithms and to include them both for treatment planning and treatment assessment. All the work developed in this dissertation was programmed in MATLAB, version R2023b, and incorporated in matRad.

The entire statistical analyses were performed using IBM® SPSS® Statistics software, version 29.0.0.0.

3.1. Preliminary Study: studying the impact of uncertainty when varying the number of fractions and the number of irradiation directions

In this first computational study, a case of head-and-neck cancer was chosen to analyse the impact of the number of beams and fractions in a RT treatment plan robustness with intensity-modulated photons. The justification for the use of a head-and-neck case when the final objective is to test robust approaches for prostate cancer treatment plans has to do with the expected behaviour of the treatment plans in both cases. It is expected that impacts derived from the use of different sets of beam angles are more noticeable in a head-and-neck case that, most of the time, require 5 to 11 beams than in a prostate case that seldom is treated with no more than 5 angles.

3.1.1. Materials

This preliminary study used a head-and-neck cancer case available in the matRad examples library.

Since head-and-neck cancer cases have several OARs, their treatment planning procedure is usually very complex. This complexity makes these cases ideal subjects for studying the impact of angles in RT treatment planning.

In this cancer case, seven structures were considered: brainstem, left and right parotids, skin, spinal cord, PTV63 and PTV70. The first five structures mentioned are OARs, while the last two are PTVs. In this case, one PTV has a medical prescription of 63 Gy and the other 70 Gy, named PTV63 and PTV70, respectively.

Also, a variety of dose metrics were contemplated, namely D_{98}, D_2, D_{mean}, and D_{max}, in order to ensure the dose prescription is delivered effectively. Prescribed and tolerance doses considered in this study are presented in Table 1 (based on [56]).

Table 1. Prescribed and tolerance doses for a head-and-neck cancer patient in the preliminary study.

Structure	Dose constraints (Gy)	
Brainstem	$D_{max} \leq 54$	
Left Parotid	$D_{mean} \leq 26$	
Right Parotid	$D_{mean} \leq 26$	
PTV63		$D_{95} \geq 61.7$
PTV70	$D_{max} \leq 74.9$	$D_{95} \geq 68.6$
Skin	$D_{max} \leq 80$	
Spinal Cord	$D_{max} \leq 45$	

As can be seen in Table 1, in this cancer case, two distinct structures were considered as PTVs, each one with a different dose prescription level. The PTV70 has the higher prescribed dose (70 Gy) while the PTV63 has the lower prescribed dose (63 Gy). The considered OARs are the ones that can be significantly affected by RT treatments, and that determine the main compromises that must be made between sparing of OAR and proper irradiation of the PTVs. Besides these structures, the skin is treated as a unique structure and refers to the remaining surrounding healthy tissue. All the delineated structures considered in this computational test are presented in Fig. 11.

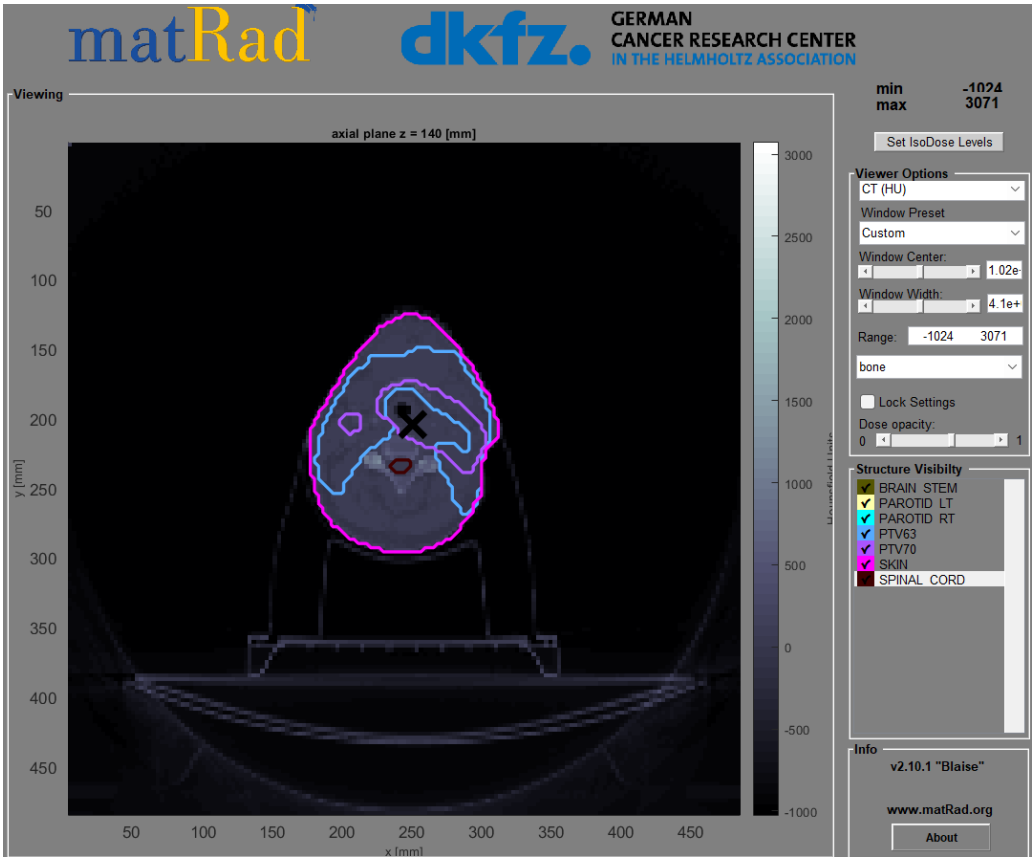

(a)

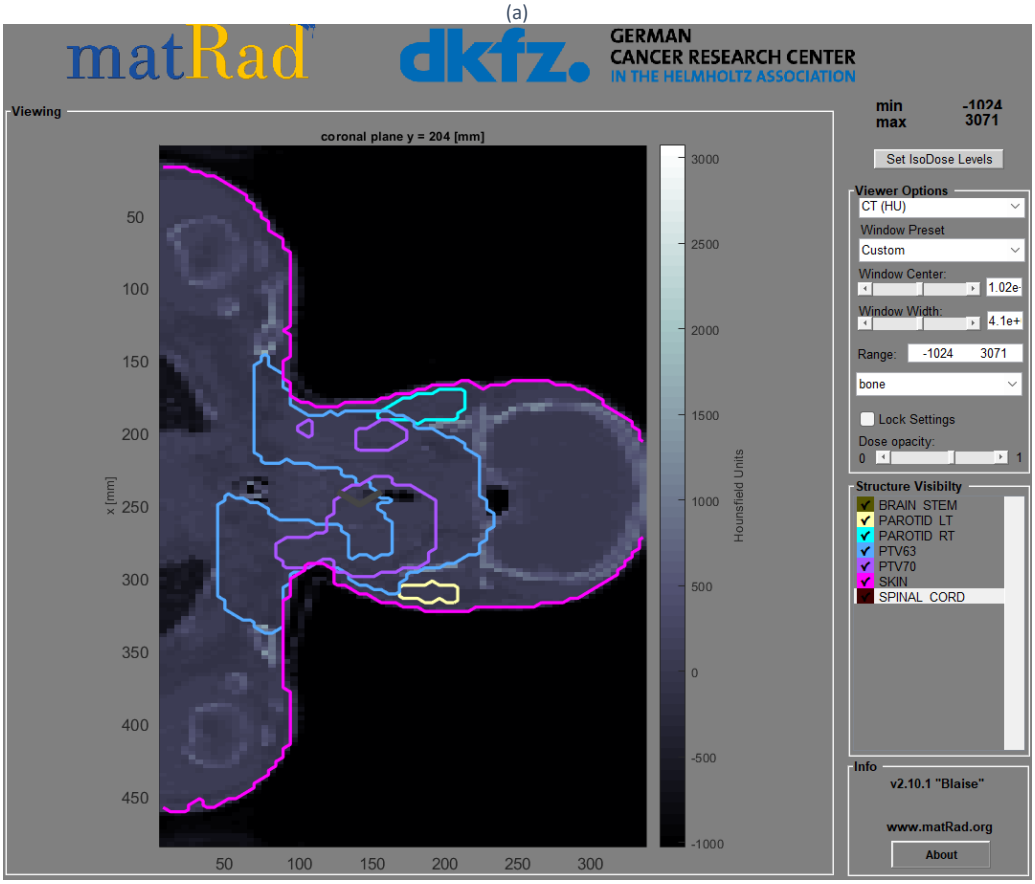

(b)

Fig. 11. Display of the delineated structures in the preliminary study computational test in matRad GUI from the planes: (a) axial, (b) coronal.

3.1.2. Methods

In order to understand the impact of uncertainty when a different number of irradiation directions is used, treatment plans with five, seven, and nine coplanar equidistant beam directions were considered. The iterative algorithm developed in [56] and described in section 2.3.2.2 was used in this computational simulation to solve the FMO problem automatically. As already explained, only the first phase of FIS is used. Therefore, in this study, the weights and bounds are automatically changed for both PTVs and OARs until an admissible plan is achieved, complying with all the constraints defined by the medical prescription.

The initial values of lower and upper bounds and weights for each structure were given following the results in [56] and are shown in Table 2.

Table 2. Initial parameters for each structure's bounds and weights used in the preliminary study.

Structure	Bound		Weight	
	Upper	Lower	Upper	Lower
Brainstem	54	0	5	5
Left Parotid	26	0	1	1
Right Parotid	26	0	1	1
PTV63	68	59.85	5	5
PTV70	75	66.5	5	5
Skin	80	0	1	1
Spinal Cord	45	0	5	5

The initial parameters (weights and bounds) of the initial FMO model do not affect the quality of the final solution once the FIS adjusts them. Nevertheless, according to [17], considering this initial set of parameters reduces computational time to yield an acceptable clinical treatment plan.

As equidistant coplanar beam sets are the most commonly used in clinical practice, this simulation tested three different sets of equidistant coplanar angles with five, seven, and nine beam directions. Thereby, this study used the following sets:

- 9 angles: 0°, 40°, 80°, 120°, 160°, 200°, 240°, 280°, 320°.
- 7 angles: 0°, 52°, 103°, 154°, 205°, 256°, 307°.
- 5 angles: 0°, 72°, 144°, 216°, 288°.

The treatment plan calculated for each one of the three sets of angles was evaluated through Monte Carlo simulations. These simulations allow the analysis of the dosimetric results obtained when uncertainty is explicitly considered.

In this case, Monte Carlo simulations were performed for each one of the three sets of angles with 50 iterations. Moreover, to understand the impact of the number of fractions, 1, 3, 5, 10, and 15 fractions are considered.

Uncertainty in treatment delivery can cause deviations between the planned and delivered dose distributions. In the Monte Carlo simulations, only positioning uncertainties are being considered, modelled as random variables following a normal distribution. The evaluation of each plan involved generating 50 scenarios, each comprising the defined number of fractions to represent the entire treatment duration. This approach allowed for the inclusion of both setup and daily positioning errors. Positioning uncertainties were simulated by shifting the isocenter position, assuming a normal distribution with a mean of zero and a standard deviation of 2.5

mm [116]. To ensure realistic scenarios, the maximum allowable positioning deviation was set to 5 mm [117].

Also, four dosimetric indicators of interest were calculated for each iteration of the simulation, namely $D_{\max}$, D_{mean}, D_{98}, and D_2. These dosimetric indicators were calculated considering the dose deposited in each one of the voxels of the respective structures during each one of the treatment fractions. Lastly, a DVH for all the structures was created for all the iterations.

The Monte Carlo simulations generate data that were analysed statistically. The comparison between means was made with ANOVA tests, while the comparison of variances used Levene's tests.

The statistical tests can be divided into two parts. First, the means and variances of the different fractions were compared for the same number of beam directions, considering D_{98} for PTV70, $D_{\max}$ for the spinal cord, and D_{mean} for the right parotid, the structures more demanding for this particular case. Secondly, the means and variances of the different beam directions were compared for the same number of fractions, considering D_{98} for PTV70, $D_{\max}$ for the spinal cord, and D_{mean} for the right parotid.

The results obtained from the statistical analysis are further explored in Chapter 4.

3.2. New approach for SBRT treatment planning and delivery

The preliminary study can help us to acknowledge that uncertainties have a greater impact when the number of fractions decreases and that an increased number of irradiation directions would result in more robust treatment plans. The main preliminary hypotheses of this dissertation can support the need for special care when planning SBRT treatment plans. Therefore, new approaches for reaching SBRT treatment plans that behave well under uncertainty are of the utmost importance.

In this computational study, a new approach for reaching plan robustness in SBRT is tested. The new approach consists of changing the treatment plan in each one of the different treatment fractions. In other words, the set of treatment plan angles used in each daily treatment fraction is changed, so there are five sets of angles to use in five fractions of a SBRT prostate cancer treatment.

This study intends to evaluate whether or not a diversification strategy, accomplished by the change of plans in each fraction, contributes to increase treatment plan robustness. To accomplish that, the new approach will be compared with the results obtained when just one of the plans is used throughout the whole treatment.

3.2.1. Materials

This study used five different prostate cancer cases, available in the MATLAB library of cases and also taken from the "Fully Automated Radiotherapy Treatment Planning Challenge" [118].

The medical prescription considered was the same for all cases. The structures considered were rectum, left and right femoral heads, bladder, body, CTV, and PTV. The first five structures mentioned are OARs, while the last two are volumes to treat. PTV represents the usual volume to treat planning structure, that tries to account for uncertainty. CTV will be used when assessing the quality of the treatment plans under uncertainty, since the definition of the PTV tries to guarantee that the CTV is properly irradiated during treatment deliver. CTV is also going to be

assessed considering homogeneity, which is a common concern in SBRT treatment planning. Table 3 presents the medical prescription.

Table 3. Prescribed and tolerance doses used for prostate cancer cases.

Structure	Dose constraints	
Rectum	$D_{50} \leq 20$ [Gy]	$D_{90} \geq 36$ [Gy]
Right Femoral Head	$V_{20} \leq 0.065$ [%]	
CTV	$D_{max} \leq 36.8$ [Gy]	$D_{98} \geq 35$ [Gy]
PTV	$D_{max} \leq 42$ [Gy]	$D_{95} \geq 34.3$ [Gy]
Bladder	$D_{max} \leq 42$ [Gy]	$D_{50} \leq 20$ [Gy]
Body	$D_{max} \leq 42$ [Gy]	
Left Femoral Head	$V_{20} \leq 0.065$ [%]	

To exemplify the delineation of all the considered structures, Fig. 12 depicts the structures for one of the prostate cancer cases.

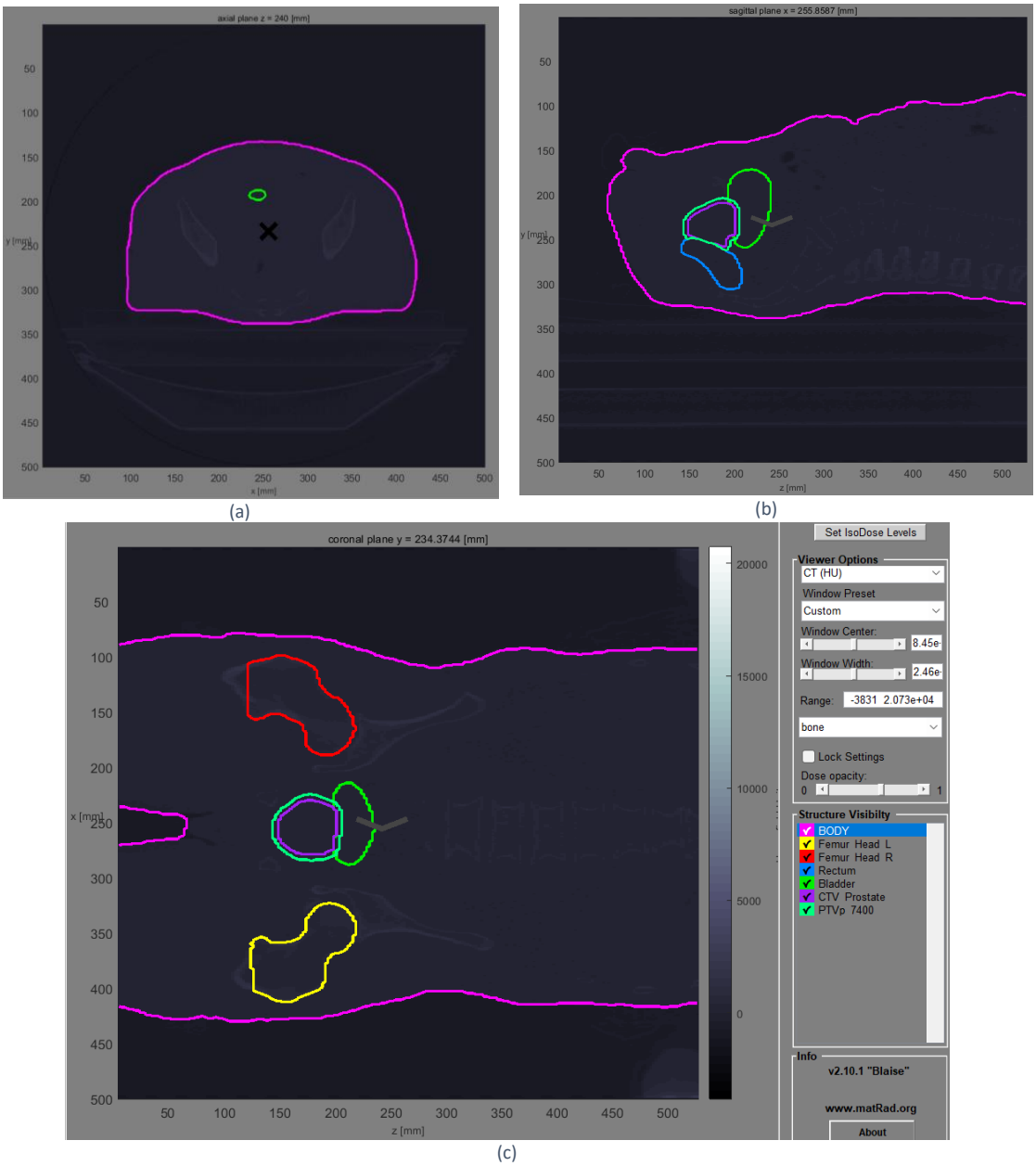

(a) (b) (c)

Fig. 12. Delineated structures for one prostate cancer case from the viewing planes: (a) axial; (b) sagittal; (c) coronal.

3.2.2. Methods

For each one of the cases, five treatment plans considering five equidistant angle configurations were automatically calculated using the same FIS-based FMO procedure already described.

Table 4 presents the initial values of lower and upper bounds and weights for each structure used in the new approach.

Table 4. Initial parameters for each structure's bounds and weights used in the new approach.

Structure	Bound		Weight	
	Upper	Lower	Upper	Lower
Body	30	0	5	1
Left Femoral Head	0.05	0	5	1
Right Femoral Head	0.05	0	5	1
Rectum	20	0	5	5
Bladder	20	0	50	100
CTV	35	35	250	2000
PTV	35	35	250	2000

Then, Monte Carlo simulation with 50 iterations was used so that six different treatment delivery alternatives are compared: each one of the five equidistant angle configurations are tested, with the treatment plan being always the same during the whole treatment; a new approach where in each day a different treatment plan is delivered. This means that in day 1, the treatment plan using the first equidistant angle configuration is delivered, in day 2 the treatment plan using the second equidistant angle configuration is delivered, and so on until day 5 (last fraction).

The five equidistant angle configurations are:

- Plan 1: 0°, 72°, 144°, 216°, 288°;
- Plan 2: 14°, 86°, 158°, 230°, 302°;
- Plan 3: 28°, 100°, 172°, 244°, 316°;
- Plan 4: 42°, 114°, 186°, 258°, 330°;
- Plan 5: 56°, 128°, 200°, 272°, 344°.

It is important to note that, for each cancer case, in order to be able to compare the six treatment plan approaches, the random number series that are used in the Monte Carlo simulations are exactly the same for each case. This is to assure that any differences that are found are not due to differences in the random number generation.

For each case and approach to be tested, 50 iterations where considered, with each iteration corresponding to a whole treatment (5 fractions).

In each iteration, eight dosimetric indicators of interest were saved, namely $D_{\max}$, D_{mean}, D_{98}, D_{95}, D_{90}, D_{50}, D_2, and V_{20}. These dosimetric indicators were calculated considering the dose deposited in each one of the voxels of the respective structures during each one of the treatment fractions.

The statistical analysis consisted of calculating the mean value of each dose constraint and dose homogeneity index for each structure. As each patient is only treated once, considering the total number of fractions that constitute the treatment, it is also important to understand how many times, out of the 50 treatments simulated, are the medical prescription constraints being respected.

The results obtained from the analysis made are detailed in Chapter 4.

Chapter 4 Results and Discussions

This chapter will present the main results obtained through the computational experiments made and will also discuss these results.

All the values in this chapter's tables have been rounded according to the following rule: the values should be presented with four significant figures. Furthermore, for rounding purposes, when the final digit is exactly 5, the preceding digit is only incremented if it is an odd number.

4.1. Preliminary Study: studying the impact of uncertainty when varying the number of fractions and the number of irradiation directions

The impact of the number of fractions was assessed considering a fixed angle configuration and using Monte Carlo simulation. An equidistant five angle configuration was chosen. Fig. 13 depicts the results obtained considering 50 Monte Carlo iterations.

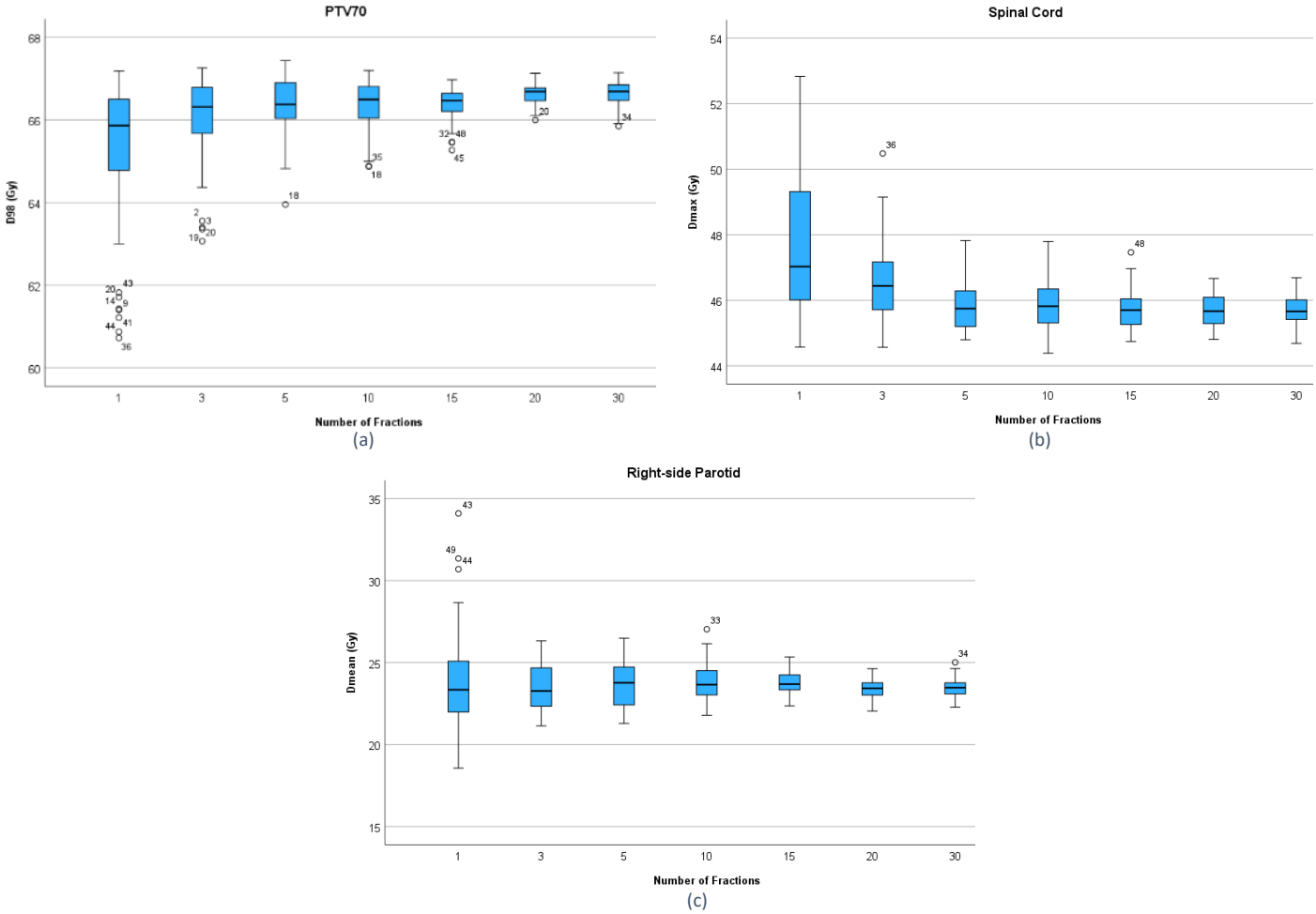

Fig. 13. Boxplots of the dosage values considering a fixed 5-angles configuration for each number of fractions for (a) PTV 70, (b) Spinal cord, (c) Right-side parotid.

From the observation of Fig. 13, it is clear that an increase in the number of fractions decreases the range of dosimetric measures obtained for the three structures considered. This range can be considered as a metric of robustness: a smaller variance in these values show a better behaviour under uncertainty, so it corresponds to more robust treatment plans. There are significant differences between the means for the PTV70 and the Spinal Cord ($p<0.001$) where

more fractions imply better results. There are significant differences between the variances for all structures ($p<0.001$) where more fractions imply also better results, i.e., more robust.

A descriptive analysis was made for each one of the three structures, allowing for the knowledge of the variation of the standard deviation and 95% confidence intervals for the dosage for each number of fractions. These values are compiled in Table 5.

Table 5. Descriptive statistics of the dosage values considering a fixed 5-angles configuration for each number of fractions for PTV 70, Spinal cord and Right-side parotid.

Structure	Number of Fractions	Standard Deviation	Standard Error	95% Confidence Interval for Mean	
				Lower Bound	Upper Bound
PTV 70	1	1.847	0.2612	64.72	65.77
	3	1.061	0.1500	65.70	66.30
	5	0.6837	0.09669	66.16	66.55
	10	0.6039	0.08541	66.18	66.52
	15	0.3922	0.05546	66.26	66.48
	20	0.2424	0.03428	66.56	66.70
	30	0.3223	0.04558	66.54	66.72
Spinal Cord	1	2.418	0.3419	47.14	48.52
	3	1.214	0.1716	46.22	46.91
	5	0.8336	0.1179	45.61	46.08
	10	0.7047	0.09966	45,64	46,04
	15	0.5266	0.07447	45.56	45.86
	20	0.5091	0.07200	45.58	45.87
	30	0.4268	0.06036	45.59	45.84
Right-side Parotid	1	3.190	0.4512	23.00	24.81
	3	1.316	0.1862	23.09	23.84
	5	1.408	0.1992	23.28	24.08
	10	1.104	0.1561	23.52	24.14
	15	0.7924	0.1120	23.56	24.02
	20	0.5923	0.08377	23.28	23.61
	30	0.5572	0.07881	23.30	23.62

As mentioned in the introduction of this chapter, the second part of this study's data consisted of fixing the number of fractions and varying the number of angles. Thus, the boxplots in Fig. 14 show the dosage variation as a function of the number of angles for the three studied structures when the treatment plan uses fifteen fractions. Equidistant angle configurations are being considered, beginning at 0^{o}.

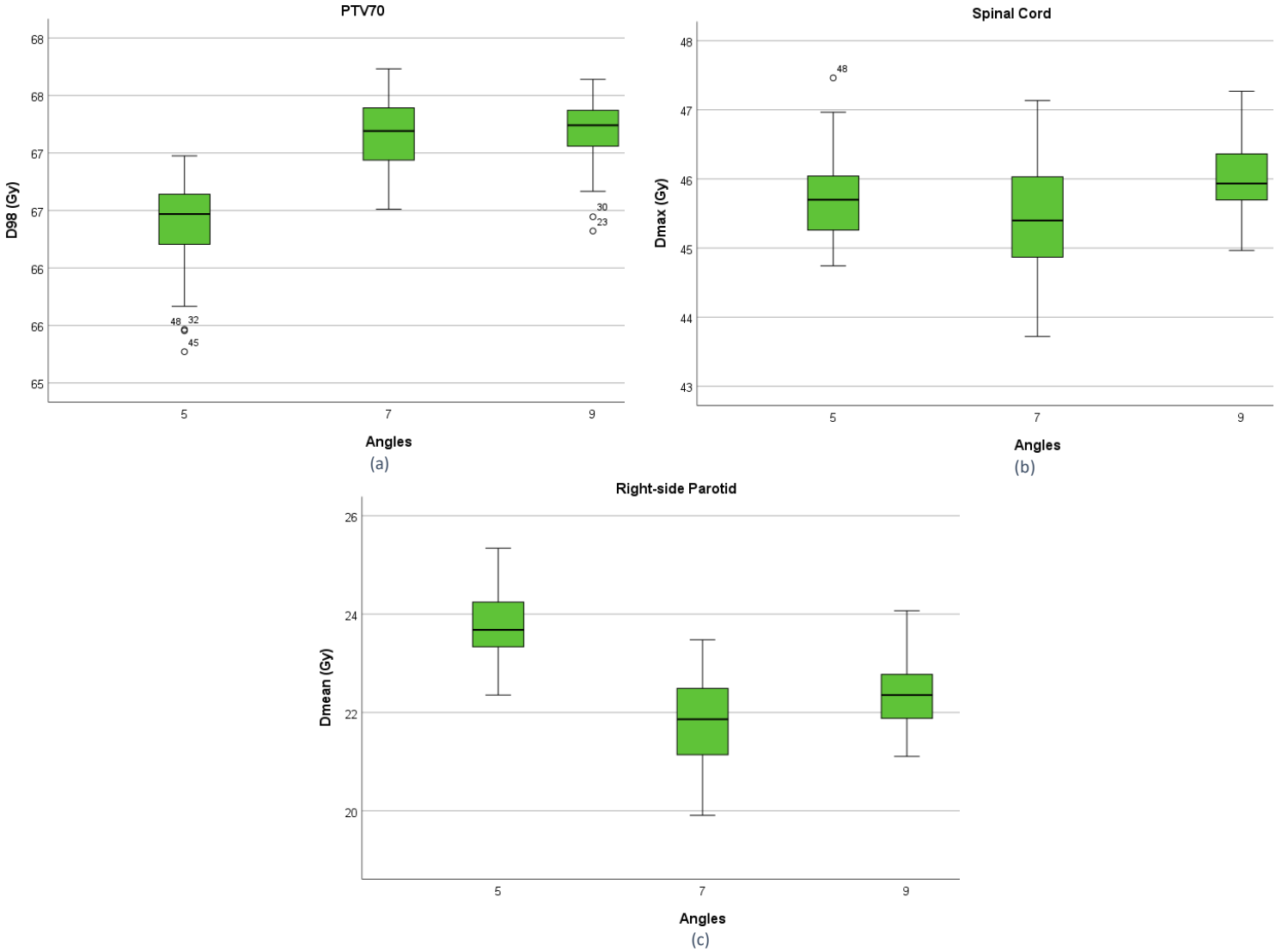

Fig. 14. Boxplots for fifteen fractions of the dosage values for each number of angles for (a) PTV 70, (b) Spinal cord, (c) Right-side parotid.

From the observation of Fig. 14, it is clear that an increase in the number of angles improves target coverage but not necessarily organ sparing. There are significant differences between the means for the PTV70 ($p<0.001$), the Spinal Cord ($p<0.001$) and the Right-side Parotid ($p<0.01$) where more angles imply better target coverage but not necessarily better organ sparing. There are significant differences between the variances only for spinal cord ($p<0.001$).

A descriptive analysis was made for each one of the three structures, allowing for the knowledge of the variation of the standard deviation and 95% confidence intervals for the dosage for each number of angles. These values are compiled in Table 6.

Table 6. Compilation of the values obtained for each structure's angles for fifteen fractions of the standard deviation, standard error, and 95% confidence interval.

Structure	Number of Angles	Standard Deviation	Standard Error	95% Confidence Interval for Mean	
				Lower Bound	Upper Bound
PTV 70	5	0.3922	0.05546	66.26	66.48
	7	0.2988	0.04226	67.10	67.27
	9	0.2829	0.04000	67.12	67.28
Spinal Cord	5	0.5266	0.07447	45.56	45.86
	7	0.7999	0.1131	45.20	45.66
	9	0.5284	0.07472	45.86	46.16
Right-side Parotid	5	0.7924	0.1120	23.56	24.02
	7	0.8478	0.1199	21.54	22.02
	9	0.7362	0.1041	22.13	22.55

Lastly, this study also assessed the variation in the delivered dosage as a function of the number of angles for the three studied structures when the treatment plan uses five fractions. This examination was conducted to support the results of the second examination. The obtained results are compiled in Fig. 15.

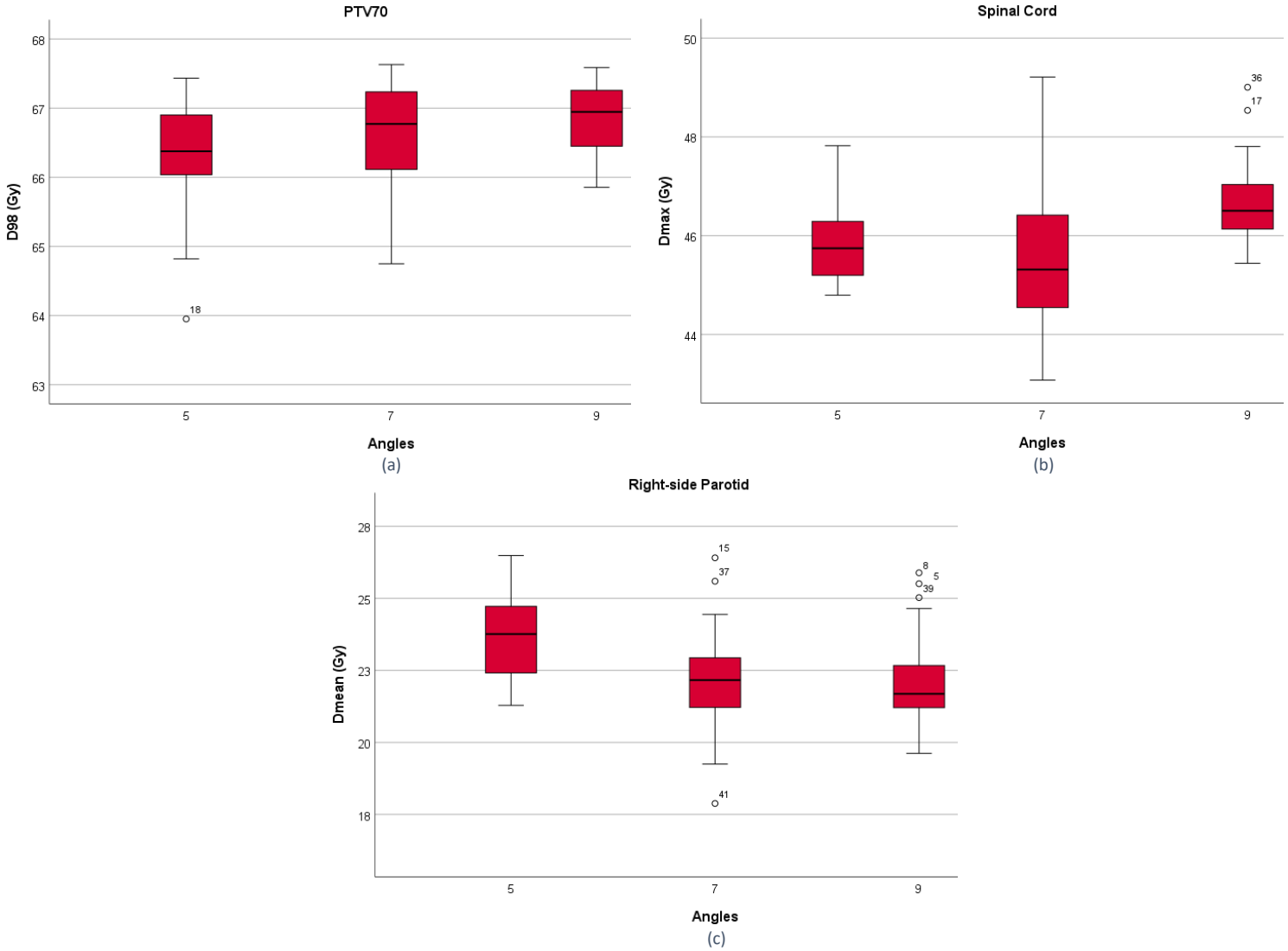

Fig. 15. Boxplots for five fractions of the dosage values for each number of angles for (a) PTV 70, (b) Spinal cord, (c) Right-side parotid.

From the observation of Fig. 15, it can be seen that an increase in the number of angles decreases the range of dosimetric measures obtained for the three structures considered, in particular for spinal cord that shows significant differences between the variances ($p<0.001$) where more angles imply better results, i.e., more robust. There are significant differences between the means for the PTV70 ($p<0.001$), the Spinal Cord ($p<0.001$) and the Right-side Parotid ($p<0.01$) where more angles imply better target coverage but not necessarily better organ sparing.

Then, a descriptive analysis was made for each one of the three structures, allowing for the knowledge of the variation of the standard deviation and 95% confidence intervals for the dosage for each number of angles. These values are compiled in Table 7.

Table 7. Compilation of the values obtained for each structure's angles for five fractions of the standard deviation, standard error, and 95% confidence interval.

Structure	Number of Angles	Standard Deviation	Standard Error	95% Confidence Interval for Mean	
				Lower Bound	Upper Bound
PTV 70	5	0.6837	0.09669	66.16	66.55
	7	0.7046	0.09965	66.42	66.82
	9	0.4892	0.06919	66.72	67.00
Spinal Cord	5	0.8336	0.1179	45.61	46.08
	7	1.528	0.2162	45.17	46.04
	9	0.7716	0.1091	46.38	46.82
Right-side Parotid	5	1.408	0.1992	23.28	24.08
	7	1.655	0.2341	21.64	22.58
	9	1.372	0.1940	21.71	22.49

Thereby, with the two statistical test results and the observation of both Fig. 15 and Table 7, it is possible to state that results are in line with the results obtained for fifteen fractions.

In summary, the initial hypothesis was corroborated since the first study results showed that increasing the number of fractions leads to higher robustness and reveals better or equal sparing. Thus, the impact of uncertainties decreases when the number of fractions increases.

Regarding the second hypothesis, increasing the number of angles does not always result in more robust treatments. For the PTV70, increasing the number of angles led to better structure coverage and equal robustness. On the other hand, the results for the OARs do not present a specific relation between the increase in the number of angles and the increase in robustness or sparing. This may mean that as important as the number of angles used is what are the irradiation directions chosen.

Therefore, the results obtained from these examinations support the need for novel treatment planning robust approaches when a reduced number of fractions (and angles) is used.

4.2. New approach for SBRT treatment planning and delivery

Five different prostate cancer cases were considered to understand the importance of uncertainty and its impact on the quality of the treatment delivered. For each one of these cancer cases, five treatment plans were created, all of them complying with the medical prescription. Each one of these plans considered a different equidistant five angle configuration.

These five plans were compared with a different approach that tested the role of diversification as a measure to deal with uncertainty. In this new approach, a different plan is considered in each fraction: five fractions will be delivered with five different treatment plans, each one corresponding to one of the calculated equidistant plans.

When using Monte Carlo simulation to assess a given treatment plan then, instead of a DVH with a single line for each structure, as presented in Fig. 5, a DVH with a set of lines (one for each simulation performed) is obtained, as illustrated in Fig. 16.

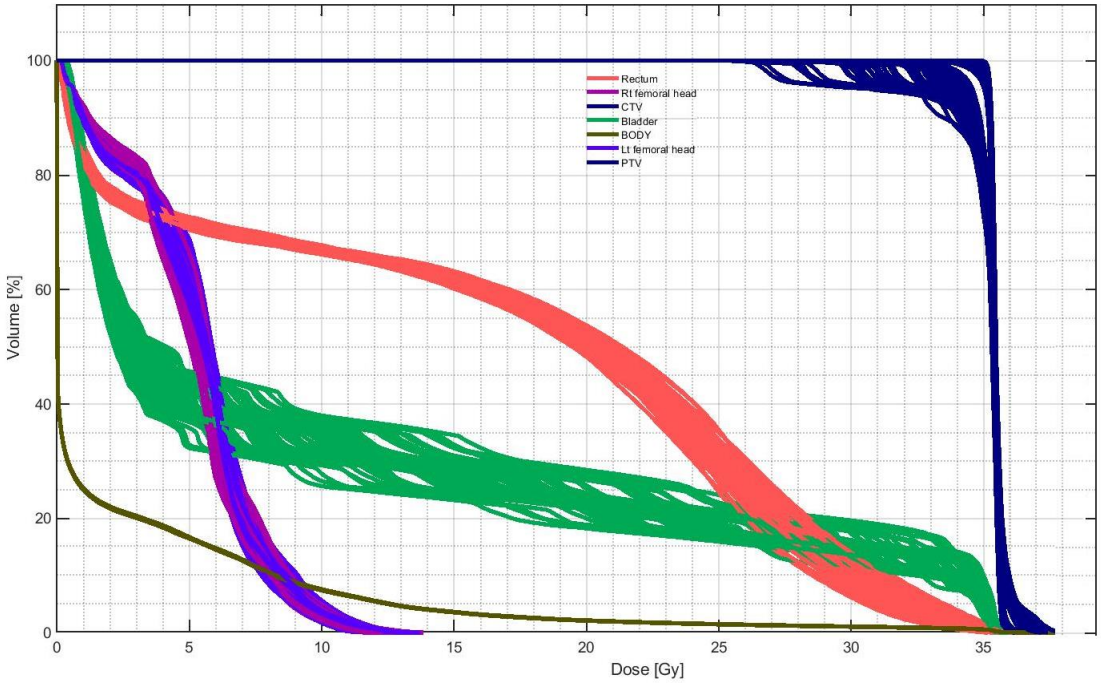

Fig. 16. Example of one of the DVHs obtained in one of the tested treatment plans for prostate cancer case 1.

The three more challenging structures were chosen for this study, more specifically, the CTV, the body, and the rectum. Each one of the structures was analysed regarding its dose constraint parameters. Comparison of the six treatment approaches will consider what is happening with these three structures for which the medical prescription is not totally fulfilled in all the conducted simulations. This means that its being compared D_{98} and D_{max} for CTV, D_{max} for body and D_{50} for the rectum.

Graphs were created to analyse the data of each case for each one of the six treatment delivery alternatives (as mentioned in 3.2.2). These graphs show the percentage of times the rectum complies with D_{50} as a function of the percentage of times that the CTV complies with D_{98}.

The results from the six scenarios were obtained consider 50 Monte Carlo iterations.

All the statistical significances in this section were calculated through Wilcoxon Signed-Rank Test, since median values are being compared with a reference value.

4.2.1. Prostate cancer case 1

For prostate cancer case 1, the percentage of compliance with the dose prescription for each one of the six approaches is presented in Fig. 17.

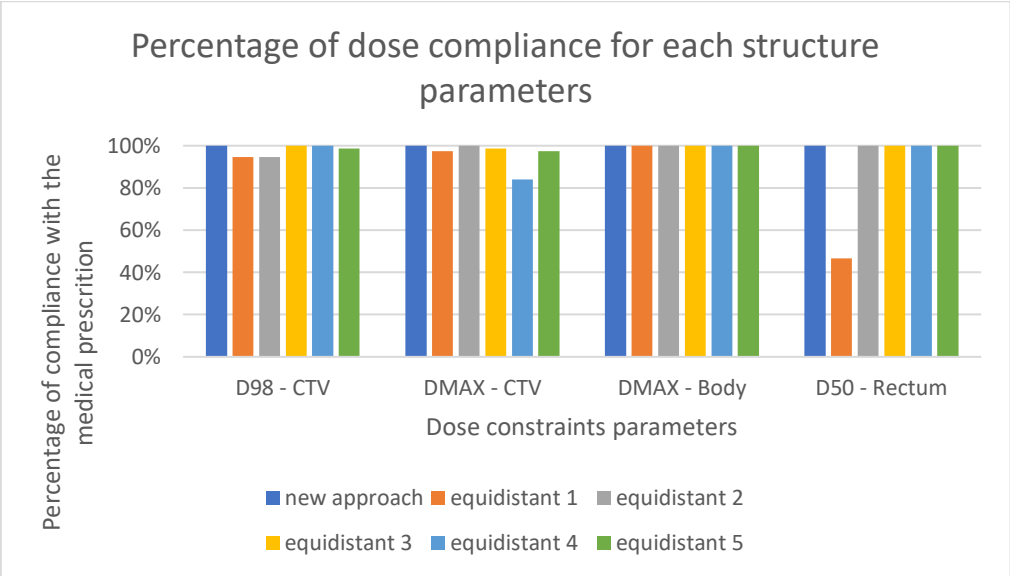

Fig. 17. Percentage of scenarios where the treatment delivered complied with the medical prescription for cancer case 1.

By analysing Fig. 17, the OARs constraints are all being met in 100% of the scenarios considered, except for the treatment plan with the first equidistant angle configuration. Considering the CTV, D_{98} is above the defined threshold for at least 95% of the scenarios, and this value is 100% for three treatment plans: the new approach being tested and equidistant configurations 3 and 4. Furthermore, only the new approach can respect the maximum dose admissible for the CTV in 100% of the scenarios.

Therefore, for cancer case 1, it is possible to conclude that the new approach is the best one, with all the constraints fully fulfilled and obtaining the best CTV homogeneity index value (1.026426 which is the smaller index between all the scenarios).

Additionally, this cancer case obtained the best results under uncertainty out of the five cases.

4.2.2. Prostate cancer case 2

Fig. 18 presents the percentage of compliance with the dose prescription for each one of the six approaches for the prostate cancer case 2.

Considering the results obtained with case 2, it is much more difficult to choose one single approach as being the best one, and the multiobjective nature of the treatment planning optimisation becomes clear. Analysing Fig. 18 and considering the values D_{98} for the CTV and D_{50} for the rectum, it can be seen that the achieved values for the new approach, equidistant 3, equidistant 4 and equidistant 5, are not immediately comparable, as they present different compromises between the two objectives.

It is important to note that, equidistant 5 reached 0% in both parameters, $D_{\max}$ for the CTV and D_{50} for the rectum.

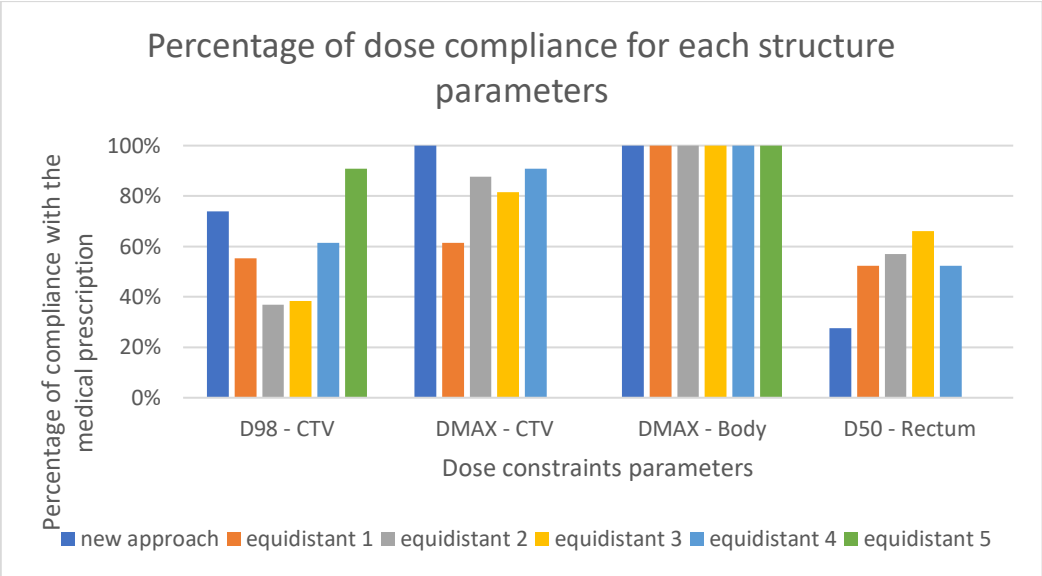

Fig. 18. Percentage of scenarios where the treatment delivered complied with the medical prescription for cancer case 2.

Once again, the new approach achieved the best CTV homogeneity index value, 1.035981, the smaller index between all the six scenarios.

The tradeoff between CTV coverage and rectum sparing is the most difficult and important to obtain and is analysed in Fig. 19.

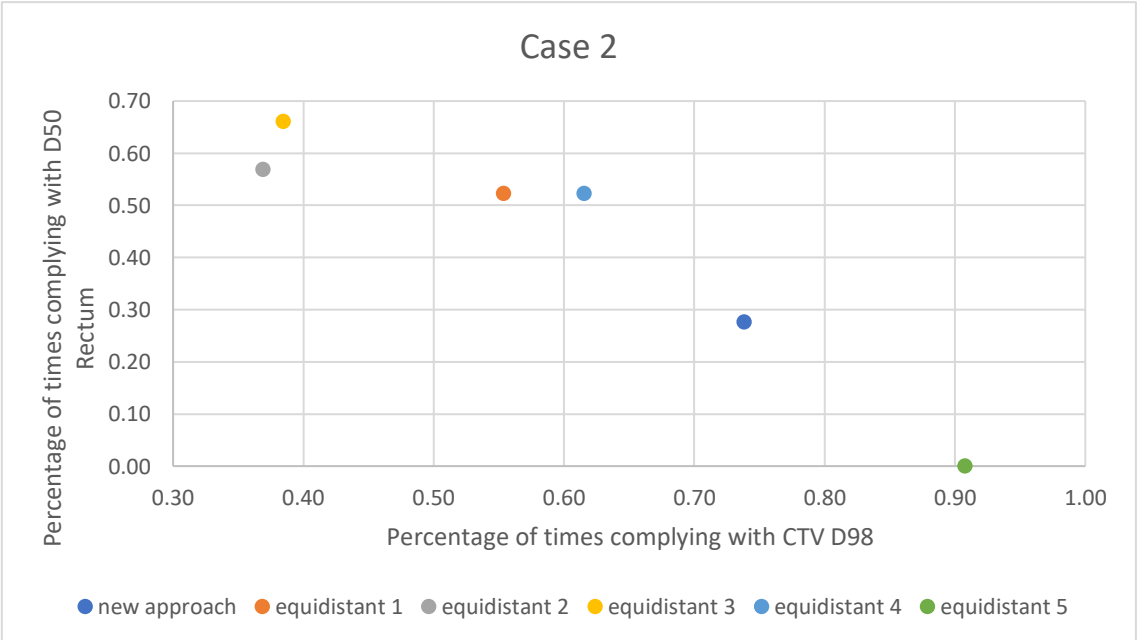

Fig. 19. Percentage of times complying with D50 for the rectum and D98 for CTV in case 2 (in the range of 0 to 1).

Considering Fig. 19, equidistant 5 is the approach that better irradiates the CTV but does not perform well when it comes to preserving the rectum. It has not been able to respect the defined medical prescription threshold in any of the scenarios considered. On the other hand, the new approach is the second best in terms of the number of times the desired value for CTV D_{98} was achieved, satisfying the medical prescription minimum threshold value 74% of the times. The median value obtained is significantly greater than the threshold ($p<0.00001$). It is also the approach presenting the best homogeneity index value. In terms of preserving the rectum, it only complies with the medical prescription 28% of the times but the mean value obtained, although statistically greater than 20Gy, is 20.39Gy. The median values obtained for the equidistant approach 3 and 4 are not significantly greater than 35Gy ($p=0.999$ and $p=0.2242$, respectively).

Looking at the mean value of the deviations from the medical prescription when it is not being fulfilled, the new approach presents the best results for the maximum dose deposited in the body and in the CTV. The mean deviation in terms of D_{98} is only 0.11 Gy. Regarding D_{50} rectum, it behaves much better than equidistant 5, which presents a mean deviation of 1.13 Gy, whilst the new approach has a mean deviation of 0.63 Gy.

4.2.3. Prostate cancer case 3

Fig. 20 presents the percentage of compliance with the dose prescription for each one of the six approaches for prostate cancer case 3.

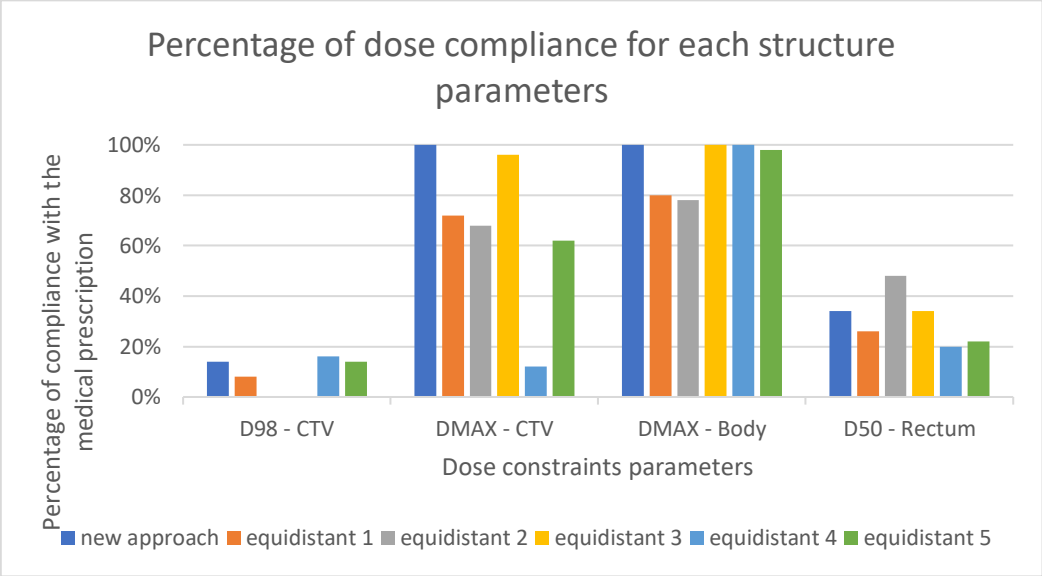

Fig. 20. Percentage of scenarios where the treatment delivered complied with the medical prescription for cancer case 3.

Considering the results obtained with case 3 and Fig. 20, it is possible to observe that the new approach is again one of the best approaches, although the simulation results are not favourable for any of the approaches considered when it comes to CTV irradiation since, for D_{98}, both equidistant 2 and 3 treatment plans have a compliance percentage of 0%, followed by 8% with plan equidistant 1, then the new approach and equidistant 5 have a compliance percentage of 14%, and finally the higher percentage is for equidistant 4 with a value of 16%.

The tradeoff between CTV coverage and rectum sparing for case 3 is presented in Fig. 21.

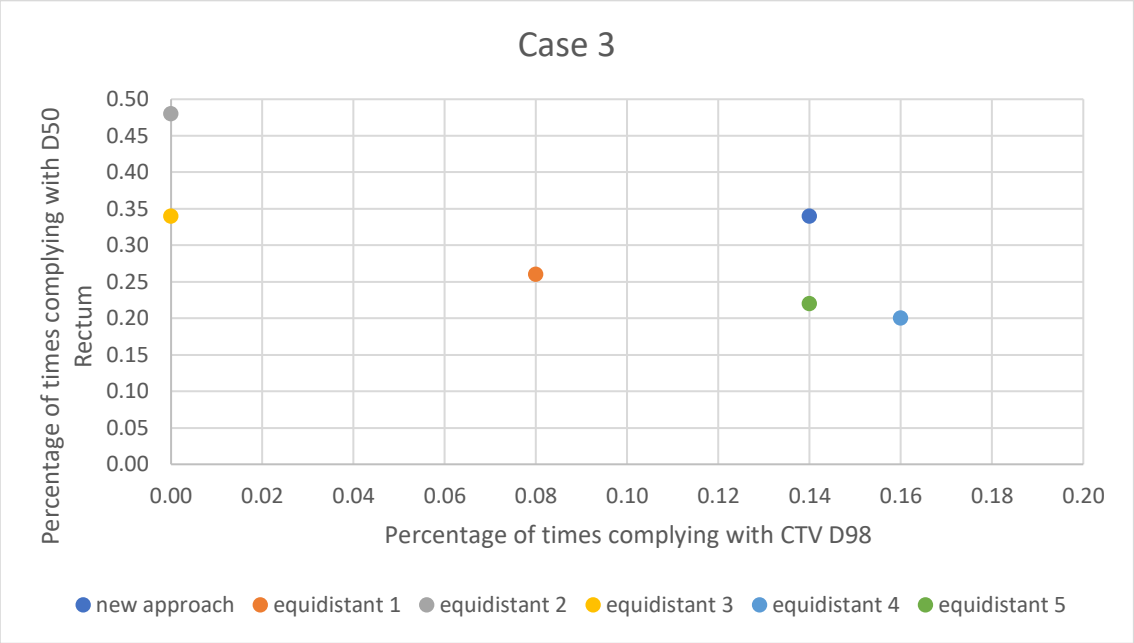

Fig. 21. Percentage of times complying with D50 for the rectum and D98 for CTV in case 3 (in the range of 0 to 1).

Analysing Fig. 21, it is possible to state that the new approach and equidistant approaches 2 and 4 are non-comparable when looking at the number of times the respective thresholds are being fulfilled in the simulations for D_{98} for the CTV and D_{50} for the rectum.

On the other hand, the new approach presents the second-best CTV coverage and the best homogeneity index value (equal to 1.084811). It is also the second best preserving both the rectum and the body. It is also the second best, considering the worst value obtained for both CTV coverage and D_{50} rectum.

4.2.4. Prostate cancer case 4

Fig. 22 presents the percentage of compliance with the dose prescription for each one of the six approaches for prostate cancer case 4.

Considering case 4, the best approach seems to be equidistant 4 which presents better CTV coverage and OAR sparing when analysing the simulations' results. Actually, equidistant 4 presents a compliance of 100% for both OARs and $D_{\max}$ for the CTV, meanwhile its D_{98} for the CTV is 50%. Nevertheless, it is the best value obtained for D_{98} in this simulation. Furthermore, the best homogeneity index is given by equidistant 4 with a value of 1.080445.

Nevertheless, the new approach presents the second-best homogeneity index value (1.085089), and it is one of the three best approaches: it is clearly surpassed by the solution equidistant 4, but it appears right after, being difficult to compare with equidistant 1.

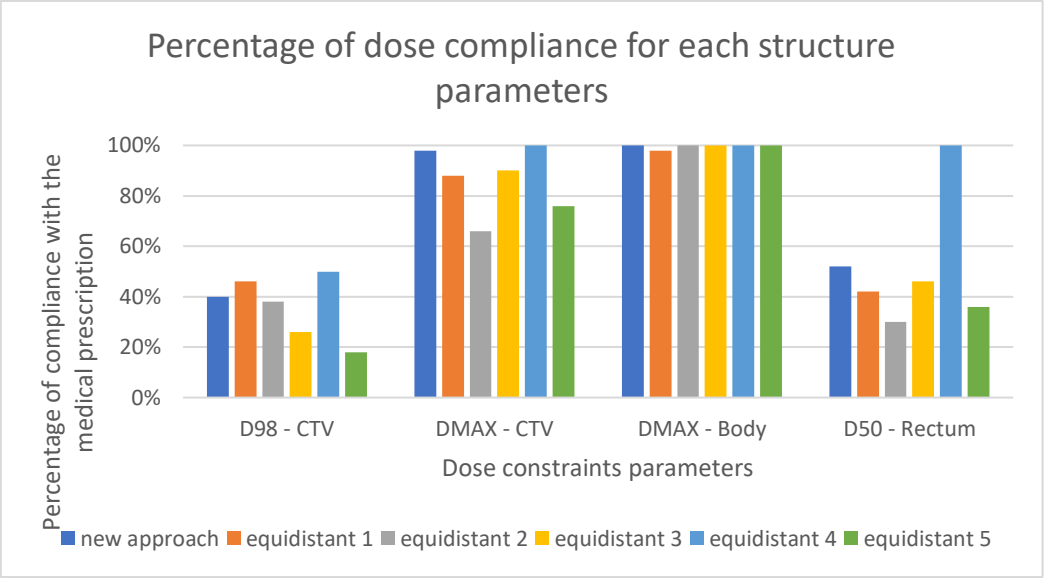

Fig. 22. Percentage of scenarios where the treatment delivered complied with the medical prescription for cancer case 4.

These facts are further highlighted in Fig. 23, where approach equidistant 4 is clearly the best compared with the other five when looking at the number of times the respective thresholds are being fulfilled in the simulations for D_{98} for the CTV and D_{50} for the rectum. Also, the new approach presents to be the second-best regarding rectum D_{50} threshold fulfil and the third-best in CTV coverage, being surpassed by equidistant 1 in this last parameter.

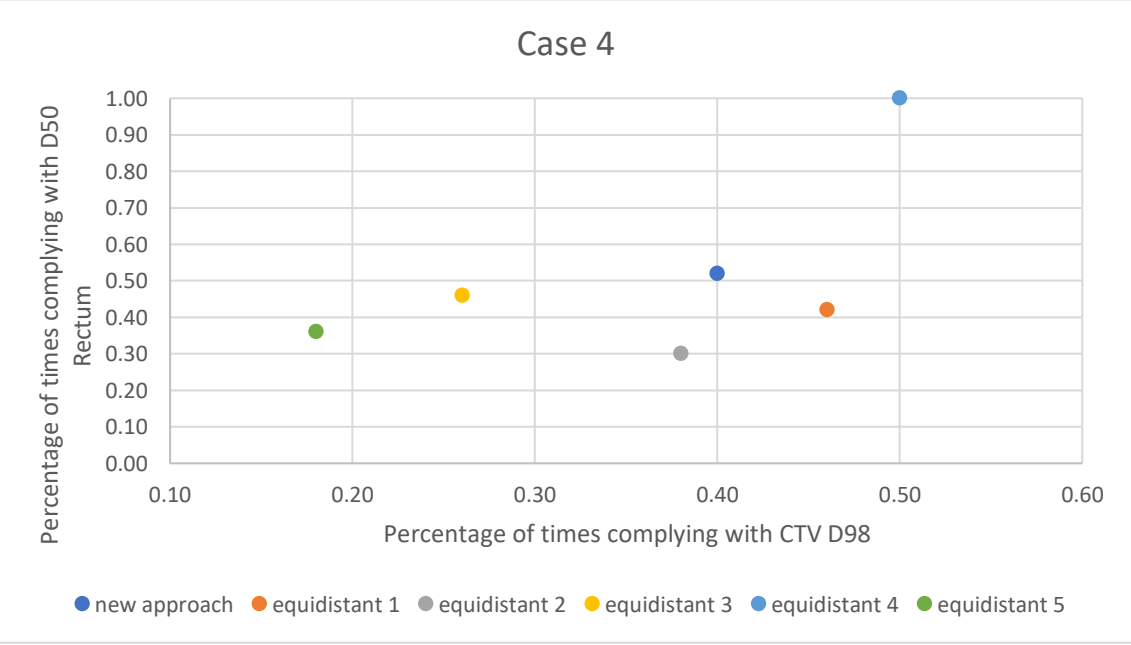

Fig. 23. Percentage of times complying with D50 for the rectum and D98 for CTV in case 4 (in the range of 0 to 1).

4.2.5. Prostate cancer case 5

For prostate cancer case 5, the percentage of compliance with the dose prescription for each one of the six approaches is presented in Fig. 24. In this case, all approaches achieved the value of 100% for $D_{\max}$ of both body and CTV. Regarding CTV coverage, the best result was obtained with the new approach due to its higher value in CTV D_{98} (38%). In contrast, its rectum-sparing value is the fifth best, with a value of 86%, which nevertheless is an excellent result. Thus, analysing best OARs sparing, it was achieved with approach equidistant 5 since it achieved the highest percentage of 98% for D_{50} of the rectum. Despite presenting the best results for OARs sparing, the value for CTV D_{98} of equidistant 5 is the fourth best with a value of 22%.

Additionally, the new approach presents the best homogeneity index value (1.018355).

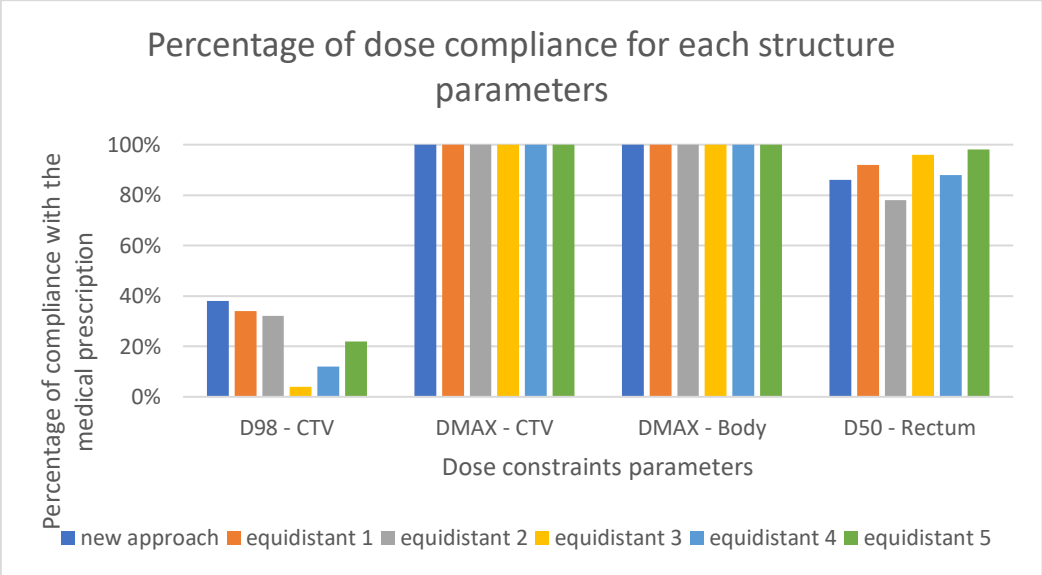

Fig. 24. Percentage of scenarios where the treatment delivered complied with the medical prescription for cancer case 5.

For a better understanding of case 5, Fig. 25 can also be observed. In this case, and once again, the new approach is one of the best alternatives when looking at the compromises between PTV coverage and rectum sparing.

Thus, this case shows that, once again, the choice of the approach will be highly dependent on the patient-specific multiobjectives of the treatment.

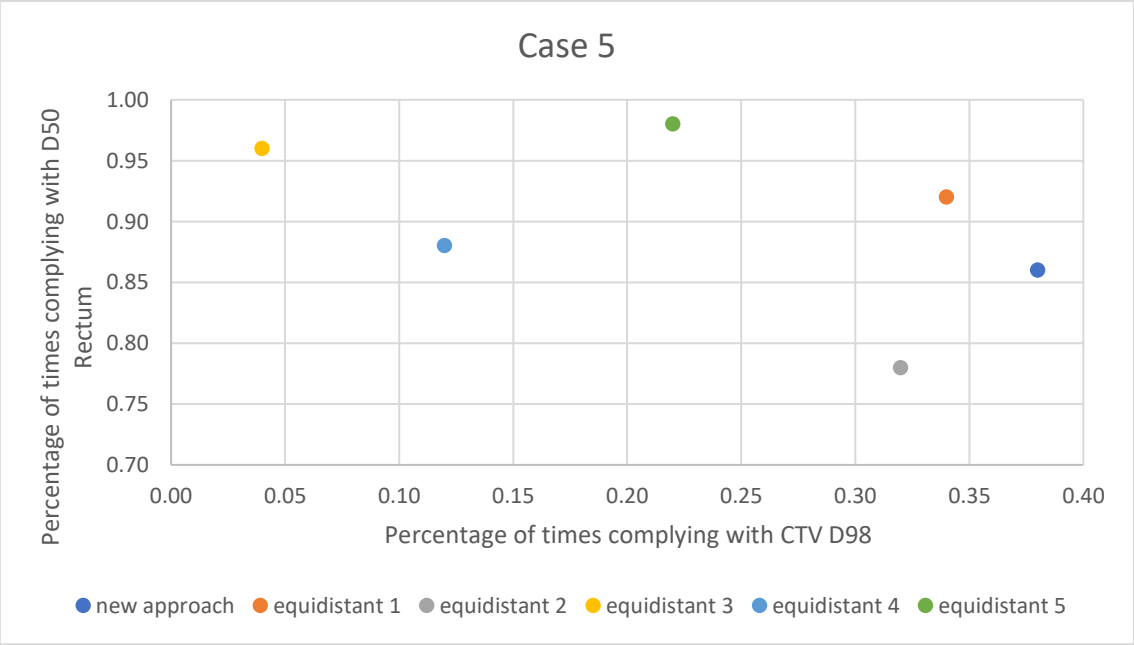

Fig. 25. Percentage of times complying with D50 for the rectum and D98 for CTV in case 5 (in the range of 0 to 1).

Chapter 5 Conclusions and Future Work

5.1. Conclusions

One very important conclusion of the experimental work that was developed is that the use of PTV as the main mitigation measure against uncertainty is not sufficient to guarantee that the desired doses are indeed being delivered. In almost all cases it was not possible to provide an adequate irradiation of the CTV or to appropriately spare the OARs, being the delivered radiation doses statistically different from the prescribed doses and doses that were achieved during treatment planning.

So, it is worth it to assess treatment plans not only looking at a single DVH, but also considering simulations where the real impact of the uncertainty can be assessed.

It is also clear from these computational results that beam angle choice is very important and can be interpreted as a measure of treatment plan robustness. There are clearly some angle configurations that are less prone to uncertainty impact.

The diversification strategy that was tested shows some interesting and promising results that need further exploration in future works. It is not the best one for all the cases tested, but it is always among the best alternatives. Actually, it appears as a valid alternative in four out of the five cases when looking at the compromise between CTV coverage and rectum sparing, which does not happen with any other approach. It is also the best approach considering the average homogeneity index in four out of five cases.

Looking at the situations where the medical prescription is not being respected, the new approach always presents the best average deviation from the prescribed value for the maximum CTV dose and maximum dose to the body.

With the results presented and discussed in the previous chapter, the new approach is always one of the best alternatives. Nonetheless, in several cases, a final balance between the treatment's objective and the patient's specificities is necessary to choose the adequate treatment planning approach.

5.2. Limitations of this work

The experimental studies that were conducted present several limitations that must be mentioned and that limit the generalisation of the results. Only five prostate cancer cases were considered, which is definitely not enough for these results to be generalisable. Even so, there is a clear trend in the results obtained, that show that diversification can indeed be a tool that deserves further studies. It is also clear that care must be taken when considering only PTV as a mitigation strategy because, most of the times, it will not be sufficient to assure a proper CTV coverage. This is a valid conclusion even considering the limited number of cases tested since it would be sufficient to have one such case to conclude that PTV is not enough.

During treatment planning, PRV delineated structures were not considered. The consideration of these structures could improve the results obtained for OAR sparing when uncertainties were explicitly considered in the simulations performed.

Only uncertainties related with patient position were taken into consideration.

5.3. Future Works

The code used for the simulations worked well for the first phase of the automated FMO FIS method, however the total time for one simulation was too long, sometimes needing between 8 and 20 days to finish all the Monte Carlo iterations for one simulation. Thus, one main aspect in future works is to optimise the code used in this dissertation's computational simulations.

Additionally, in terms of treatment planning automation, it would be interesting to compute the second phase of the automated FMO FIS method and analyse whether it would bring advantages in target coverage or organ sparing. It would be interesting to understand the impact that further improvements in OAR sparing and PTV coverage during the treatment planning stage can have when uncertainty is explicitly taken into account in treatment assessment.

The new approach presented in this dissertation brought excellent results in terms of the homogeneity index and it is always one of the best choices as a treatment planning approach, considering the multiobjective nature of treatment assessment. Thus, in future works, it would be advisable to do further tests with this new approach in other SBRT cancer cases where the homogeneity index of the CTV is highly relevant, such as lung, pancreatic, and liver cancers. It would also be interesting to perform beam angle optimisation and try other diversification measures considering different beam angle configurations other than the equidistant solutions.

Besides that, it would be interesting to compare the results obtained with the new approach for photon and proton SBRT to verify if there is a clear advantage in using one of them.

References

[1] R. L. Siegel Mph, A. N. Giaquinto, | Ahmedin, J. Dvm, and R. L. Siegel, “Cancer statistics, 2024,” 2024, doi: 10.3322/caac.21820.

[2] “Causes of death statistics - Statistics Explained,” Eurostat, European Comission. Accessed: Jun. 28, 2024. [Online]. Available: https://ec.europa.eu/eurostat/statistics-explained/index.php?title=Causes_of_death_statistics#Major_causes_of_death_in_the_EU_in_2021

[3] “Global cancer data by country | World Cancer Research Fund International.” Accessed: Mar. 02, 2023. [Online]. Available: https://www.wcrf.org/cancer-trends/global-cancer-data-by-country/

[4] “Global cancer burden growing, amidst mounting need for services,” World Health Organization. Accessed: Jun. 28, 2024. [Online]. Available: https://www.who.int/news/item/01-02-2024-global-cancer-burden-growing--amidst-mounting-need-for-services

[5] Joint Research Centre, “Cancer cases and deaths on the rise in the EU,” European Commission. Accessed: Jun. 28, 2024. [Online]. Available: https://joint-research-centre.ec.europa.eu/jrc-news-and-updates/cancer-cases-and-deaths-rise-eu-2023-10-02_en

[6] European Union, “Data explorer | ECIS,” ECIS - European Cancer Information System. Accessed: Mar. 06, 2023. [Online]. Available: https://ecis.jrc.ec.europa.eu/explorer.php?$0-4$1-All$4-1,2$3-0$6-0,85$5-2020,2040$7-8$21-0$2-All$CLongtermChart1_1$X0_-1-AE27$CLongtermChart1_2$X1_-1-AE27$CLongtermChart1_3$X2_-1-AE27$CLongtermChart1_4$X3_14-$X3_-1-AE27$CLongtermTable1_6$X4_-1-AE27

[7] H. Rocha and J. M. Dias, “On the Optimization of Radiation Therapy Planning,” *INESC - Instituto de Engenharia de Sistemas e Computadores de Coimbra*, no. 15, Sep. 2009.

[8] S. J. Otter, A. J. Stewart, and P. M. Devlin, “Modern Brachytherapy,” *Hematol Oncol Clin North Am*, vol. 33, no. 6, pp. 1011–1025, Dec. 2019, doi: 10.1016/J.HOC.2019.08.011.

[9] R. Baskar, K. A. Lee, R. Yeo, and K. W. Yeoh, “Cancer and Radiation Therapy: Current Advances and Future Directions,” *Int J Med Sci*, vol. 9, no. 3, p. 193, Feb. 2012, doi: 10.7150/IJMS.3635.

[10] A. Ahnesjö, B. Hårdemark, U. Isacsson, and A. Montelius, “The IMRT information process—mastering the degrees of freedom in external beam therapy,” *Phys Med Biol*, vol. 51, no. 13, p. R381, Jun. 2006, doi: 10.1088/0031-9155/51/13/R22.

[11] K. Spoormans, M. Crabbé, L. Struelens, M. De Saint-Hubert, and M. Koole, “A Review on Tumor Control Probability (TCP) and Preclinical Dosimetry in Targeted Radionuclide Therapy (TRT),” *Pharmaceutics 2022, Vol. 14, Page 2007*, vol. 14, no. 10, p. 2007, Sep. 2022, doi: 10.3390/PHARMACEUTICS14102007.

[12] I. Skvortsova, P. Debbage, V. Kumar, and S. Skvortsov, “Radiation resistance: Cancer stem cells (CSCs) and their enigmatic pro-survival signaling,” *Semin Cancer Biol*, vol. 35, pp. 39–44, Dec. 2015, doi: 10.1016/J.SEMCANCER.2015.09.009.

[13] K. J. Marcus and D. Haas-Kogan, *Pediatric Radiation Oncology*. W.B. Saunders, 2009. doi: 10.1016/B978-1-4160-3431-5.00008-X.

[14] M. F. Osti and M. Massaro, "Principles of Radiotherapy," *Nucl Med Mol Imaging*, pp. 412–421, Jan. 2022, doi: 10.1016/B978-0-12-822960-6.00070-3.

[15] A. Chandra *et al.*, "Feasibility of using intensity-modulated radiotherapy to improve lung sparing in treatment planning for distal esophageal cancer," *Radiother Oncol*, vol. 77, no. 3, pp. 247–253, Dec. 2005, doi: 10.1016/J.RADONC.2005.10.017.

[16] J. Gomez-Millan, J. R. Fernández, and J. A. Medina Carmona, "Current status of IMRT in head and neck cancer," *Reports of Practical Oncology and Radiotherapy*, vol. 18, no. 6, p. 371, 2013, doi: 10.1016/J.RPOR.2013.09.008.

[17] J. M. Dias, H. Rocha, P. Carrasqueira, B. C. Ferreira, T. Ventura, and M. C. Lopes, "Operations research contribution to totally automated radiotherapy treatment planning: A noncoplanar beam angle and fluence map optimization engine based on optimization models and algorithms," *Oper Res Health Care*, vol. 36, p. 100378, Mar. 2023, doi: 10.1016/J.ORHC.2023.100378.

[18] S. O. Hunte, C. H. Clark, N. Zyuzikov, and A. Nisbet, "Volumetric modulated arc therapy (VMAT): a review of clinical outcomes—what is the clinical evidence for the most effective implementation?," *British Journal of Radiology*, vol. 95, no. 1136, Jul. 2022, doi: 10.1259/BJR.20201289/ASSET/IMAGES/LARGE/BJR.20201289.G001.JPEG.

[19] M. Guckenberger *et al.*, "Definition and quality requirements for stereotactic radiotherapy: consensus statement from the DEGRO/DGMP Working Group Stereotactic Radiotherapy and Radiosurgery," *Strahlentherapie und Onkologie*, vol. 196, no. 5, pp. 417–420, May 2020, doi: 10.1007/S00066-020-01603-1/METRICS.

[20] M. Guckenberger *et al.*, "Definition of stereotactic body radiotherapy: Principles and practice for the treatment of stage I non-small cell lung cancer," *Strahlentherapie Und Onkologie*, vol. 190, no. 1, p. 26, Jan. 2014, doi: 10.1007/S00066-013-0450-Y.

[21] W. Wang *et al.*, "Fluence Map Prediction Using Deep Learning Models - Direct Plan Generation for Pancreas Stereotactic Body Radiation Therapy," *Front Artif Intell*, vol. 3, Sep. 2020, doi: 10.3389/FRAI.2020.00068.

[22] A. Martin and A. Gaya, "Stereotactic Body Radiotherapy: A Review," *Clin Oncol*, vol. 22, no. 3, pp. 157–172, Apr. 2010, doi: 10.1016/J.CLON.2009.12.003.

[23] M. J. LaRiviere, P. M. G. Santos, C. E. Hill-Kayser, and J. M. Metz, "Proton Therapy," *Hematol Oncol Clin North Am*, vol. 33, no. 6, pp. 989–1009, Dec. 2019, doi: 10.1016/J.HOC.2019.08.006.

[24] R. P. Johnson, "Review of medical radiography and tomography with proton beams," *Reports on Progress in Physics*, vol. 81, no. 1, p. 016701, Nov. 2017, doi: 10.1088/1361-6633/AA8B1D.

[25] W. Cao *et al.*, "Reflections on beam configuration optimization for intensity-modulated proton therapy," *Phys Med Biol*, vol. 67, no. 13, p. 13TR01, Jun. 2022, doi: 10.1088/1361-6560/AC6FAC.

[26] A. C. Moreno *et al.*, “Intensity Modulated Proton Therapy (IMPT) – The Future of IMRT for Head and Neck Cancer,” *Oral Oncol*, vol. 88, p. 66, Jan. 2019, doi: 10.1016/J.ORALONCOLOGY.2018.11.015.

[27] W. Owadally and J. Staffurth, “Principles of cancer treatment by radiotherapy,” *Surgery (Oxford)*, vol. 33, no. 3, pp. 127–130, Mar. 2015, doi: 10.1016/J.MPSUR.2014.12.008.

[28] J. Seuntjens *et al.*, “ICRU REPORT 91. Prescribing, Recording, and Reporting of Stereotactic Treatments with Small Photon Beams,” *J ICRU*, vol. 14, no. 2, pp. 1–160, Dec. 2014, Accessed: Apr. 30, 2023. [Online]. Available: https://academic.oup.com/journals/pages/access_purchase/

[29] C. E. Cardenas, J. Yang, B. M. Anderson, L. E. Court, and K. B. Brock, “Advances in Auto-Segmentation,” *Semin Radiat Oncol*, vol. 29, pp. 185–197, 2019, doi: 10.1016/j.semradonc.2019.02.001.

[30] M. P. A. Starmans, S. R. van der Voort, J. M. C. Tovar, J. F. Veenland, S. Klein, and W. J. Niessen, “Radiomics: Data mining using quantitative medical image features,” in *Handbook of Medical Image Computing and Computer Assisted Intervention*, S. K. Zhou, D. Rueckert, and G. Fichtinger, Eds., Academic Press, 2020, pp. 429–456. doi: 10.1016/B978-0-12-816176-0.00023-5.

[31] H. Mcgrath *et al.*, “Manual segmentation versus semi-automated segmentation for quantifying vestibular schwannoma volume on MRI,” *Int J Comput Assist Radiol Surg*, vol. 15, pp. 1445–1455, 2020, doi: 10.1007/s11548-020-02222-y.

[32] M. Shahedi, M. Halicek, R. Guo, G. Zhang, D. M. Schuster, and B. Fei, “A semiautomatic segmentation method for prostate in CT images using local texture classification and statistical shape modeling,” *Med Phys*, vol. 45, no. 6, pp. 2527–2541, Jun. 2018, doi: 10.1002/MP.12898.

[33] K. Harrison, H. Pullen, C. Welsh, O. Oktay, J. Alvarez-Valle, and R. Jena, “Machine Learning for Auto-Segmentation in Radiotherapy Planning,” *Clin Oncol*, vol. 34, no. 2, pp. 74–88, Feb. 2022, doi: 10.1016/J.CLON.2021.12.003.

[34] C. Sjöberg, M. Lundmark, C. Granberg, S. Johansson, A. Ahnesjö, and A. Montelius, “Clinical evaluation of multi-atlas based segmentation of lymph node regions in head and neck and prostate cancer patients,” *Radiat Oncol*, vol. 8, no. 1, Oct. 2013, doi: 10.1186/1748-717X-8-229.

[35] H. A. Kirişli *et al.*, “Evaluation of a multi-atlas based method for segmentation of cardiac CTA data: a large-scale, multicenter, and multivendor study,” *Med Phys*, vol. 37, no. 12, pp. 6279–6291, 2010, doi: 10.1118/1.3512795.

[36] T. Vrtovec, D. Močnik, P. Strojan, F. Pernuš, and B. Ibragimov, “Auto-segmentation of organs at risk for head and neck radiotherapy planning: From atlas-based to deep learning methods,” *Med Phys*, vol. 47, no. 9, pp. e929–e950, Sep. 2020, doi: 10.1002/MP.14320.

[37] J. J. Lucido *et al.*, “Validation of clinical acceptability of deep-learning-based automated segmentation of organs-at-risk for head-and-neck radiotherapy treatment planning,” *Front Oncol*, vol. 13, p. 1137803, 2023, doi: 10.3389/FONC.2023.1137803/FULL.

[38] A. Kuisma *et al.*, “Validation of automated magnetic resonance image segmentation for radiation therapy planning in prostate cancer,” *Phys Imaging Radiat Oncol*, vol. 13, pp. 14–20, Jan. 2020, doi: 10.1016/J.PHRO.2020.02.004.

[39] B. Fraass *et al.*, “American Association of Physicists in Medicine Radiation Therapy Committee Task Group 53: quality assurance for clinical radiotherapy treatment planning,” *Med Phys*, vol. 25, no. 10, pp. 1773–1829, 1998, doi: 10.1118/1.598373.

[40] T. Halabi, D. Craft, and T. Bortfeld, “Dose–volume objectives in multi-criteria optimization,” *Phys Med Biol*, vol. 51, no. 15, p. 3809, Jul. 2006, doi: 10.1088/0031-9155/51/15/014.

[41] A. Sadeghnejad Barkousaraie, O. Ogunmolu, S. Jiang, and D. Nguyen, “A fast deep learning approach for beam orientation optimization for prostate cancer treated with intensity-modulated radiation therapy,” *Med Phys*, vol. 47, no. 3, pp. 880–897, Mar. 2020, doi: 10.1002/MP.13986.

[42] H. Rocha, J. M. Dias, B. C. Ferreira, and M. C. Lopes, “Noncoplanar beam angle optimization in IMRT treatment planning using pattern search methods,” *J Phys Conf Ser*, vol. 616, no. 1, p. 012014, May 2015, doi: 10.1088/1742-6596/616/1/012014.

[43] B. W. K. Schipaanboord, B. J. M. Heijmen, and S. Breedveld, “TBS-BAO: fully automated beam angle optimization for IMRT guided by a total-beam-space reference plan,” *Phys Med Biol*, vol. 67, no. 3, p. 035004, Jan. 2022, doi: 10.1088/1361-6560/AC4B37.

[44] S. Haseai, H. Arimura, K. Asai, T. Yoshitake, and Y. Shioyama, “Similar-cases-based planning approaches with beam angle optimizations using water equivalent path length for lung stereotactic body radiation therapy,” *Radiol Phys Technol*, vol. 13, no. 2, pp. 119–127, Jun. 2020, doi: 10.1007/S12194-020-00558-3.

[45] S. Breedveld, P. R. M. Storchi, P. W. J. Voet, and B. J. M. Heijmen, “iCycle: Integrated, multicriterial beam angle, and profile optimization for generation of coplanar and noncoplanar IMRT plans,” *Med Phys*, vol. 39, no. 2, pp. 951–963, 2012, doi: 10.1118/1.3676689.

[46] W. Gu *et al.*, “Integrated beam orientation and scanning-spot optimization in intensity-modulated proton therapy for brain and unilateral head and neck tumors,” *Med Phys*, vol. 45, no. 4, pp. 1338–1350, Apr. 2018, doi: 10.1002/MP.12788.

[47] W. Cao *et al.*, “Uncertainty incorporated beam angle optimization for IMPT treatment planning,” *Med Phys*, vol. 39, no. 8, pp. 5248–5256, Aug. 2012, doi: 10.1118/1.4737870.

[48] G. J. Lim, L. Kardar, and W. Cao, “A hybrid framework for optimizing beam angles in radiation therapy planning,” *Ann Oper Res*, vol. 217, no. 1, pp. 357–383, Mar. 2014, doi: 10.1007/S10479-014-1564-Z.

[49] T. Magome *et al.*, “Computer-aided beam arrangement based on similar cases in radiation treatment-planning databases for stereotactic lung radiation therapy,” *J Radiat Res*, vol. 54, no. 3, pp. 569–577, 2013, doi: 10.1093/JRR/RRS123.

[50] L. Rossi, S. Breedveld, S. Aluwini, and B. Heijmen, “Physics Contribution Noncoplanar Beam Angle Class Solutions to Replace Time-Consuming Patient-Specific Beam Angle Optimization in Robotic Prostate Stereotactic Body Radiation Therapy Radiation

Oncology," *Int J Radiation Oncol Biol Phys*, vol. 92, no. 4, pp. 762–770, 2015, doi: 10.1016/j.ijrobp.2015.03.013.

[51] G. Meedt, M. Alber, and F. Nüsslin, "Non-coplanar beam direction optimization for intensity-modulated radiotherapy," *Phys Med Biol*, vol. 48, no. 18, p. 2999, Sep. 2003, doi: 10.1088/0031-9155/48/18/304.

[52] J. A. de Pooter, A. M. Romero, W. Wunderink, P. R. M. Storchi, and B. J. M. Heijmen, "Automated non-coplanar beam direction optimization improves IMRT in SBRT of liver metastasis," *Radiotherapy and Oncology*, vol. 88, no. 3, pp. 376–381, Sep. 2008, doi: 10.1016/J.RADONC.2008.06.001.

[53] T. Ventura, M. do C. Lopes, H. Rocha, B. da Costa Ferreira, and J. Dias, "Advantage of Beam Angle Optimization in Head-and-Neck IMRT: Patient Specific Analysis," *IFMBE*, vol. 76, pp. 1256–1263, Jan. 2020, doi: 10.1007/978-3-030-31635-8_153.

[54] H. Kamal Sayed, M. G. Herman, and C. J. Beltran, "A Pareto-based beam orientation optimization method for spot scanning intensity-modulated proton therapy," *Med Phys*, vol. 47, no. 5, pp. 2049–2060, Jun. 2020, doi: 10.1002/MP.14096.

[55] H. Rocha, J. Dias, P. Carrasqueira, T. Ventura, B. Ferreira, and M. do C. Lopes, "Comparison of Different Strategies for Arc Therapy Optimization," *LNCS*, vol. 12251, pp. 552–563, Jan. 2020, doi: 10.1007/978-3-030-58808-3_40.

[56] J. Dias, H. Rocha, T. Ventura, B. Ferreira, and M. D. C. Lopes, "Automated fluence map optimization based on fuzzy inference systems," *Med Phys*, vol. 43, no. 3, pp. 1083–1095, Mar. 2016, doi: 10.1118/1.4941007.

[57] H. Rocha, J. M. Dias, B. C. Ferreira, and M. C. Lopes, "Discretization of optimal beamlet intensities in IMRT: A binary integer programming approach," *Math Comput Model*, vol. 55, no. 7–8, pp. 1969–1980, Apr. 2012, doi: 10.1016/J.MCM.2011.11.056.

[58] S. C. M. Ten Eikelder, A. Ajdari, T. Bortfeld, and D. Den Hertog, "Conic formulation of fluence map optimization problems," *Phys Med Biol*, vol. 66, no. 22, p. 225016, Nov. 2021, doi: 10.1088/1361-6560/AC2B82.

[59] M. Zaghian, G. Lim, W. Liu, and R. Mohan, "An Automatic Approach for Satisfying Dose-Volume Constraints in Linear Fluence Map Optimization for IMPT," *J Cancer Ther*, vol. 5, no. 2, pp. 198–207, 2014, doi: 10.4236/JCT.2014.52025.

[60] W. Wang *et al.*, "Deep Learning–Based Fluence Map Prediction for Pancreas Stereotactic Body Radiation Therapy With Simultaneous Integrated Boost," *Adv Radiat Oncol*, vol. 6, no. 4, p. 100672, Jul. 2021, doi: 10.1016/J.ADRO.2021.100672.

[61] V. Hernandez *et al.*, "Optimization of intensity modulated radiotherapy under constraints for static and dynamic MLC delivery," *MEDICINE AND BIOLOGY Phys. Med. Biol*, vol. 46, pp. 3229–3239, 2001.

[62] G. Bednarz *et al.*, "The use of mixed-integer programming for inverse treatment planning with pre-defined field segments," *MEDICINE AND BIOLOGY Phys. Med. Biol*, vol. 47, pp. 2235–2245, 2002.

[63] C. Cotrutz and L. Xing, "Segment-based dose optimization using a genetic algorithm," *MEDICINE AND BIOLOGY Phys. Med. Biol*, vol. 48, pp. 2987–2998, 2003.

[64] C. Men, H. E. Romeijn, Z. C. Taşkin, and J. F. Dempsey, “An exact approach to direct aperture optimization in IMRT treatment planning,” *Phys Med Biol*, vol. 52, no. 24, pp. 7333–7352, Dec. 2007, doi: 10.1088/0031-9155/52/24/009.

[65] H. E. Romeijn, R. K. Ahuja, J. F. Dempsey, and A. Kumar, “A COLUMN GENERATION APPROACH TO RADIATION THERAPY TREATMENT PLANNING USING APERTURE MODULATION *,” *SIAM J. OPTIM*, 2005, doi: 10.1137/040606612.

[66] T. Kalinowski, “A duality based algorithm for multileaf collimator field segmentation with interleaf collision constraint,” *Discrete Appl Math (1979)*, vol. 152, no. 1–3, pp. 52–88, Nov. 2005, doi: 10.1016/J.DAM.2004.10.008.

[67] D. Baatar, M. Ehrgott, H. W. Hamacher, and I. M. Raschendorfer, “Minimizing the number of apertures in multileaf collimator sequencing with field splitting,” *Discrete Appl Math (1979)*, vol. 250, pp. 87–103, Dec. 2018, doi: 10.1016/J.DAM.2018.04.016.

[68] H. Rocha, J. M. Dias, B. C. Ferreira, and M. C. Lopes, “Combinatorial optimization for an improved transition from fluence optimization to fluence delivery in IMRT treatment planning,” *Optimization*, vol. 61, no. 8, pp. 969–987, Aug. 2012, doi: 10.1080/02331934.2011.607498.

[69] D. M. Shepard, M. A. Earl, X. A. Li, S. Naqvi, and C. Yu, “Direct aperture optimization: a turnkey solution for step-and-shoot IMRT,” *Med Phys*, vol. 29, no. 6, pp. 1007–1018, 2002, doi: 10.1118/1.1477415.

[70] M. Moyano, G. Cabrera-Guerrero, G. Tello-Valenzuela, and C. Lagos, “An Hybrid Local Search for the Direct Aperture Optimisation Problem,” *IEEE Trans Emerg Top Comput Intell*, 2023, doi: 10.1109/TETCI.2023.3265360.

[71] M. Clements, N. Schupp, M. Tattersall, A. Brown, and R. Larson, “Monaco treatment planning system tools and optimization processes,” *Medical Dosimetry*, vol. 43, no. 2, pp. 106–117, Jun. 2018, doi: 10.1016/J.MEDDOS.2018.02.005.

[72] P. Meyer *et al.*, “Automation in radiotherapy treatment planning: Examples of use in clinical practice and future trends for a complete automated workflow,” *Cancer/Radiothérapie*, vol. 25, no. 6–7, pp. 617–622, Oct. 2021, doi: 10.1016/J.CANRAD.2021.06.006.

[73] S. Naccarato *et al.*, “Automated Planning for Prostate Stereotactic Body Radiation Therapy on the 1.5 T MR-Linac,” *Adv Radiat Oncol*, vol. 7, no. 3, p. 100865, May 2022, doi: 10.1016/J.ADRO.2021.100865.

[74] X. Zhang, X. Li, E. M. Quan, X. Pan, and Y. Li, “A methodology for automatic intensity-modulated radiation treatment planning for lung cancer,” *Phys Med Biol*, vol. 56, no. 13, p. 3873, Jun. 2011, doi: 10.1088/0031-9155/56/13/009.

[75] R. Bijman *et al.*, “Automated Radiotherapy Planning for Patient-Specific Exploration of the Trade-Off Between Tumor Dose Coverage and Predicted Radiation-Induced Toxicity-A Proof of Principle Study for Prostate Cancer,” *Front Oncol*, vol. 10, Jun. 2020, doi: 10.3389/FONC.2020.00943.

[76] M. Huiskes *et al.*, “Validation of Fully Automated Robust Multicriterial Treatment Planning for Head and Neck Cancer IMPT,” *International Journal of Radiation Oncology*Biology*Physics*, Jan. 2024, doi: 10.1016/J.IJROBP.2023.12.034.

[77] B. W. K. Schipaanboord, M. K. Giżyńska, L. Rossi, K. C. de Vries, B. J. M. Heijmen, and S. Breedveld, “Fully automated treatment planning for MLC-based robotic radiotherapy,” *Med Phys*, vol. 48, no. 8, pp. 4139–4147, Aug. 2021, doi: 10.1002/MP.14993.

[78] R. Bijman *et al.*, “First system for fully-automated multi-criterial treatment planning for a high-magnetic field MR-Linac applied to rectal cancer,” *Acta Oncol (Madr)*, vol. 59, no. 8, pp. 926–932, Aug. 2020, doi: 10.1080/0284186X.2020.1766697.

[79] M. Zarepisheh *et al.*, “A DVH-guided IMRT optimization algorithm for automatic treatment planning and adaptive radiotherapy replanning,” *Med Phys*, vol. 41, no. 6Part1, p. 061711, Jun. 2014, doi: 10.1118/1.4875700.

[80] Q. Jia *et al.*, “OAR dose distribution prediction and gEUD based automatic treatment planning optimization for intensity modulated radiotherapy,” *IEEE Access*, vol. 7, pp. 141426–141437, 2019, doi: 10.1109/ACCESS.2019.2942393.

[81] L. A. Zadeh, “Fuzzy sets,” *Information and Control*, vol. 8, no. 3, pp. 338–353, Jun. 1965, doi: 10.1016/S0019-9958(65)90241-X.

[82] R. Seising, “Proposals for future developments in fuzzy set technology,” *IEEE International Conference on Fuzzy Systems*, pp. 1655–1662, 2006, doi: 10.1109/FUZZY.2006.1681929.

[83] F. Stieler, H. Yan, F. Lohr, F. Wenz, and F. F. Yin, “Development of a neuro-fuzzy technique for automated parameter optimization of inverse treatment planning,” *Radiation Oncology*, vol. 4, no. 1, p. 39, Sep. 2009, doi: 10.1186/1748-717X-4-39.

[84] H. Yan, F. F. Yin, H. Guan, and J. H. Kim, “Fuzzy logic guided inverse treatment planning,” *Med Phys*, vol. 30, no. 10, pp. 2675–2685, Oct. 2003, doi: 10.1118/1.1600739.

[85] H. Yan, F. F. Yin, H. Q. Guan, and J. H. Kim, “AI-guided parameter optimization in inverse treatment planning,” *Phys Med Biol*, vol. 48, no. 21, pp. 3565–3580, Nov. 2003, doi: 10.1088/0031-9155/48/21/008.

[86] A. E. Torshabi, “Investigation of the robustness of adaptive neuro-fuzzy inference system for tracking moving tumors in external radiotherapy,” *Australas Phys Eng Sci Med*, vol. 37, no. 4, pp. 771–778, Dec. 2014, doi: 10.1007/S13246-014-0313-6.

[87] B. Mzenda, M. Hosseini-Ashrafi, A. Gegov, and D. J. Brown, “Implementation of a fuzzy model for computation of margins in cancer treatment,” *2010 IEEE World Congress on Computational Intelligence, WCCI 2010*, 2010, doi: 10.1109/FUZZY.2010.5584468.

[88] R. Timmerman *et al.*, “Stereotactic Body Radiation Therapy for Inoperable Early Stage Lung Cancer,” *JAMA : the journal of the American Medical Association*, vol. 303, no. 11, p. 1070, Mar. 2010, doi: 10.1001/JAMA.2010.261.

[89] R. Kumar *et al.*, “Stereotactic body radiation therapy planning with duodenal sparing using volumetric-modulated arc therapy vs intensity-modulated radiation therapy in locally advanced pancreatic cancer: A dosimetric analysis,” *Med Dosim*, vol. 38, no. 3, p. 243, 2013, doi: 10.1016/J.MEDDOS.2013.02.003.

[90] S. S. Kumar *et al.*, “Comparison of outcomes of stereotactic body radiation therapy delivered with three different technologies to the lung,” *J Radiosurg SBRT*, vol. 5, no. 3, p. 209, 2018, Accessed: Mar. 28, 2023. [Online]. Available: /pmc/articles/PMC6018041/

[91] Z. Ouyang, D. V. LaHurd, E. H. Balagamwala, S. T. Chao, J. H. Suh, and P. Xia, “Treatment planning of VMAT and step-and-shoot IMRT delivery techniques for single fraction spine SBRT: An intercomparative dosimetric analysis and phantom-based quality assurance measurements,” *J Appl Clin Med Phys*, vol. 21, no. 1, pp. 62–68, Jan. 2020, doi: 10.1002/ACM2.12788.

[92] D. E. Heron, M. S. Huq, and J. M. Herman, *Stereotactic Radiosurgery and Stereotactic Body Radiation Therapy (SBRT)*, 1st ed. New York: Demos Medical Publishing, 2018.

[93] J. Unkelbach *et al.*, “Robust radiotherapy planning,” *Phys Med Biol*, vol. 63, no. 22, p. 22TR02, Nov. 2018, doi: 10.1088/1361-6560/AAE659.

[94] K. L. Moore, “Automated Radiotherapy Treatment Planning,” *Semin Radiat Oncol*, vol. 29, no. 3, pp. 209–218, Jul. 2019, doi: 10.1016/J.SEMRADONC.2019.02.003.

[95] A. D. Yock *et al.*, “Robustness Analysis for External Beam Radiation Therapy Treatment Plans: Describing Uncertainty Scenarios and Reporting Their Dosimetric Consequences,” *Pract Radiat Oncol*, vol. 9, no. 4, pp. 200–207, Jul. 2019, doi: 10.1016/J.PRRO.2018.12.002.

[96] L. P. Kaplan *et al.*, “Plan quality assessment in clinical practice: Results of the 2020 ESTRO survey on plan complexity and robustness,” *Radiotherapy and Oncology*, vol. 173, pp. 254–261, Aug. 2022, doi: 10.1016/J.RADONC.2022.06.005.

[97] V. Hernandez *et al.*, “What is plan quality in radiotherapy? The importance of evaluating dose metrics, complexity, and robustness of treatment plans,” *Radiotherapy and Oncology*, vol. 153, pp. 26–33, Dec. 2020, doi: 10.1016/J.RADONC.2020.09.038.

[98] D. Bertsimas, D. B. Brown, and C. Caramanis, “Theory and Applications of Robust Optimization,” *SIAM Review*, vol. 53, no. 3, pp. 464–501, Jan. 2011, doi: 10.1137/080734510.

[99] X. Liang *et al.*, “ITV-Based Robust Optimization for VMAT Planning of Stereotactic Body Radiation Therapy of Lung Cancer,” *Pract Radiat Oncol*, vol. 9, no. 1, pp. 38–48, Jan. 2019, doi: 10.1016/J.PRRO.2018.08.005.

[100] A. Fredriksson and R. Bokrantz, “A critical evaluation of worst case optimization methods for robust intensity-modulated proton therapy planning,” *Med Phys*, vol. 41, no. 8Part1, p. 081701, Aug. 2014, doi: 10.1118/1.4883837.

[101] X. Zhang *et al.*, “Robust optimization in lung treatment plans accounting for geometric uncertainty,” *J Appl Clin Med Phys*, vol. 19, no. 3, pp. 19–26, May 2018, doi: 10.1002/ACM2.12291.

[102] R. Bokrantz and A. Fredriksson, “Scenario-based radiation therapy margins for patient setup, organ motion, and particle range uncertainty,” *Phys Med Biol*, vol. 62, no. 4, p. 1342, Jan. 2017, doi: 10.1088/1361-6560/AA524D.

[103] S. Teoh, B. George, F. Fiorini, K. A. Vallis, and F. Van den Heuvel, “Assessment of robustness against setup uncertainties using probabilistic scenarios in lung cancer: A comparison of proton with photon therapy,” *British Journal of Radiology*, vol. 93, no. 1107, Mar. 2020, doi: 10.1259/BJR.20190584/SUPPL_FILE/BJR.20190584.SUPPL-01.DOCX.

[104] M. Chu, Y. Zinchenko, S. G. Henderson, and M. B. Sharpe, “Robust optimization for intensity modulated radiation therapy treatment planning under uncertainty,” *Phys Med Biol*, vol. 50, no. 23, p. 5463, Nov. 2005, doi: 10.1088/0031-9155/50/23/003.

[105] D. A. Ripsman, F. Rahimi, H. Abouee-Mehrizi, and H. Mahmoudzadeh, “Light Pareto robust optimization for IMRT treatment planning,” *Med Phys*, vol. 50, no. 5, pp. 2637–2648, May 2023, doi: 10.1002/MP.16298.

[106] H. Mahmoudzadeh, J. Lee, T. C. Y. Chan, and T. G. Purdie, “Robust optimization methods for cardiac sparing in tangential breast IMRT,” *Med Phys*, vol. 42, no. 5, pp. 2212–2222, May 2015, doi: 10.1118/1.4916092.

[107] M. Byrne, Y. Hu, and B. Archibald-Heeren, “Evaluation of RayStation robust optimisation for superficial target coverage with setup variation in breast IMRT,” *Australas Phys Eng Sci Med*, vol. 39, no. 3, pp. 705–716, Sep. 2016, doi: 10.1007/S13246-016-0466-6.

[108] H. Miura, S. Ozawa, and Y. Nagata, “Efficacy of robust optimization plan with partial-arc VMAT for photon volumetric-modulated arc therapy: A phantom study,” *J Appl Clin Med Phys*, vol. 18, no. 5, pp. 97–103, Sep. 2017, doi: 10.1002/ACM2.12131.

[109] Y. Miyasaka *et al.*, “A robust treatment planning approach for chest motion in postmastectomy chest wall intensity modulated radiation therapy,” *J Appl Clin Med Phys*, vol. 25, no. 1, p. e14217, Jan. 2024, doi: 10.1002/ACM2.14217.

[110] D. A. Iancu and N. Trichakis, “Pareto Efficiency in Robust Optimization,” *Manage Sci*, vol. 60, no. 1, pp. 130–147, Sep. 2013, doi: 10.1287/MNSC.2013.1753.

[111] H. Miura *et al.*, “Characterization of robust optimization for VMAT plan for liver cancer,” *Reports of Practical Oncology & Radiotherapy*, vol. 25, no. 3, pp. 376–381, May 2020, doi: 10.1016/J.RPOR.2020.03.012.

[112] J. L. Bedford, I. Blasiak-Wal, and V. N. Hansen, “Dose prescription with spatial uncertainty for peripheral lung SBRT,” *J Appl Clin Med Phys*, vol. 20, no. 1, pp. 160–167, Jan. 2019, doi: 10.1002/ACM2.12504.

[113] R. W. K. Leung, M. K. H. Chan, C. L. Chiang, M. Wong, and O. Blanck, “On the pitfalls of PTV in lung SBRT using type-B dose engine: An analysis of PTV and worst case scenario concepts for treatment plan optimization,” *Radiation Oncology*, vol. 15, no. 1, pp. 1–16, May 2020, doi: 10.1186/S13014-020-01573-9.

[114] L. C. Goddard, N. P. Brodin, W. R. Bodner, M. K. Garg, and W. A. Tomé, “Comparing photon and proton-based hypofractioned SBRT for prostate cancer accounting for robustness and realistic treatment deliverability,” *British Journal of Radiology*, vol. 91, no. 1085, May 2018, doi: 10.1259/BJR.20180010/7449393.

[115] H. P. Wieser *et al.*, “Development of the open-source dose calculation and optimization toolkit matRad,” *Med Phys*, vol. 44, no. 6, pp. 2556–2568, Jun. 2017, doi: 10.1002/MP.12251.

[116] A. Fredriksson, A. Forsgren, and B. Hårdemark, “Minimax optimization for handling range and setup uncertainties in proton therapy,” *Med Phys*, vol. 38, no. 3, pp. 1672–1684, Mar. 2011, doi: 10.1118/1.3556559.

[117] M. Zhang, V. Moiseenko, and M. Liu, “PTV margin for dose-escalated radiation therapy of prostate cancer with daily online realignment using internal fiducial markers: Monte Carlo approach and dose population histogram (DPH) analysis,” *J Appl Clin Med Phys*, vol. 7, no. 2, pp. 38–49, Mar. 2006, doi: 10.1120/JACMP.V7I2.2210.

[118] “Grand Challenge - Fully Automated Radiotherapy Treatment Planning Challenge.” Accessed: Jul. 08, 2024. [Online]. Available: https://auto-rtp.grand-challenge.org/